Regionally optimized high resolution input datasets enhance the representation of snow cover ~~and ecophysiological processes~~ in CLM5

Johanna Teresa Malle[1,2], Giulia Mazzotti[2,3], Dirk Nikolaus Karger[1+], and Tobias Jonas[2+]

[1]Swiss Federal Research Institute for Forest, Snow, and Landscape Research (WSL), Zürcherstrasse 111, 8903, Birmensdorf, Switzerland
[2]WSL Institute for Snow and Avalanche Research SLF, Davos Dorf, Switzerland
[3]Univ. Grenoble Alpes, Université de Toulouse, Météo-France, CNRS, CNRM, Centre d'Études de la Neige, 38100 St. Martin d'Hères, France
[*]These authors contributed equally to this work.

Correspondence: Johanna Malle (johanna.malle@wsl.ch)

Abstract. Land surface processes, crucial for exchanging carbon, nitrogen, water, and energy between the atmosphere and terrestrial Earth, significantly impact the climate system. Many of these processes vary considerably at small spatial and temporal scales, in particular in mountainous terrain and complex topography. To examine the impact of spatial resolution and ~~quality~~ representativeness of input data on modeled land surface processes, we conducted simulations using the Community Land Model 5 (CLM5) at different resolutions and based on a range of input datasets over the spatial extent of Switzerland. Using high-resolution meteorological forcing and land-use data, we found that increased resolution ~~not only~~ substantially improved the representation of snow cover in CLM5 (up to 52% enhancement)~~but also propagated through the model, directly affecting gross primary productivity and evapotranspiration. These findings highlight the significance of high spatial resolution and high-confidence input datasets in land surface models, enabling better quantification and constraint of process uncertainties. They~~ , allowing CLM5 to closely match performance of a dedicated snow model. However, a simple lapse-rate based temperature downscaling provided large positive effects on model performance, even if simulations were based on coarse-resolution forcing datasets, only. Results demonstrate the need for resolutions higher than 0.25° for accurate snow simulations in topographically complex terrain. These findings have profound implications for climate impact studies. As improvements were observed across the cascade of dependencies in the land surface model, high spatial resolution as well as high-quality forcing data becomes necessary for accurately capturing the ~~impacts of recent climate change~~effects of a reclining snowcover and consequent shifts in the vegetation period, particularly in mountainous regions. This study further highlights the utility of multi-resolution modeling experiments when aiming to improve ~~process-based~~ representation of variables in land surface models. By embracing high-resolution modeling, we can enhance our understanding of ~~Earth's systems and their responses~~ the land surface and its response to climate change.

1 Introduction

The Earth's changing climate is causing ~~increasingly severe impacts on ecosystems worldwide (Pachauri et al., 2014; IPCC, 2022) . Human activity has played a significant role in past land-cover changes and will continue to have both direct and indirect impacts in the future (Vitousek et al., 1997; Pitman, 2003; Sterling et al., 2013; Pongratz et al., 2021).~~ profound alterations in ecosystems globally, with large impacts on ecological, hydrological, and climatological processes (Pachauri et al., 2014; IPCC, 2022) . In the context of the climate system, land surface processes control the exchange of carbon, nitrogen, water and energy between the atmosphere and ~~the terrestrial Earth, making them critical components of the current~~ terrestrial ecosystems, hence profoundly influencing contemporary and future climate ~~(Ferguson et al., 2012; Dirmeyer et al., 2006; Seneviratne et al., 2006) .~~ dynamics (Ferguson et al., 2012; Dirmeyer et al., 2006; Seneviratne et al., 2006). Seasonal snow cover greatly impacts this complex interplay, as it plays a vital role in the Earth's energy balance and hydrological cycle (Flanner and Zender, 2005; Barnett et al., 200 . More specifically, snow's characteristic high reflectivity (Flanner et al., 2011) substantially modulates land surface albedo and energy balance, while its low thermal conductivity (Zhang, 2005) allows snow to act as an insulating blanket for soil and organisms. More generally, agricultural irrigation often heavily relies on snow-melt for food production (Qin et al., 2020), while more than one sixth of the world's population is dependent on water from glaciers or snow melt (Barnett et al., 2005), highlighting the importance of glaciers and snow for human water demand (Mankin et al., 2015; Pritchard, 2019).

~~Important~~ Within the integrated Earth System, important interactions and feedback mechanisms exist between energy, water, and nutrient cycles. In seasonally snow-covered areas, the snowpack creates numerous such ~~feedbacks: it controls~~ interactions: it influences the energy balance by modulating the exchange of heat and moisture between the land surface and the atmosphere (Thackeray et al., 2019). It ~~determines~~ influences the partitioning of energy fluxes, ~~influencing~~ affecting the magnitudes of both sensible and latent heat fluxes (Male and Granger, 1981), which, in turn, regulate the transfer of energy and water vapor, shaping the local and regional climate patterns (Ban-Weiss et al., 2011). Moreover, the duration and extent of snow cover has direct implications for vegetation periods, which has the potential to impact gross primary production (GPP), a measure of vegetation's ability to convert solar energy into chemical energy (and carbon dioxide to organic matter) through photosynthesis (Slatyer et al., 2022). ~~Thus~~Therefore, the presence or absence of snow cover directly influences the availability of water and sunlight for plants, influencing the productivity and carbon cycling within terrestrial ecosystems and resulting in direct links between melt-out date and biomass production (Jonas et al., 2008).

~~As snow plays a vital role in the Earth's energy balance (e.g., due to its high reflectivity (Flanner et al., 2011) and low thermal conductivity (Zhang, 2005)) and hydrological cycle (Flanner and Zender, 2005; ?), understanding and quantifying the intricate interactions among snow cover and ecophysiological processes is essential for accurate predictions of environmental change and its impacts on the Earth's systems. Experimental studies, including snow manipulation experiments (Rixen et al., 2022; Slatyer et al., 2 , have observed and assessed these feedbacks at the local scale (e.g., Zeeman et al. (2017); Cooper et al. (2020)); Extrapolating these findings to regional and global scales , however, is only possible through modelling studies and remains challenging today. Ecohydrological models such as Tethys&Chloris (Fatichi et al., 2012; Mastrotheodoros et al., 2020) and RHESSys (Son and Tague, 2019; are specifically designed to represent interactions between water, energy, and the carbon cycles, but are not suitable for~~

~~global-scale applications~~The Global Climate Observing System (GCOS, https://gcos.wmo.int/) has identified Snow Cover Extent as an essential climate variable, which further underlines the importance of snow for monitoring climate change and the critical role it has in regulating the energy balance of the planet. In physically-based models, the representation of seasonal snow and its evolution are usually based on mass- and energy balance calculations. Representations of snowpack structure range from simple, one-layer approaches (Douville et al., 1995) to complex schemes that resolve up to 50 snowpack layers and track the evolution of their microstructural properties (Vionnet et al., 2012; Bartelt and Lehning, 2002). For model applications at large scales and coarse resolutions, snowpack representations with few (3 to ca. 10) layers (Essery et al., 2013; Niu et al., 2011) have been found to be an adequate compromise between model complexity and accuracy (Dutra et al., 2012; Magnusson et al., 2015) .

Land surface models (LSM) ~~, in contrast,~~ specifically target global-scale applications, as they were initially developed to represent the lower atmospheric boundary condition of Global Circulation Models. Land surface modeling has seen remarkable progress in recent years, evolving from simple biophysical parametrizations to complex frameworks that incorporate key processes such as soil moisture dynamics, land surface heterogeneity, and plant and soil carbon cycling (Fisher and Koven, 2020; Lawrence et al., 2019). Today's LSMs are thus principally suitable for, and even intended to, study process interactions and feedbacks within the Earth's systems (e.g., Lawrence et al. (2019). However, large challenges in land surface modeling today remain due to uncertainties in process representation, unresolved sub-grid heterogeneity, and the projection of spatial and temporal dynamics of model parameters (Beven and Cloke, 2012; Fisher and Koven, 2020; Fisher et al., 2019; Blyth et al., 2021). It is these limitations that make it difficult to reconcile site-scale experimental data and LSM simulations, hampering their evaluation and further development. Multi-resolution modelling setups (including the point/site scale) overcome this very limitation ~~, as it allows to evaluate~~ (e.g. (Singh et al., 2015; Meissner et al., 2009)), as they allow evaluating a spatially distributed LSM simulation over a large spatial extent, while at the same time certain aspects of the model (i.e. snow depth / snow cover duration) can be validated at the point scale using in-situ observations. This is especially of value if meteorological forcing data (e.g. station data) and/or land-use information as well as model evaluation data is available for a specific point-location.

Today, a strong push is evident towards higher resolution modeling, such as 1km simulations (Schär et al., 2020). While achieving this level of resolution globally over extended periods remains a challenge due to computational limitations, higher resolution allows for a more precise representation of land surface heterogeneity, which directly influences the representation of various key parameters and their associated processes (e.g., Ma and Wang (2022); Rimal et al. (2019); Zhang et al. (2017)). Because ~~snow cover dynamics~~ depth, duration and variability of seasonal snow cover is strongly affected by topography and thus highly variable in space (e.g., Clark et al. (2011)), higher resolution enables a more detailed characterization of snow distribution, depth, and duration, capturing the spatial variability of snow cover across diverse landscapes (Lei et al., 2022; Magnusson et al., 2019; Essery, 2003). Improved representation of snow cover dynamics has the potential to enhance simulation of surface albedo, which affects the amount of solar radiation reflected back into the atmosphere, and thus influences ~~surface temperatures (Thackeray and Fletcher, 2016; Flanner et al., 2011). Further variables and processes such as sensible and latent heat fluxes (Singh et al., 2015), surface temperature and evapotranspiration rates, and GPP, are highly variable in space (Anav et al., 2015). Increasing spatial resolution in land surface models, therefore has the potential to enhance not~~

only the simulation of snow cover dynamics, but also helps understand for which related ecophysiological processes higher spatial resolutions is paramount. Improved representation of the intricate interactions within the Earth's systems makes LSMs a powerful tool to study these feedback processes across scales and advance our understanding of themthe overall simulated surface energy balance (Thackeray and Fletcher, 2016; Flanner et al., 2011). An improved representation of snow melt-out date can further directly affect simulation of land surface phenology (Xie et al., 2020).

In this study, we explore how model resolution, and the quality of meteorological and land surface datasets affect the representation of seasonal snow cover dynamics and dependent ecophysiological variables. Based in the Community Land Model 5 (CLM5), a state-of-the-art LSM. More specifically and based on the ideas highlighted above, we formulate the following hypotheses:

Hypothesis 1: *With increasing spatial resolution and quality of meteorological input datasets, the representation of snow cover dynamics and its associated variables in CLM5 can achieve an accuracy comparable to that of a dedicated snow model.*

However, differences in snow cover development (especially on the grid scale) raise the question of whether corresponding changes in growing season length arising from differences in simulated snow-cover have a substantial impact on phenology, ecosystem functions, and the water budgethypothesize that with increasing spatial resolution and quality of meteorological and land surface input datasets, the representation of snow cover dynamics and its associated variables in CLM5 can achieve an accuracy comparable to that of a dedicated snow model.

Hypothesis 2: *Higher spatial resolution and increased level of detail in input datasets systematically affect the simulation of snow cover-dependent ecophysiological variables. We therefore predict that an increasing spatial resolution also improves the simulation of evapotranspiration, and gross primary production, leading to better estimates of carbon fluxes.*

To test these hypothesesTo test this hypothesis, we implement a multi-resolution modelling framework using CLM5, a state-of-the-art LSM. This framework bridges the gap between point/site-scale and spatially distributed land surface modeling, thus allowing us to compare process representation model accuracy across a hierarchy of spatial scales and using diverse evaluation data, while preserving model architecture. This way, confounding effects due to differences in process parametrizations are eliminated, isolating and clarifying the effects of model resolution and input-data, and allowing us to assess the importance of an accurate representation of sub-grid variability within coarser resolution models.

We apply our framework to the spatial extent of Switzerland, including relevant watersheds of neighboring countries. This region provides an ideal setting due to its diverse topography, encompassing both the Swiss Alps and the Swiss plateau. We test our hypotheses 1 and 2 by investigating relative differences between different Through a set of modelling experiments, we assess the relative impact of detailed meteorological and land cover information on snow simulations with CLM5 configurations with regards to the (a) snow dynamics, (b) terrestrial carbon cycle by focusing on heat fluxes and photosynthetic activity (GPP) and (c) the terrestrial water budget by focusing on the sum of water returning back to the atmosphere (evapotranspiration, ET)across topographically complex landscapes. Our findings can inform the optimal design of further offline applications of LSMsto , for instance 1) to extrapolate local-scale experimental findings, and ; 2) provide context to to address the limitations of global-scale, coarse resolution simulations; and 3) to support the interpretation of snow cover information contained in Earth System simulations.

2 Methodology

2.1 Land surface modelling

To investigate the effects of spatial resolution and input datasets in LSMs, we use the land component of the Community Earth System Model (CLM5), ~~a~~ an open-source, state-of-the-art, and widely used LSM that simulates carbon, nitrogen, water and energy exchange between the atmosphere and the land surface (Lawrence et al., 2019, 2018). It offers two operational modes: prognostic biogeochemistry (BGC) mode ~~, which fully prognostically calculates all state variables,~~ and prescribed satellite phenology (SP) mode. For this study, we focused on running CLM5 in SP mode, where ~~latest~~ remote sensing-based datasets are used to prescribe ~~part of the state variables in natural vegetation,~~ spatial extents of Plant Functional Types (PFTs) and Crop Functional Types as well as the PFT-specific monthly Plant Area Index (PAI, sum of Leaf Area Index and Stem Area Index), hence reducing the degrees of freedom compared to prognostic calculations. See Section 2.3.2 for more information.

It's important to note that in SP mode, carbon-nitrogen cycling is not considered, and certain processes such as leaf nutrient limitation and respiration terms are omitted. GPP ~~in CLM5 SP is~~ for the context of this study was approximated by photosynthetic activity, with photosynthesis being limited by carboxylation, light, and export limitations for different plant functional types (Thornton and Zimmermann, 2007; Farquhar et al., 1980). The photosynthesis module in CLM5 is described in detail by Thornton and Zimmermann (2007), Bonan et al. (2011), and Oleson et al. (2010). Simulations were performed with the Leaf Use of Nitrogen for Assimilation (LUNA) routine turned on (Ali et al., 2016). Evapotranspiration in CLM5 is calculated as the sum of transpiration, evaporation (considering soil/snow evaporation, ~~soil~~ice/snow sublimation as well as dew), and canopy evaporation following Lawrence et al. (2007).

~~Snow cover provides a convenient means of observing and validating the internal energy turnover of LSMs, and it is the duration of snow cover that influences vegetation periods, ecophysiological processes, and carbon cycles. In CLM5, general snow parametrizations are based on Anderson (1976), Jordan (1991), and Dai and Zeng (1997), with fractional snow cover calculations being based on the method of Swenson and Lawrence (2012). In recent years there have been several updates to the snow-related parametrizations, most notably an inclusion of wind and temperature effects on fresh snow density and an increase in maximum snow layers from 5 to 12 (Lawrence et al., 2019). A detailed description of snow related calculations in CLM5 can be found in Lawrence et al. (2018).~~

~~Spatial resolution mostly~~ Spatial resolution influences the representation of spatial heterogeneity in CLM5 which is represented by a sub-grid hierarchical system. Each grid cell is split into different land units (vegetation, glacier, lake, urban, crop)~~,~~ ~~and vegetated land-units~~ . On the second sub-grid level (column-level), potential variability in the soil and snow state variables within the same land-unit is accounted for. However, the vegetation and lake land unit only allow for a single column. Each vegetated column can be further divided up into up to 15 Plant Functional Types (PFTs) or bare ground (this is the ~~second~~ third sub-grid level in CLM5, often referred to as the ~~column-level~~patch-level). Vegetation structure for each PFT is described by monthly varying Leaf Area Index (LAI) and Stem Area Index (SAI), as well as canopy top and bottom heights. All of these values are prescribed in our model setup (satellite phenology mode).

Here, we applied CLM5 both to the regional scale, and to the point-scale, for which CLM5 features a dedicated point mode (PTCLM). It is worth noting that what we refer to as point-scale simulations incorporates fractional state variables (e.g., fractional snow-cover), as the gridded modeling algorithms (~~e.g.~~i.e., exactly the same ~~algorithms that are applied to~~ as used for large-scale gridded simulations) are directly applied to a single point. From a snow-cover modeling perspective such an approach would be referred to as site-scale, but in order to be consistent with LSM conventions we refer to them as point-scale simulations. As there is no lateral exchange in our model setup (river routing is off), there is no difference in running a dedicated point-simulation and taking out individual grid cells from a regional simulation, apart from the fact that we have additional information at these station locations (e.g. meteorological station data for forcing, exact GPS location for downscaling temperature). We elaborate on our experiments setup for point-scale and gridded simulations in Section 2.2.

2.1.1 Snow and fractional snow cover schemes in CLM5

Snow cover provides a convenient means of observing and validating the internal energy turnover of LSMs, and it is the duration of snow cover that influences vegetation periods, ecophysiological processes, and carbon cycles. The snow scheme in CLM5 classifies as a multi-layer snow model with detailed internal-snow-process schemes (Boone and Etchevers, 2001). General snow parametrizations are based on Anderson (1976), Jordan (1991), and Dai and Zeng (1997), with fractional snow cover calculations being based on the method of Swenson and Lawrence (2012). In recent years there have been several updates to the snow-related parametrizations, most notably an inclusion of wind and temperature effects on fresh snow density and an increase in maximum snow layers from 5 to 12 (Lawrence et al., 2019). A detailed description of snow related calculations in CLM5 can be found in Lawrence et al. (2018), but for convenience we also give a brief summary of snow related parametrizations used in CLM5 here. In CLM5, a snowpack can be made up of up to 12 layers, with the lowest being at the snow/soil interface and the uppermost at the snow/atmosphere interface. Each layer is described by mass of water, mass of ice, layer thickness and temperature. Any snowpack smaller than 10cm is treated as a single layer and only described by mass of snow.

Upon falling of solid precipitation on a column, either a new snow layer is initialized (if >10cm) or the snow is added to the present one, whereby combination and subdivision of snow layers is based on Jordan (1991). Mass of ice in each snow layer is calculated based on the rate of solid precipitation reaching the ground, taking into account gains due to frost and losses due to sublimation as well as change in ice due to phase change (melting). Bulk density of newly fallen snow is calculated dependent on air temperature and further increased if wind speeds exceed 0.1 m-1 due to wind compaction, following van Kampenhout et al. (2017). CLM5 includes 4 processes leading to overall snow compaction: (1) destructive metamorphism of new snow (2) snow load (3) melting (4) drifting snow. Mass of water in each layer is dependent on liquid water flow in and out of the layer and change in liquid water due to phase change (melting). For the top snow layer this includes rate of liquid precipitation falling, and evaporation as well as liquid dew. Any water flowing out of the lowest snow layer contributes to surface runoff and infiltration calculations in different CLM5 subroutines.

An essential variable for the energy balance due to its effects on surface albedo is fractional snow-covered area (FSno). FSno is further of importance as CLM5 calculates surface energy fluxes separately for snow-free and snow-covered land unit fractions. FSno in CLM5 is calculated following Swenson and Lawrence (2012), which uses separate parametrizations for the

snow accumulation and depletion phase. During accumulation, FSno is calculated as:

$$FSno^{n+1} = 1 - ((1 - tanh(0.1 q_{sno} \Delta t))(1 - FSno^{n})) \quad (1)$$

where $q_{sno}\Delta t$ quantifies the amount of new snow; $FSno^{n}$ and $FSno^{n+1}$ denote FSno at the previous and current time step, respectively. During snow-melt, the following parametrization is used:

$$FSno^{n+1} = 1 - [\frac{1}{\pi} acos(2\frac{W}{W_{max}} - 1)]^{n_{melt}} \quad (2)$$

W is the simulated snow water equivalent (SWE) at the current time step and W_{max} is the maximum simulated SWE of the snow season. n_{melt} is the snow covered area shape function, which is determined from σ_{topo}, the standard deviation of topography within a grid cell by:

$$n_{melt} = \frac{200}{\sigma_{topo}} \quad (3)$$

2.1.2 Rain-snow partioning in CLM5

CLM5 partitions total precipitation into rain and snow according to a linear temperature ramp, resulting in all snow below 0°C, all rain above 2°C, and a mix of rain and snow for intermediate temperatures. More specfically, the fraction of total precipitation P falling as rain (q_{rain}) and snow (q_{snow}) at each timestep is calculated as follows:

$$q_{rain} = P(f_p) \quad (4)$$

$$q_{snow} = P(1 - f_p) \quad (5)$$

$$f_p = 0 < 0.5(T_{atm} - T_f) < 1 \quad (6)$$

where T_f is set to 0°C.

2.2 Model experiments with CLM5

Figure 1 provides a general overview of the experimental setup, which includes three ~~main~~ aspects. Firstly, we varied the spatial resolution, ranging from 0.5°(10x6 grid cells) to 0.25°(19x11 grid cells) to 1 km (365x272 grid cells) over the study domain. As the 0.5°and 0.25°grids were chosen to closely match the extent of the pre-determined 1km grid, grid anchoring might slightly vary between resolutions. Secondly, we used different meteorological forcing datasets, including a globally available coarse-resolution dataset ($Clim_{CRU}$), the same global dataset with lapse-rate corrected temperature ($Clim_{CRU*}$), and a high-resolution regional dataset ($Clim_{OSHD}$). Lastly, we considered two options for land-use information: a global dataset

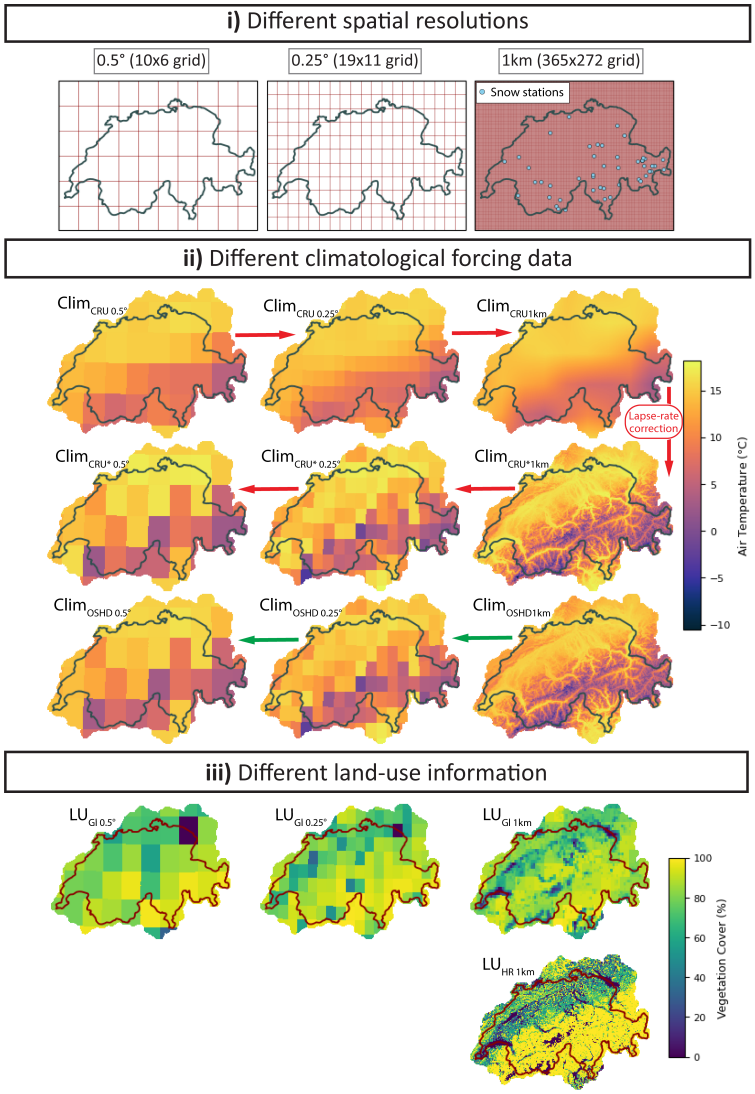

Figure 1. Schematic overview specifying the 3 facets of the experimental setup: Variation of i) spatial resolution, ii) meteorological forcing data and iii) land-use information. i) shows the different grids used, including the locations of the snow stations. ii) shows monthly mean temperature (May 2018) from the different data sources: Globally-available coarse-scale dataset (Clim_{CRU}), the same but with a lapse-rate corrected temperature ($\text{Clim}_{\text{CRU*}}$), and a high-resolution regional dataset ($\text{Clim}_{\text{OSHD}}$). Note that Clim_{CRU} data is provided at 0.5°(top left-most panel in ii), and bilinearly regridded to 0.25°and 1km. $\text{Clim}_{\text{CRU1km}}$ is then downscaled via a lapse-rate correction to obtain $\text{Clim}_{\text{CRU*1km}}$, before being up-scaled to 0.25°and 0.5°. Apart from temperature, meteorological forcing data is identical for Clim_{CRU1km} and $\text{Clim}_{CRU*1km}$ simulations. $\text{Clim}_{\text{OSHD}}$ data is provided at 1km, and upscaled to 0.25°and 0.5°. iii) shows differences in land-use information considered in this study by the example of percentage vegetation cover (sum of vegetation PFTs and crop CFTs).

(LU_{GI}) and a high-resolution dataset (LU_{HR}). This approach is intended to cover the multiple facets of resolution: on the one hand, the spatial resolution of the CLM5 simulations themselves; on the other hand, the 'native' resolution, or level of detail, of the input datasets, with higher resolution implying better quality of the datasets. Different CLM5 configurations were set up to cover the variations in spatial resolution, meteorological forcing, and land-use information.

At the 1km scale, CLM5 was run with six different configurations, each using different combinations of meteorological forcing and land-use information. At the 0.5°and 0.25°resolutions, CLM5 was run with three configurations corresponding to the respective meteorological forcing datasets and using the global land-use dataset. These regional CLM5 simulations across the spatial extent of Switzerland and adjacent watersheds of neighboring countries, covering an area of 44,050 km^2, were set up in an identical way as global simulations.

Additionally, point-scale simulations were conducted at 36 snow-monitoring station locations within the model domain. At the snow monitoring stations, we focus on the impact of meteorological forcing and land-surface input on CLM5 simulations by first running the same six configurations as for the 1km gridded experiment. ~~Land surface information for each site location was thereby extracted from the nearest~~ While exactly the same modelling framework was used for these point-scale simulations as for the gridded simulations, meteorological forcing was station-specific (e.g. not just the extracted meteorological forcing from the closest 1km ~~tile of the gridded dataset (either LU_{GI1km} or LU_{HR1km}).~~ gridcell, see 2.3.1 for additional information). Knowing that all 36 snow-monitoring stations are located on non-forested land, we set up 3 additional simulations enabling direct comparison of observations with respective simulations: For each meteorological forcing dataset ($Clim_{CRU}$, $Clim_{CRU^*}$, $Clim_{OSHD}$) we set up a simulation where the land-unit was set to be 100% vegetated with PFT 0 (bare ground) rather than using the composite grid-cell from the LU_{HR} and LU_{GI} dataset, respectively. This additional land use dataset is further refereed to as LU_{nofor}. Model performance evaluation was carried out based on in-situ observations at these stations (see Section 2.4.1 and 2.5.1 for more information). ~~We also set up simulations at 6 FLUXNET tower locations (Pastorello et al., 2020), setup and results of which can be found in Appendix **??**.~~

The performance of all gridded CLM5 configurations in simulating seasonal snow cover was assessed against simulations obtained with a ~~the~~ dedicated snow model (see Section 2.4.2 and 2.5.2 for more information). Outcomes from the snow cover analyses were complemented by ~~examining the link between spatially distributed CLM5 simulations of seasonal snow and their subsequent effects on ecophysiological variables through~~ a relative comparison of the different gridded CLM5 ~~model configurations , with a particular focus on~~ configurations for the ecophysiological variables gross primary production and evapotranspiration.

2.3 Input datasets

Each CLM5 model configuration requires the following meteorological driving data: incident short and long-wave radiation, air temperature, relative humidity, wind speed, pressure, and precipitation. Additionally, a land surface information file is required.

CLM5 simulations were set-up to run between January 2016 and December 2019, in order to maximize the temporal overlap between the various meteorological forcing datasets and available data for model ~~bench-marking~~benchmarking. We further performed 10 years of spin-up ~~in accelerated decomposition mode, followed by a final spin-up of 10 years, both by~~ by re-cycling

through the available input-data. A spin-up was necessary to ensure soil moisture and soil temperature were in approximate equilibrium and not affecting temporal dynamics and physical properties e.g., of the simulated snow cover evolution.

2.3.1 Meteorological Forcing

To assess the impact of meteorological input data quality, we considered three meteorological forcing datasets with increasing level of detail. As an example of a standard global dataset, we used the recent state-of-the-art dataset CRU-JRA (University of East Anglia Climatic Research Unit; of East Anglia Climatic Research Unit; Harris (2019)), which provides near-global (excluding Antarctica) six-hourly meteorological data on a 0.5°latitude x 0.5°longitude grid. CRU-JRA is a merged product of the monthly Climate Research Unit (CRU) gridded climatology (Harris et al., 2014) with the Japanese Reanalysis product (JRA, Kobayashi et al. (2015)). We selected CRU-JRA due to its large timespan (1901-2020), which includes recent years and hence ensures sufficient overlap with our high-resolution forcing dataset (see below), ~~data~~ as well as due to its application in the annual Global Carbon Budget assessments (e.g., TRENDY, Friedlingstein et al. (2020)) and in the Land Surface, Snow and Soil Moisture Model Intercomparison Project (LS3MIP, Hurk et al. (2016)). The original 0.5°CRU-JRA dataset was first projected to our model domain using nearest neighbor techniques ($\text{Clim}_{\text{CRU0.5°}}$), before re-gridding it to 0.25°~~and~~, 1km and all point locations using bilinear interpolation to obtain $\text{Clim}_{\text{CRU0.25°}}$~~and~~, $\text{Clim}_{\text{CRU1km}}$ as well as $\text{Clim}_{\text{CRU}^{pt}}$.

As a dataset representing an intermediate level of detail, we upgraded the $\text{Clim}_{\text{CRU1km}}$ ~~dataset~~ as well as $\text{Clim}_{\text{CRU}^{pt}}$ datasets by downscaling temperature data using a temperature lapse rate of -6.5K/1000m, which resulted in the $\text{Clim}_{\text{CRU}*}$ ~~dataset~~and the $\text{Clim}_{\text{CRU}*^{pt}}$ datasets. This approach was intended to account for variations of air temperature within the complex topography of the Swiss Alps and subsequent refinement of the partitioning of precipitation into snow and rain. We use a global DEM at 0.5°to first bring temperature to sea-level temperatures by applying negative lapse rates, before using a high-resolution DEM of Switzerland to re-lapse temperature (see Figure C1 in the Appendix for both DEMs). For the snow station locations we used the actual GPS measurement of each station, resulting in $\text{Clim}_{\text{CRU}*^{pt}}$. The updated 1km fields were upscaled back to 0.25°and 0.5°to inherit this correction also to the coarser-resolution simulations. This resulted in the $\text{Clim}_{\text{CRU}*}$ dataset. All other forcing variables were left identical for $\text{Clim}_{\text{CRU1km}}$ and $\text{Clim}_{\text{CRU}*\text{1km}}$, as well as $\text{Clim}_{\text{CRU}^{pt}}$ and $\text{Clim}_{\text{CRU}*^{pt}}$ simulations.

As input datasets with the highest level of detail, we used meteorological forcing generated according to methods developed by the Operational Snow Hydrological Service (OSHD), at 1km spatial and 1hour temporal resolution as well as all point locations at 1 hour temporal resolution. Necessary meteorological input variables were all provided by MeteoSwiss (COSMO1 and COSMOE product), and specific downscaling routines were applied e.g., to incoming solar radiation and wind velocity to optimally capture the influence of complex topography. Of particular relevance to this study is the correction of snowfall input fields by assimilation of station data according to Magnusson et al. (2014). In the context of this study, this dataset can be considered a meteorological input specifically optimized for accurate gridded snow cover simulations. The 1km forcing data was then upscaled to the desired target resolution (0.25°and 0.5°) with no smoothing applied. We refer to Mott et al. (2023) for further details with regards to the $\text{Clim}_{\text{OSHD}}$ product. The OSHD downscaling algorithms were also applied for each specific snow station location, resulting in the $\text{Clim}_{\text{OSHD}^{pt}}$ dataset for the point-scale simulations.

2.3.2 Land-use information

Global-scale land-use information: Input datasets for the land surface are based on the global-scale input dataset commonly used in CLM5, where extents of each land unit and percent plant functional type for each grid cell are derived from MODIS satellite data (Lawrence and Chase, 2007), as are monthly LAI and SAI values. ~~These global-scale surface input-datasets have an initial resolution of 0.05. We firstly re-projected and re-gridded the dataset to the model domain using~~ In a first step, which was performed separately for each target resolution (including all point-locations), we used the standard CLM tools (including the Earth System Modelling Framework (ESMF) regridding tools~~, which resulted in~~), to obtain our "global info" land surface dataset (LU_{Gl}, see Figure 1)~~and~~ . This represents a land surface dataset equivalent to that which would be used in a typical large scale LSM/General Circulation Model application. ~~This step was performed separately for each target resolution , resulting~~ Note that the resolution of the underlying global datasets varied (0.05° for urban/lake/glacier, 0.25° for vegetated/PFT fractions/LAI and SAI), since we used the most commonly applied CLM5 datasets. This step resulted in the $LU_{Gl0.5°}$, $LU_{Gl0.25°}$ as well as the LU_{Gl1km} ~~dataset.~~ datasets (see Figure 1). In Appendix B we show obtained land unit distributions per grid cell for all 3 target resolutions (Figure B2, Figure B1 and Figure B2 for LU_{Gl1km}, $LU_{Gl0.25°}$ and $LU_{Gl0.5°}$, respectively), patch-level PFT distributions (Figures B4, B5, B6) and monthly PAI for temperate needle leaf evergreen trees (Figures B8, B9, B10) as well as boreal broad-leaf deciduous trees (Figures B12, B13, B14).

High resolution land-use information: To obtain an alternative land-use input dataset (LU_{HR1km}) with a higher level of detail and based on a more up-to-date land use dataset, the LU_{Gl1km} dataset was updated based on a combination of ~~the official land-use and land-cover Data of Switzerland (Arealstatistik,~~ high-resolution data sources: (1) Copernicus Global Land Service PROBA-V data (2) Copernicus Sentinel-3/OLCI data, and (3) high-resolution national forest mixing ratios derived specifically for Switzerland (100m ~~resolution, updated every 6-8 years and derived by visual interpretation of aerial photographs (Office., 2001), forest mixing ratios (~~resolution, Swiss-Federal-Statistical-Office (2013)). In a first step, land unit distributions per grid cell (first sub-grid level in CLM5) were computed using the Copernicus PROBA-V 100m ~~resolution, Swiss-Federal-Statistical-Office (2013)) and~~ 2019 landcover datasets, which have been shown to be of high spatiotemporal quality (e.g. 79.9% accuracy over Europe for the Discrete Classification dataset, (Tsendbazar et al., 2021)). The native 100m fractional cover datasets were reprojected and regridded to our domain using ESMF tools (with a bilinear interpolation algorithm). We used the Copernicus Builtup-Cover Fraction to obtain the spatial extent of the urban landunit (assumed to be all at medium density), the Crops-Cover Fraction for the crop landunit (assumed to all be rainfed, non-irrigated land), and the level 1 Discrete Classification dataset for lake and glacier land units. The vegetated landunit was derived by adding Copernicus PROBA-V Grass-Cover Fraction, Tree-Cover Fraction, Shrub-Cover Fraction as well as Bare-Cover Fraction together. Minor adjustments were necessary due to regridding artifacts to ensure (a) no pixel exceeded 100% (e.g. around edges of lakes) and (b) each pixel added up exactly to 100% (any non-classified pixels were classified as non-vegetated). Figure B1 in Appendix B shows extents of the LU_{HR1km} dataset for each CLM5 land unit.

For the third sub-grid level (patch-level) of the vegetated landunit, we merged the 100m Copernicus Forest Type layer as well as the 100m Copernicus ~~Sentinel-3 data (333m resolution). More specifically we merged arealstatistics Switzerland and~~ shrub-

and grass cover fraction with Swiss national 100m forest mixing ratio data. The Copernicus Forest Type layer distinguishes between 6 forest classes (needle leaf and broad leaf evergreen forests; needle leaf and broad leaf deciduous forests; mixed forests and unclassified) which were translated to CLM5 PFTs in the following manner: Evergreen trees (both deciduous and broad-leaf) were classified as needle leaf evergreen temperate trees (PFT2), deciduous needle-leaf trees were classified as needle leaf deciduous boreal trees (PFT4) and deciduous broad-leaf trees were classified as broad-leaf deciduous temperate trees (PFT8). All shrubs from Copernicus shrub cover were assumed to be broad-leaf deciduous shrubs (PFT12), and all grass as well as sparsely vegetated cells were classified as C_3 grass. Mixed and unknown pixels were then updated based on the Swiss-wide dataset. If the Swiss-dataset classified it as needle leaf forest, it was set to PFT2, if it was a deciduous forest it was PFT 8, needle-mix and deciduous-mix forest were set to PFT 4 and no wood was classified as C_3 grass (PFT 13). Figure B3 in Appendix B shows percentage PFT fractions of the LU_{HR1km} dataset.

In order to obtain an updated LAI dataset, Copernicus Sentinel-3/~~OLCI,~~ OLCI/PROBA-V ~~@333m and forest mixing ratios to obtain vegetation, lake, urban, glacier, crop-fraction at the land-unit level and monthly LAI, SAI, fraction per PFT (incl. bare ground) at the column level. This resulted in the high-resolution~~ data at 333m spatial resolution was used, which has a temporal resolution of 3 timesteps per month. We used data for the year 2020, and averaged the 3 monthly timesteps to obtain one layer of LAI data per month. For evergreen PFTs August LAI was used year round, whereas for deciduous PFTs the respective monthly values were used. LAI of pixels where satellite data was not available (snow, clouds) was set to 1. LAIs of crops, shrubs and grasses remained unchanged in the LU_{HR1km} dataset. Figure B7 and B11 in Appendix B show monthly PAI for temperate needle leaf evergreen trees (PFT2) and boreal broad-leaf deciduous tree (PFT 4).

2.4 Test datasets

We used two ~~observational datasets as test datasets~~ datasets to assess model performance. The first, consisting of daily snow depth observations from 36 snow stations, ~~served~~ allowed to evaluate the performance of CLM5 point-scale configurations in simulating seasonal snow cover ~~. For the second dataset~~against ground truth data. For an evaluation of the gridded CLM5 simulations, we employed the Flexible Snow Model (FSM2) as a reference snow model for validation~~and comparison with the gridded CLM5 simulations of seasonal snow development.~~ .

2.4.1 Snow stations

The 36 snow stations considered cover an elevational gradient~~and~~ , are spread throughout Switzerland (see Figure 1~~i))~~)) and were selected from an exceptionally dense and accurate network of snow observations. Table A1 in the Appendix specifies locations and characteristics of each of these sites. Observations at the station locations consist of daily monitored snow depth (HS), which are collected as part of the snow monitoring networks of either the WSL Institute for Snow and Avalanche Research (SLF) or the Federal Office for Meteorology and Climatology (MeteoSwiss). HS measurements were extracted at a daily timestep and cleaned from obvious outliers (assessed against neighboring stations at similar elevations), which can occur e.g. due to ~~transmission or~~ measurement errors (see Mott et al. (2023) for more details).

2.4.2 Snow cover simulations with FSM2

The Flexible Snow Model (FSM2, Mazzotti et al. (2020)), a recent upgrade of the Factorial Snow Model (FSM, Essery (2015)), is an open-source, ~~spatially distributed,~~ physics-based snow model ~~. Gridded simulations~~ of intermediate complexity. Simulations at 250m resolution and point simulations at snow station locations have been specifically set up and calibrated by SLF to run over the extent of Switzerland for the purpose of operational snow water resources monitoring (Griessinger et al., 2019; Mott et al., 2023). At the 250m resolution, model grid cells are subdivided into forest, open, and glacier fractions, with forest cover descriptors derived from a 1m-resolution, LiDAR-based canopy height model available for Switzerland (Mott et al., 2023; Waser et al., 2017). In the absence of high-quality, spatially distributed snow depth observations over the entire extent of Switzerland, these FSM2 simulations were served as ground truth for this study. For comparison with CLM5 output, 250m resolution ~~FSM~~ FSM2 output results were upscaled to 1km without smoothing (e.g. conservative regridding).

2.5 Evaluation of model ~~performance~~experiments

2.5.1 Comparing point-scale CLM5 model simulations to station observations of snow depth

Observations at the snow monitoring stations (Figure 1 ~~i and Table S1)~~ and Table A1) provide an exceptional opportunity to allow proper assessment of regional model performance. Sub-sampled from a dense, high-quality network of snow observations, these measurements of snow height were used to assess the ability of each station-specific point-scale CLM5 configuration to simulate seasonal snowpack in Switzerland, and were additionally compared to ~~offline~~ FSM2 simulations. The evaluation of FSM2 runs allowed to assess whether FSM2 is a suitable model to be used as a reference for the gridded simulations.

The stations were binned into three elevational bands (<1000 m.a.s.l, 1000 – 2000 m.a.s.l, >2000 m.a.s.l) resulting in 10, 12 and 14 stations for the low, mid- and high elevation band, respectively. For each station location, the various CLM5 point-scale simulations ($Clim_{CRU\,1km}$+$LU_{Gl/HR\ 1km}$, $Clim_{CRU^{*}1km}$+$LU_{Gl/HR\ 1km}$, $Clim_{OSHD\,1km}$+$LU_{Gl/HR\ 1km}$) as well as the FSM2 simulation were compared to observations of snow depth (HS), by computing relative and absolute differences as well as Root Mean Square Errors (RMSE) and Mean Absolute Errors (MAE) for the ~~timeframe between November and May of each simulation year (2016-2019)~~time frame between October and July across all 4 simulated snow seasons.

Additionally we use wiggle plots to show the seasonal evolution of model errors for all the point-scale simulations across the 2017/18 season.

2.5.2 Comparing gridded CLM5 model simulations to FSM2 simulations of snow depth

~~For the~~ Given that the point-scale evaluation against station data offers an incomplete picture of CLM5 performance in its 'typical' setting (coarse-resolution, gridded) as it is limited to point locations with a narrow range of topographic and vegetation characteristic, we provide a complementary evaluation of all gridded CLM5 simulations against FSM2. This model evaluation was performed at 0.25° resolution, which is a fair target given the complexity of the topography across our modelling domain and its relatively small size, and considering today's ever-increasing computational resources. FSM2 as well as 1km CLM5

simulation results were hence upscaled to 0.25°using a conservative upscaling approach which preserves areal averages. For this purpose, we had to decrease our evaluation domain slightly, as we performed the 1km simulations with a mask running exactly along the edges of our modelling domain, making it impossible to upscale these areas to 0.25°without crude assumptions. The 0.5°simulations were downscaled to 0.25°, and all simulations were evaluated across the same domain.

For the evaluation and quantification of snow-related CLM5 model experiment's performance we used a Taylor diagram (Taylor, 2001), with FSM2 simulations of snow depth at 0.25°as our reference. A Taylor diagram combines centered RMSE, correlation coefficients as well as the spatial/temporal standard deviation and hence describes overestimation or underestimation of the models relative to a benchmark. ~~In order to calculate the values for the Taylor diagram the output of the low resolution~~

Additionally, in order to better understand patterns in model discrepancy as they relate to topography and land cover, we compared simulated snow depth (HS) as a function of elevation for three dates during the 2018/19 winter season (early winter 1-Dec; mid winter 1-Feb; late winter 1-Apr). This comparison was performed at 1km, and only included the six 1km CLM5 simulations ~~(0.25and 0.5resolution) was interpolated to the finer 1km grid without smoothing~~as well as FSM2, hence no up-/down-sampling was necessary and the effect of elevation could be assessed over a larger distribution. We further compared changes in land-use information and simulated snow-cover for non-forested vs. forest-dominated grid-cells, allowing an assessment of whether the sensitivity to the chosen dataset depends on the land cover type.

3 Results

3.1 ~~Snow~~ Evaluation of snow simulations at point locations

3.1.1 ~~Snow dynamics using different meteorological forcing~~

~~We~~

We begin by focusing on simulated snow depth at point locations. We observed distinct differences in performance using different meteorological forcing datasets in our CLM5 experiments (see Figure 2). The point-scale CLM5 model using global meteorological forcing data ($\text{Clim}_{\text{CRU}\,1\text{km}}\text{CRU}^{pt}$+$\text{LU}_{\text{GI/HR}\,1\text{km}}\text{GI/HR/nofor}$) showed poor performance in modeling seasonal snow development ~~. RMSEs exceeded~~ across all snow station locations. RMSEs were close to 1m for mid-elevation stations and only marginally ~~improved~~ better for high- and low-elevation stations. This demonstrates that these runs fail to accurately represent elevational gradients in temperature and snow amounts, making the error dependent on how closely the characteristics of the station happen to match the characteristics of the coarse resolution grid-cells of the Clim_{CRU} forcing dataset.

When the lapse-rate based downscaled temperature input was used ($\text{Clim}_{\text{CRU*}\,1\text{km}}\text{CRU*}^{pt}$+$\text{LU}_{\text{GI/HR}\,1\text{km}}\text{GI/HR/nofor}$) instead, the model's performance improved significantly, particularly at low elevations. At mid- and high elevations the positive impact of a better temperature representation is masked by the overestimated precipitation input when compared to the OSHD dataset (see Figure C2 and Figure C4 in the Appendix for a comparision of precipitation forcing between the CRU and the OSHD

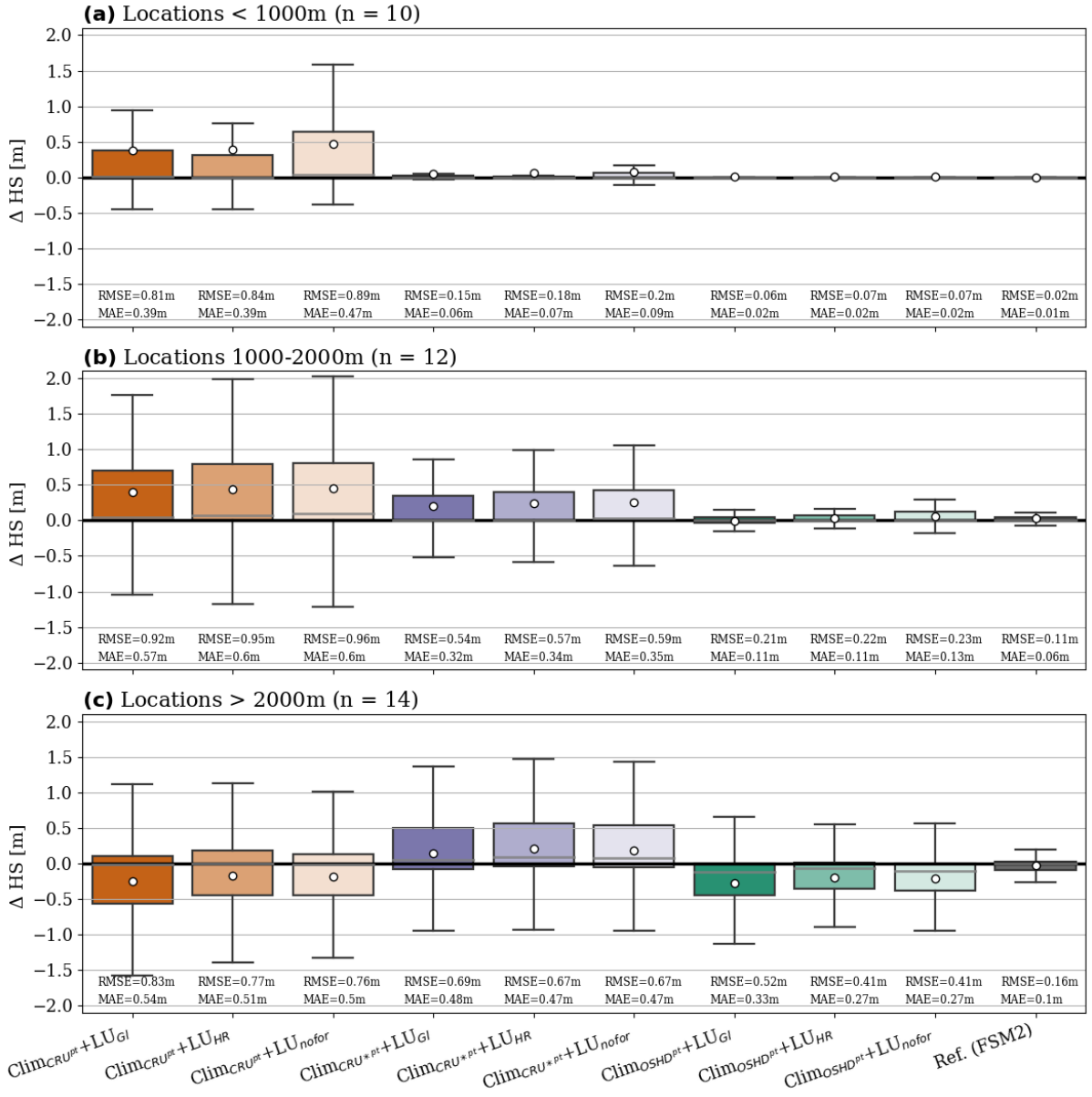

Figure 2. Comparisons of point-scale model simulations to observations of snow depth (HS) ~~during the 2017/18~~ across all simulated snow ~~season~~ seasons (~~November-May~~October-July) for combined (a) low elevation, (b) mid-elevation and (c) high elevation snow station locations. Negative values depict under-estimations of the simulations. Means are shown by the white dots.~~The reference snow simulation (FSM2) matches observations the closest, with negligible errors for low and mid-elevation points and slight underestimation for high elevation points. CLM5 forced with OSHD data and based on high-resolution land-use information is the next best. For a more detailed assessment of seasonal snow dynamics per station and simulation, refer to Figure ?? in the Appendix.~~

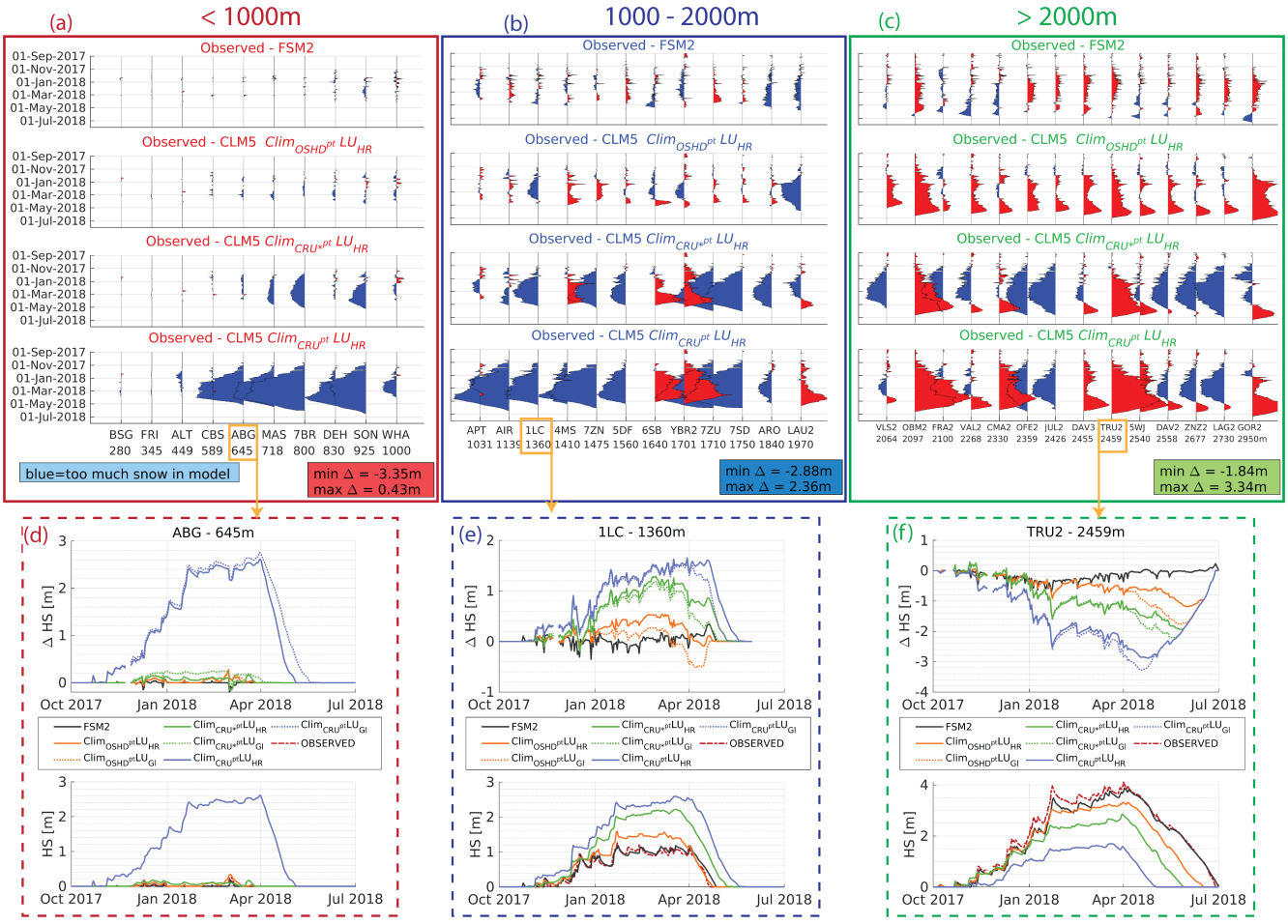

Figure 3. Wiggle plots comparing point-scale model simulations to observations of snow depth (HS) throughout the 2017/18 season for low elevation (a), mid-elevation (b) and high elevation (c) point locations whereby blue denotes too much and red too little snow in the models when compared to observations. (d-f): Absolute difference to observations and seasonal snow depth development for 3 example point locations.

forcing dataset). The overestimation of snow at mid- and high elevations of the $Clim_{CRU*}$ dataset is hence a direct result of overestimated precipitation along the Alps.

The CLM5 model forced with OSHD data ($Clim_{\sout{OSHD1km}OSHD^{pt}}$+$LU_{\sout{GI/HR 1km}GI/HR/nofor}$) demonstrated the best performance across all three elevation bands, with only minor errors in low- and mid-elevation locations (e.g., RMSE/MAE of ~~0.25~~0.22/~~0.15~~0.11m for mid-elevation $Clim_{\sout{OSHD1km}OSHD^{pt}}$+$LU_{\sout{HR 1km}HR}$ simulations). ~~Results were consistent throughout all simulated years.~~ These simulations overcome the 'too much solid precipitation problem' outlined above as the OSHD precipitation forcing dataset is optimized by data assimilation. The underestimation at high elevations is likely due to snow process representation in the model

(combination of too fast settling and too efficient melt, see Figure 3f). Generally, these results indicate that the CLM5 model forced with OSHD data approach the accuracy of a dedicated snow model (FSM2), at least when assessed at point locations.

3.1.1 ~~Snow dynamics using different land use information~~

Figure 3 further illustrates these results, as it features wiggle plots as well as seasonal snow development for selected snow station location throughout the 2017/18 winter season. It is apparent across all elevation bands that FSM2 simulations match observations the closest (discussed in more detail in Section 3.1.1), and that CLM5 forced with OSHD data is the next best. CLM5 with global meteorological forcing data ($Clim_{CRU^{pt}}$) performs poorly with maximal errors of over 3m. These biases are persistent throughout the snow season, whereas snow depth is mostly overestimated below, and underestimated above 2000m, respectively.

Regarding the effects of the land-use information dataset, we observed that the choice of land-use information ~~had a smaller impact compared to the meteorological forcing data~~ only had a small impact on simulated snow depth (Figure 2). We include simulations using the global, the high-resolution, as well as the non-forested land use dataset (LU_{Gl}, LU_{HR}, LU_{nofor} respectively). While a slight improvement was seen when using the high-resolution land-use information dataset ($LU_{\text{~~HR1km~~}HR}$) at high elevations for all three sets of meteorological forcing data (reducing RMSE by ~~-0.13~~-0.06m/-0.02m/~~-0.06~~-0.11m for $Clim_{\text{~~CRU1km~~}CRUpt}$/ $Clim_{\text{~~CRU*1km~~}CRU^{*}pt}$/ $Clim_{\text{~~OSHD1km~~}OSHDpt}$ simulations, respectively), no ~~significant~~ substantial differences or marginal decreases in model performance were observed for ~~$Clim_{OSHD1km}$, $Clim_{CRU1km}$ and $Clim_{CRU*1km}$ across all elevation bands.~~ the lower two elevation bands. This is further underlined by Figure 3d-f. Simulating open, non-forested sites (LU_{nofor}) only had marginal effects on model performance: For low and mid-elevations a slight decrease in model performance is apparent for all three meteorological forcing datasets, whereas at high elevations differences are virtually non-existent. This can be explained by the larger variety in land-unit distributions at lower elevations, while at high elevations differences between the two datasets remained small. Ultimately, it can be seen that, at coarse model resolution, the effect of meteorological forcing data is substantially larger in comparison to differences arising from the choice of land surface information.

3.1.1 Accuracy of FSM2 point-scale simulations

Across all elevation bands, the FSM2 simulations closely matched the observations, with only minor errors at low and mid elevations during the 2017/18 season (Figure 2). At high elevations, the FSM2 model slightly underestimated snow depths, which can be assessed in more detail in Figure ~~S1 in the supplementary material. Figure ?? in the Appendix features wiggle plots as well as absolute difference and seasonal snow development for selected snow station locations, visualizing the~~ 3. Figure 3 visualizes the superior performance of FSM2 in comparison to ~~various~~ all CLM5 model experiments, further justifying using FSM2 model simulations as our ground truth for the gridded simulation comparisons in Section ~~3.1.4~~3.2.

3.1.2 ~~Spatially distributed snow cover~~

3.2 Evaluation of gridded snow simulations

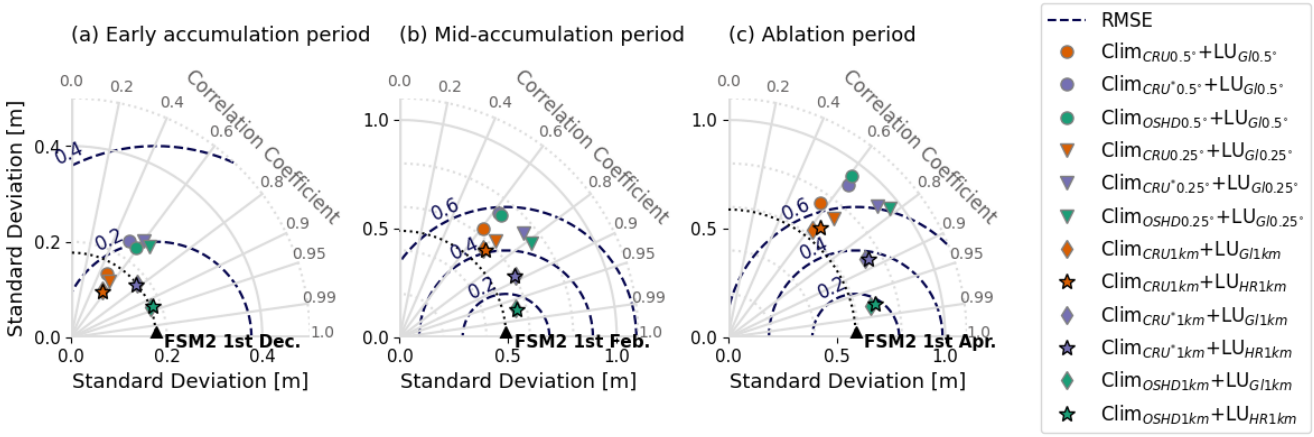

Figure 4. Taylor plots (Taylor, 2001) for comparisons of simulated snow-depth (HS) between all 12 different CLM5 configurations and the reference snow simulation (FSM2, dark grey) during (a) early accumulation season (1-Dec), (b) mid-accumulation period (1-Feb) and (c) ablation period (1-Apr) throughout four winter seasons (2015/16, 2016/17, 2017/18, 2018/19). The plotted statistical metrics allow for evaluation and quantification of CLM5 model experiments performance, based on centered RMSE (directly proportional to the distance away from the reference (=FSM2)), correlation coefficients (azimuthal position) and the spatial/temporal standard deviation (radial position from the origin) which determines overestimation or underestimation of the models. ~~An increase in resolution results in improved representation of snow for all 3 time periods and across all meteorological/land-use information combinations. Simulations with high-resolution meteorological forcing data substantially outperform global meteorological forcing cases, whereas simulations with different land-use information only differ marginally. Clim$_{OSHD1km}$+LU$_{Gl1km}$ performs closest to the reference FSM2 simulation during all 3 time periods. The global case simulations (e.g., Clim$_{CRU0.5°}$+LU$_{Gl0.5°}$) do not perform well with low correlations and high standard deviations. See Figure 1(ii) and (iii) for the various combination setups.~~

~~Here we investigate all 3~~ The comparison of gridded simulations with CLM5 to FSM2 reference simulations allows us to investigate all three facets of this study: Effects of resolution, effects of meteorological forcing data, and effects of land-use information data. ~~We focus on~~ To this end, we consider gridded simulations of snow depth from all 12 different CLM5 configurations (see Figure 1(ii) and (iii)) and compare them to FSM2 simulations ~~.~~ (Figure 4). Our analysis is performed across all four snow seasons, and at 0.25°. Additionally we investigate how the accuracy of CLM5 varies as a function of elevation by comparing all 1km simulations against FSM2 (Figure 5) for the 2018/19 season. For both analysis we differentiate between early accumulation period (1st December), mid-accumulation period (1st of February) and ablation period (1st of April).

Increasing the level of detail in meteorological forcing data ~~plays the largest role in modulating~~ has the largest effect on accuracy of simulated seasonal snow cover, especially when simulating at 1km. CLM5 runs with OSHD-based input data outperform all CRU- and CRU*-based simulations at all three points in time during winter (e.g., RMSE Clim$_{OSHD1km}$+LU$_{Gl1km}$: ~~0.13, 0.28, 0.32~~0.07, 0.14, 0.18m vs. RMSE Clim$_{CRU*1km}$+LU$_{Gl1km}$: ~~0.19, 0.47, 0.59~~0.12, 0.29, 0.37m vs. RMSE Clim$_{CRU1km}$+LU$_{Gl1km}$: ~~0.23, 0.62, 0.79~~0.15, 0.41, 0.53m for early, mid, and end-winter respectively~~).~~

~~When running CLM5 with global-based forcing data, increasing spatial resolution in isolation (e.g., regridding) only has a marginal effect on accuracy of simulated seasonal snow cover during early and mid-winter, with a bit more of a pronounced effect of increases to 1km during the ablation period(see difference between $Clim_{CRU0.5°}+LU_{GI0.5°}$ (red dots), ;~~ Figure 4)) as compared to FSM2 simulations. The postitive effects of lapse-rate corrected temperatures on model performance ($Clim_{CRU0.25°}$ ~~$+LU_{GI0.25°}$ (dark red dots) and~~ $_{CRU1km}$ vs. $Clim_{CRU*1km}$) are pronounced during mid-accumulation and ablation period, where performance is substantially enhanced, while during early accumulation only correlation and standard deviation is improved when moving from $Clim_{CRU1km}$ ~~$+LU_{GI1km}$ (orange dots) in Figure 4 a,b,c). The marginal effect can be attributed to the fact that increasing spatial resolution in itself (e.g., simple regridding) does not bring any added value as in better representation of topography. However, when using the down-scaled global temperature data as well as the OSHD~~ to $Clim_{CRU*1km}$. The reason behind this is that during early season snow height tends to be small anyways, but once snow amounts become substantial the effect of a lapse-rate correction in the context of partitioning precipitation into rain and snowfall becomes more evident, and simulation results diverge. A simple lapse rate correction that accounts for high-resolution topography hence already brings a lot of benefit relative to a coarse-resolution dataset.

Figure 5 further illustrates these findings: Focusing in on only one representative season (2018/19) and looking at simulated snow-depth as a function of elevation, elevational behaviour of FSM2 is matched closest by CLM5 simulations using OSHD-based forcing data, ~~there is a substantial reduction in accuracy between the 1km and the 0.5/0.25simulations (Figure 4), implying that a coarse resolution negates the benefit~~ with most discrepancies occurring during the ablation period at high elevation. Downscaling temperature has a substantial effect on performance, allowing $Clim_{CRU*1km}$ to closely match performance of $Clim_{OSHD1km}$.

However, the benefits of a higher level of detail in the meteorological forcing ~~,~~

~~Similarly to~~ are negated when model resolution itself is decreased. Comparing results of CLM5 configurations that differed in resolution only, a large decrease in accuracy is evident for the OSHD- and CRU*-based runs when moving from 1km to 0.25°, while further coarsening to 0.5° only has a marginal effect. This is because the evolution of snow cover is shaped by non-linear process interactions (e.g., temperature fields affect both snowpack energetics and its mass balance by dictating precipitation phase) that are 'lost' when meteorological input is averaged spatially. Our simulations suggest that a model resolution higher than 0.25° is essential to capture the spatial heterogeneity of snow cover evolution processes in the complex terrain present in our study domain. In accordance with this finding, resolution did not have much impact on the performance of the ~~point-scale simulations at the snow station locations, the choice of land-use information only had a marginal influence on the simulation accuracy of seasonal snow-cover development.~~ CRU-based runs, since simple regridding without additional consideration of topographic effects on the meteorological drivers does not bring any added values in capturing the non-linear processes shaping snow cover dynamics in complex terrain.

Ultimately, throughout the ~~4~~ four modeled years, and averaged over the model domain, substantial differences in simulated snow-cover between the various CLM5 configurations are ~~prevalent~~ evident (Figure 4). In a similar manner to the point-scale CLM5 simulations, results revealed ~~vast~~ considerable improvements in simulated snow cover accuracy when using high-confidence forcing data (Figure 2, Figure 4), with CLM5 in our best-effort scenario ($Clim_{OSHD1km}$+LU_{HR1km} simulation) almost

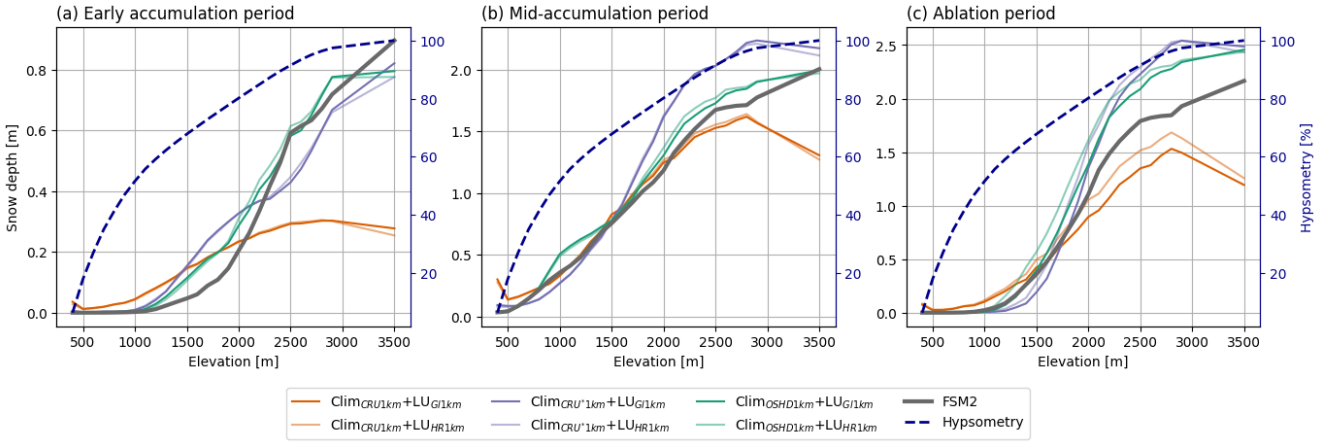

Figure 5. ~~Spatial comparison~~ Simulated snow depth (HS) as a function of ~~CLM5-simulated~~ elevation during (a) ~~GPP and b~~early accumulation season (1-Dec)~~Evapotranspiration for the following cases: i) denotes the reference case~~, ~~with "best" climate~~ (~~Clim$_{OSHD1km}$~~b) ~~+ global land-use info~~ mid-accumulation period (~~LU$_{HR1km}$~~1-Feb) ~~, ii~~and (c) ~~singles out~~ ablation period (1-Apr) for the ~~effect~~ 2018/19 winter season. We contrast elevational dependency of ~~land-use information and iii~~FSM2 (dark grey) ~~shows the combined effect climate and land-use info~~with all six 1km CLM5 configurations. ~~For the residual plots,~~ The dark blue ~~indicates underestimation and red indicates overestimation with regards to~~ dashed line represents hypsometry across the ~~reference case~~model domain (Switzerland+).

reaching the level of a dedicated snow model also in a gridded application. This becomes especially apparent when looking at the high correlation coefficient of the Clim$_{OSHD1km}$+LU$_{HR1km}$ simulation in Figure 4. However, degraded model performance between the 1km and the 0.25°configurations suggests that in order to actually benefit from the added value of high-quality forcing data, a sufficiently high model resolution remains necessary when applying CLM5 in topographically complex regions.

3.3 ~~Simulation of ecophysiological parameters~~

In order to better understand why the effect of land-use data in our results was minimal, we further investigated the link between changes in land-use information and simulated snow-cover for non-forested vs. forest-dominated grid-cells. Figure 6 compares differences in PAI (averaged across all PFTs, averaged between January-March) across the model domain between LU$_{HR1km}$ and the LU$_{Gl1km}$ with simulated snow height for 1-Feb-2018. We show that the majority of snow-dominated pixels correspond to pixels with little change in PAI between the high-resolution and the global land-use datasets (e.g. non-forested areas). Pixels with large changes in PAI on the contrary tend to be located in the lowlands, with little snow throughout the season. This demonstrates that the impact of land-use data is masked by the many pixels with much snow but little change in PAI. The low sensitivity we find with regards to land-use forcing is hence mostly a symptom of the limited overlap between snow dominated and forested areas in our model domain.

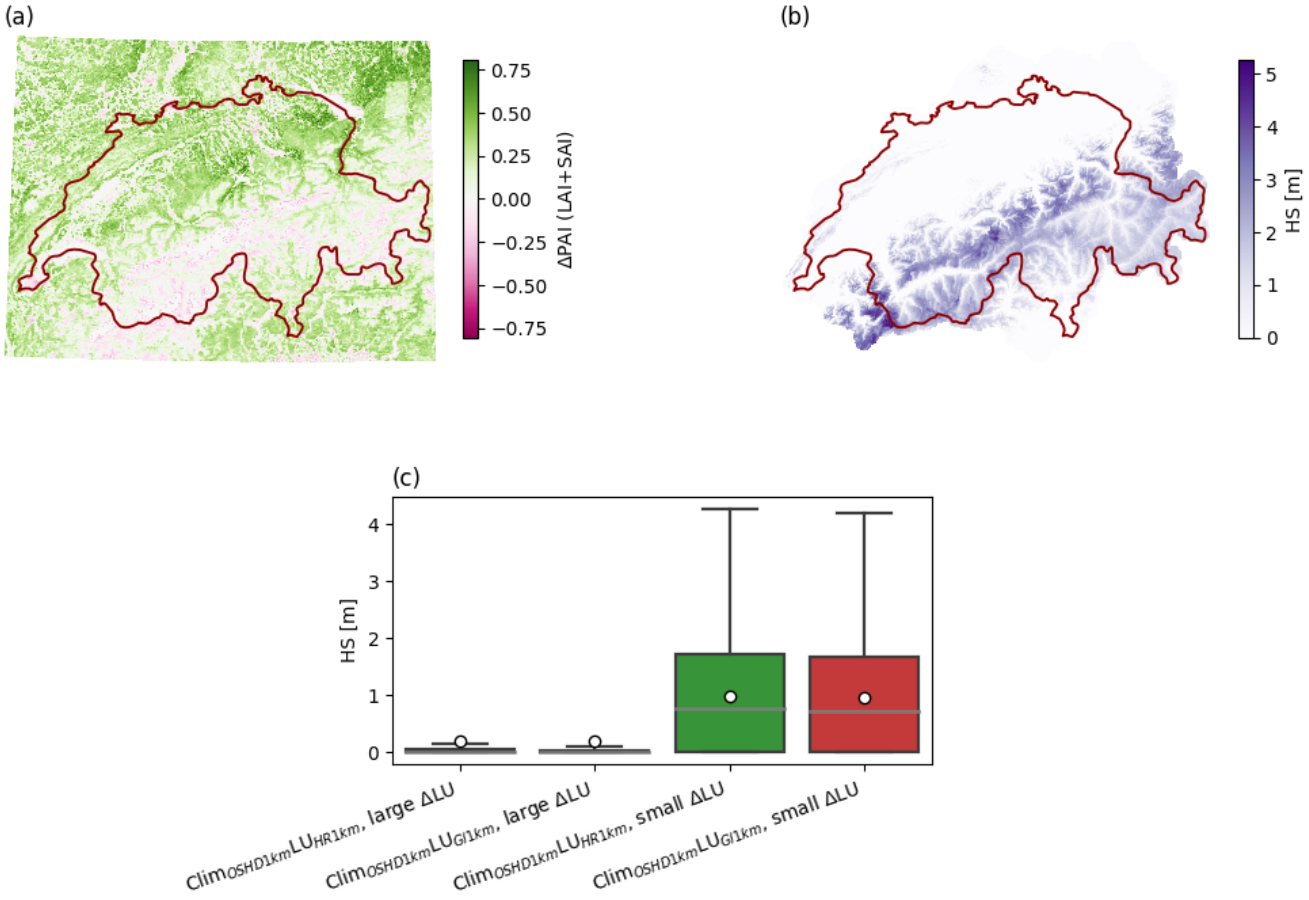

Figure 6. Links between change in land-use and simulated snow cover: (a) PAI difference between the LU_{HR1km} and LU_{Gl1km} dataset, whereby PAI (LAI+SAI) is averaged across all PFTs as well as between January and March. (b) Snow depth on 1-Feb-2018 as simulated by CLM5 $Clim_{OSHD1km}$+LU_{HR1km}. (c) Comparison of snow height distributions on 1-Feb-2018 for $Clim_{OSHD1km}$+LU_{HR1km} and $Clim_{OSHD1km}$+LU_{Gl1km}, each for pixels with a large change in overall PAI (>0.25) and a small change in overall PAI (<0.25).

3.3 Simulation of ecophysiological variables

~~A relative~~ While the previous sections focused on the representation of snow cover, an asset of LSMs relative to dedicated snow models such as FSM2 is that they include a more comprehensive description of land surface processes and state variables, allowing the interaction between these to be investigated. In this final part of our analysis, we thus extend our focus to ecophysiological parameters to showcase effects of spatial resolution, meteorological forcing and land-use information beyond snow cover. In lack of a reference model for evaluation, we present a relative comparison between spatially distributed (a) simulated mean total ~~peak (July+August) growing season GPP for 2017~~ GPP for 2016-2019 as well as (b) total ET during 2017 ~~is shown~~ in Figure 7. ~~In each~~ To single out the impact of each facet of our study, in each plot $Clim_{OSHD1km}$+LU_{Gl1km} is

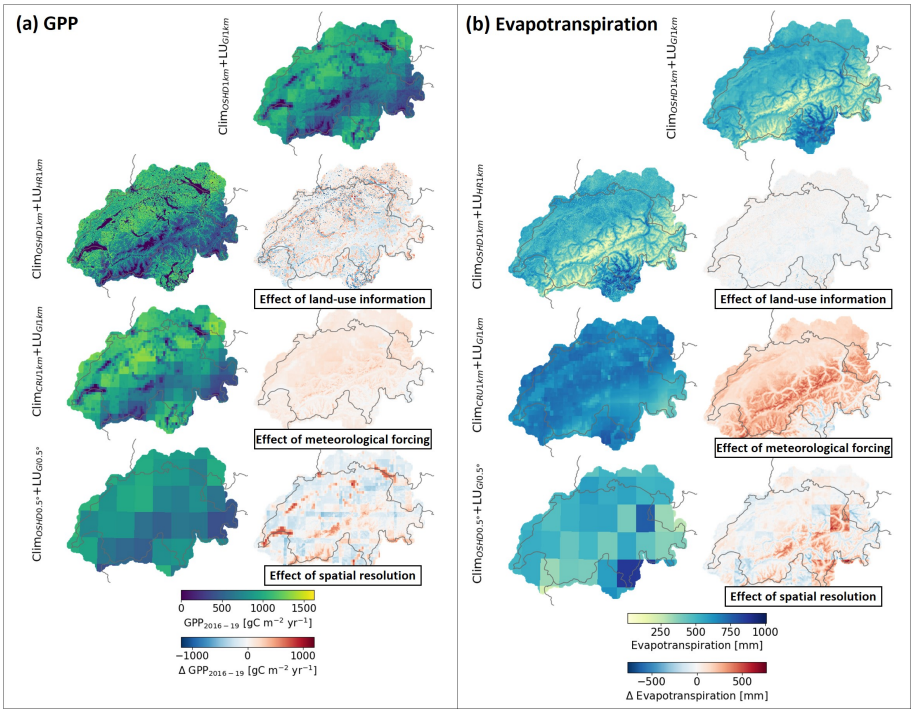

Figure 7. Spatial comparison of CLM5-simulated a) yearly GPP (mean 2016-2019) and b) Evapotranspiration for 4 different CLM5 configurations of this study, showing absolute values as well as relative differences to investigate the effect of land-use information, the effect of climatological forcing and the effect of spatial resolution.

compared with the $Clim_{OSHD1km}+LU_{HR1km}$ simulation (effect of land-use information), with the $Clim_{CRU1km}+LU_{Gl1km}$ (effect of meteorological forcing) as well as with the $Clim_{OSHD0.5°}+LU_{Gl0.5°}$ simulation (effect of spatial resolution). ~~Figures ?? D2 in the Appendix show this relative comparison for all remaining CLM5 model configurations used in this study, while Figure ?? shows monthly values for the full simulation period, averaged over the model domain.~~

For GPP, ~~effects~~ sensitivity of land-use information ~~are pronounced, with a mix of over- underestimations across the model domain. Meteorological forcingdata had a slightly smaller with relative overestimations of GPP throughout~~ outweighed sensitivity of meteorological forcing. Higher level of detail in the land use data caused both increases and decreases in GPP across the model domain~~(up to 14% during peak growing season when averaged over the model domain, see Figure ??). For the coarse-scale runs, we see that non-resolved surface heterogeneity (e.g., lakes) has a large effecton simulated GPP, underlying the effect of resolution~~, while improved meteorological input had a more systematic effect.

The choice of land surface information datasets, on the other hand, only showed marginal effects on simulated ET, but the effect of meteorological forcing results in substantial differences in simulated ET (up to 26% when averaged over the entire model domain~~, see Figure ?? in the Appendix~~). This effect is especially pronounced along the Swiss Alps, where complex terrain leads to differences in precipitation patterns captured by the two forcings (see ~~Figure ?? in the Appendix for a direct~~

Figures C2, C4, C3 in the appendix for comparison of precipitation patterns in the forcing datasets). ~~Similarly to GPP, the effect of~~ Temperature differences between the two forcing datasets further contributed to the differences, as it is precisely along the Swiss Alps where $Clim_{CRU1km}$ does not capture topographic effects on temperature.

For both GPP and ET, model resolution in isolation strongly affects the ~~patterns of simulated ET~~ spatial patterns due to non-resolved surface heterogeneity ~~, but is~~ at coarse resolution. Discrepancies between the simulations are less directional and hence difficult to quantify.

3.4 ~~Seasonal snow cover development and ecophysiological variables~~

~~a-b and c-d: Spatial comparison of differences in CLM5 simulations highlighting the cascading effects of changes in snow cover development to changes in ecophysiological variables. We compare our best-effort reference case ($Clim_{OSHD1km}$+LU_{HR1km}) and $Clim_{CRU1km}$+LU_{HR1km} for 2017 showing a) monthly-averaged GPP in May and June 2017, b) number of days with more than 2cm of snow on the ground between January and July 2017, d) yearly sum of Evapotranspiration between October 2016 and September 2017, and e) yearly cumulative sum of Snow Water Equivalent (SWE) between October 2016 and September 2017 (total positive SWE increments; 'how much water is stored in total'). c) and f) show the correlation between GPP and number of snow days and ET and total SWE for 3 elevation bands (<1000m = yellow, 1000-2000m = blue, >2000m = grey) including regression lines. The dashed red line in c) and f) is the overall regression line. For the residual (scatter) plots, blue (negative) indicates underestimation and red (positive) indicates overestimation with regards to the reference case.~~

~~Substantial differences in simulated snow-cover~~

4 Discussion

This study used CLM5 to offer a multi-scale assessment of the representation of seasonal snow in complex topographic terrain, by evaluating simulated snow depth against a wealth of station data, as well as ~~in simulated ecophysiological variables persist between the various~~ gridded FSM2 simulations. The multi-resolution setup and a suite of model experiments allowed assessment of several aspects (impact of resolution and input datasets), in spatially and temporally resolved manner, while leveraging diverse reference datasets.

Evaluation against station data showed that CLM5 ~~configurations (see Section 3.1 and 3.2, respectively). These demonstrated differences raise the question of the link between these discrepancies, more specifically whether corresponding changes in growing season length arising from differences in simulated snow-cover have substantial impacts on the simulated terrestrial carbon cycle and water budget. Here, we focus on differences between the best-effort simulation (Clim~~itself is capable of achieving performance similar to a dedicated snow model when applied in point mode and with the best available input data (land use info and meteorological forcing; $Clim_{OSHD1km}$+LU_{HR1km}~~) and the~~). Differences to station data are largest at high elevation, where CLM5 ~~configuration with global meteorological forcingdata ($Clim_{CRU1km}$+LU_{HR1km}~~underestimates snow cover. As this bias persists throughout the season, ~~'effect of meteorological forcing data')where large differences in~~

the snow-based evaluation were evident (see Section 3.1), asking whether these differences are correlated with simulation differences in gross primary production and evapotranspiration.

Simulation differences in monthly-averaged GPP during May and June are shown to be negatively correlated with simulation differences in snow duration (number of days with more than 2cm of snow on the ground between January and June, Figure **??**a-c), which becomes apparent when visually comparing spatially explicit differences (Figure **??**a-b): It is evident that locations with lower differences in GPP production coincide with a larger difference in snow duration and vice-versa. This relationship is strong for elevations above 2000m (R2 = 0.74) and relatively strong between 1000 and 2000m (R2 = 0.51). Expectedly, for pixels below 1000m this relationship is less pronounced, which can be attributed to the reduced effect of snow-cover in low elevations. More generally we confirm the hypothesis that seasonal snow cover is important for determining productivity during the growing seasonlength, with a negative correlation between snow and GPP (see Figure **??**).

Shifting from the terrestrial carbon cycle to the water budget, we focus on simulation differences in yearly evapotranspiration (ET) and the total yearly amount of water contained within the snow-pack (snow water equivalent, SWE) to investigate whether differences in ET can be explained by snow on the ground in addition to differences in precipitation input itself. Evapotranspiration differences are shown to be negatively correlated with total SWE differences across all elevationbands (Figure **??**d-f), underlining the importance of snow for quantifying water feedbacks to the atmosphere with it is likely due to a combination of accumulation and internal snowpack properties (e.g. the settling parameterization) and melt processes. Tracking down the exact mechanism would require a process-level comparison beyond the scope of this study, but it should be noted that in FSM2 as set up by OSHD parameters such as the effective roughness length and fresh snow albedo vary spatially (e.g. with elevation); future studies could assess whether such spatially variable parameters could benefit CLM5 snow simulations as well.

A summary statistic of the four discussed variables in this section ($GPP_{MayJune}$, number of snow days, total ET, total SWE) for all Rather than point-mode applications, however, CLM is intended for gridded applications over large areas. This is where our modelling experiments provided interesting insights into the performance of different CLM5 configurations of this study is provided in Figure D3 (Appendix), which underlines that our best-effort reference case ($Clim_{OSHD1km}$+LU_{HR1km}) exhibits a wider spread in simulated $GPP_{MayJune}$ and total ET when compared to remaining CLM5 configuration simulations, which reflects the wider spread of snow-duration. Figure **??** additionally shows summary statistics for $GPP_{JulyAugust}$, which when compared to Figure D3c) ($GPP_{MayJune}$) suggests that snow cover impacts on GPP are mainly visible in the beginning of the growing season, further explaining why $GPP_{MayJune}$ was used here.

5 Discussion

In this study, we used a multi-resolution modeling setup to examine how input data and spatial resolution affect the accuracy of seasonal snow cover simulations and their impact on ecophysiologial variables, with the focus being gross primary production (GPP) and evapotranspiration (ET). Availability of a wealth of snow station data in combination with operational FSM2 results provided a unique opportunity to systematically assess snow cover simulation accuracy across elevations, in a spatially and

temporally explicit manner. configurations. We found that the most accurate snow cover simulations for Switzerland, with results comparable to those of the operational snow-hydrological model (FSM2), were achieved using high-resolution meteorological forcing data (OSHD) and a 1km resolution that fully resolved landscape heterogeneityconfirming our hypothesis1, which aligns with . This confirmed our hypothesis, which stated that with increasing spatial resolution and quality of meteorological and land surface input datasets, the representation of snow cover dynamics and its associated variables in CLM5 can achieve an accuracy comparable to that of a dedicated snow model. These findings align with previous studies (e.g., Lüthi et al. (2019)). Simulation performance

Performance of snow-cover simulations were dictated is thus constrained by the capability of the meteorological input to capture topographic effects (e.g., improved estimation of precipitation phase due to the high resolution temperature fields) and precipitation patterns, which is a function of both input type (e.g., OSHD vs. CRU$Clim_{OSHD}$ vs. $Clim_{CRU}$) and model resolution(. Indeed, the fact that aggregating OSHD-based forcing data for coarser resolution simulations drastically reduced simulation accuracy)evidenced the need for resolutions higher than 0.25°for snow simulations in topographically complex terrain.

We observed a negative correlation between differences in growing season length (quantified as number of snow-free days) and GPP estimates across the model domain, highlighting the significance of accurate snow cover simulations for the carbon budget, and confirming hypothesis 2. The link between snow duration and GPP wasThe lapse-rate corrected results ($Clim_{CRU*}$) suggest that in the absence of native high-resolution input data, increasing model resolution through interpolation of input fields with a simple lapse-rate correction of temperature fields can already account for an important topographic effect and thus positively impact model results. This approach, however, much stronger during the early growing season (May-June), as compared to peak growing season (July-August), suggesting that additional differences between the CLM5 model configurations that happen in the summer period confound the effect of snow alone. Such differences can arise e.g. due to discrepancies in summer precipitation captured by the different meteorological forcings, or because inconsistencies in vegetation parameters derived from different land use datasets result in different magnitudes of ecophysiological processes.

The variations in estimated peak summer GPP between different CLM5 configurations exceeded 200 gC m-2 month-1, equivalent to a 8,810 tC month-1 difference in peak growing season GPP across Switzerland. These differences are noteworthy because errors in simulated GPP can propagate through LSMs and introduce additional errors in simulated biomass and other fluxes (Schaefer et al., 2012). They have substantial implications for climate predictions and underline the challenges that current LSMs face in predicting carbon exchanges (Beer et al., 2010; Zaehle et al., 2014). Our findings regarding GPP modeling uncertainties are consistent with a recent study that showed CLM5 overestimated summer GPP by up to 40% in an arctic boreal environment compared to observational data (Birch et al., 2021). This study emphasizes the importance of regional model analysis and development.

Another crucial variable in linking global water, carbon, and energy cycles in LSMs is ET. ET is important for the water budget, while at the same time being a relevant process for energy balance (e.g., latent heat flux) . We detected large effects of spatial resolution and choice of input data on ET estimates over the model domain, with the choice of meteorological forcing data having the largest effect. Compared to the mountainous, high-elevation areas of Switzerland, increased ET

~~was shown to occur in the low-lands, in line with other studies which showed increased evapotranspiration as temperature increases (Zhao and Dai, 2015; Cheng et al., 2017). As ET is further limited by~~ cannot provide the high-quality precipitation data achieved with data assimilation based techniques (as used in the OSHD forcing). Model errors are thus inherently linked to uncertainty in precipitation input, which can cause both over and underestimations of snow (in the ~~amount of available moisture in the soil, and hence related to precipitation input~~ case of the evaluation at the stations, errors in precipitation (overestimation) overcompensated the underestimation seen in the $Clim_{OSHD}$ simulations for the highest elevation band).

Where model simulations at high resolution are unfeasible (e.g. limited by computational constraints), results from our study suggest that developing a sub-grid parametrization that accounts for the impact of topography on precipitation partitioning as well as ~~to seasonal snow, we compared differences in ET to differences in precipitation input itself, as well as to differences in total snow water. We were able to link differences in simulated ET between model configurations with regards to meteorological forcing datato differences in total snow water, highlighting the importance of rain-snow transitions for ET calculations and further underlining results from Kraft and McNamara (2022). We were, however, not able to directly link differences between model configurations to differences in precipitation input. Significant positive correlation between precipitation and ET has been shown to predominantly occur in dry climates, where ET processes are controlled by water availability in the root zone or shallow surface (Shi et al., 2013), which is not the case in Switzerland. While some previous studies with CLM5~~ on temperature could be a promising approach.

Snow simulations were not sensitive to land-use data, but this is likely due to the distribution of land-units within our model domain, as most snow-dominated grid-cells only saw small changes when moving from the global (LU_{Glc1km}) to the high-resolution land use dataset (LU_{HR1km}). Previous mulit-resolution studies with FSM2 have shown that ~~spatial distribution and interannual variability of ET is captured well in CLM5, when compared to observations (Shi et al., 2013), and despite considerable progress in modelling terrestrial evapotranspiration in recent years, large uncertainties still exist (e.g., Miralles et al. (2016); M). The large differences we find in ET estimates across CLM5 configurations reflect this fact.~~

~~The finding that high resolution simulations improve the accuracy of seasonal snow cover development should thus not be interpreted as the main conclusion of our study. Instead, we have shown how biases in snow cover development can propagate through the model and affect ecophysiological calculations. These findings are underlining local-scale results of e.g., Harpold (2016), which demonstrate the importance of snow-disappearance date for water stress across 62 sites in the Western US. They are further consistent with observations of greening as a result of reduced snow cover in Arctic (Myers-Smith et al., 2020) and Alpine (Rumpf et al., 2022) regions. At the same time, there is evidence that longer growing season is not always associated with increased productivity (Phoenix and Bjerke, 2016), highlighting the relevance of processes beyond the snow season diagnosed in our analysis as well. Our study thus suggests the potential of LSMs applied at high spatial resolutions and fed with accurate input datasets to complement observational studies, as they allow us to quantify and better understand these still poorly constrained process dependencies across larger spatial and temporal extents, including predictions of future conditions~~land-use data does indeed affect simulated snow dynamics (Mazzotti et al., 2021). However, for other ecophysiological variables (GPP in this case) we showed a large effect of land-use data. Today, a plenitude of new detailed land cover datasets are emerging thanks to advances in satellite remote sensing datasets, which should be exploited for land surface modelling.

To gain a more comprehensive understanding, it would be beneficial to repeat such a model experiment in an arctic environment rather than just an alpine one, as high latitudes are critical components of the rapidly changing climate system. Changes in land-use datasets are likely to have a greater effect in such environments, as larger extents of forested areas overlap with seasonally snow-covered areas.

Additionally, it is important to note that all simulations in this work were conducted in satellite phenology mode. Direct assessments of linkages between simulated snow cover and ecophysiological parameters were hence not possible. Future studies should ~~also~~ compare CLM5 simulations with prognostic vegetation and biogeochemistry modes turned on to enable a more detailed analysis of the terrestrial carbon and nitrogen cycles, as well as evapotranspiration fluxes.

Uncertainty remains in ~~LSM projections of climate change~~ climate change impact assessments using LSM projections (e.g., Shrestha et al. (2022); Yuan et al. (2021, 2022)), with two major sources of uncertainty being the effects of resolution and the quality of meteorological input data (especially precipitation, Peters-Lidard et al. (2008)) on LSM simulation outputs. Quantifying such uncertainties is imperative to further increase the predictive power of climate impact models. Furthermore, given the complexity of state-of-the art LSMs, an understanding of the ways different parts/modules of LSMs interact with each other is more important than ever, as climate change impacts are not isolated, but highly interconnected processes (Zscheischler et al., 2018; Ridder et al., 2021). It is therefore of great importance to investigate how exchanges and interactions between model components are represented, rather than assessing process representation for each model component separately (Blyth et al., 2021), which ultimately requires multidisciplinary community efforts (Ciscar et al., 2019). Multi-resolution modelling frameworks as used for this study have large potential to help with such endeavors and provide critical insights into ecosystem responses to environmental change. More specifically, it can help identify both the key processes for which high spatial resolution and high-fidelity input data are necessary, as well as quantify the minimum resolution needed to resolve these processes accurately. Such modelling experiments should be prioritized in the future, ideally in combination with experimental manipulations (e.g., increase the availability of nitrogen or carbon dioxide in the system) as suggested by Wieder et al. (2019).

5 Conclusions

Using multi-resolution modeling experiments to quantify and potentially constrain uncertainties in land surface modeling, we highlight the importance of input data quality and spatial resolution in accurately representing ~~processes~~ seasonal snow cover across scales. ~~By using regionally optimized datasets, we enhance the accuracy and applicability of LSM simulations, enabling a more comprehensive understanding of ecosystem responses to environmental changes. We could demonstrate the accuracy of simulated snow-cover in~~ We found that CLM5 ~~simulations based on high-quality/high resolution~~ is capable of achieving performance similar to a dedicated snow model when using high-resolution meteorological forcing data and ~~with landscape heterogeneity fully resolved at 1km and show how performancedifferences between different CLM5 configurations propagate through the model to result in substantial differences in gross primary production as well as evapotranspiration.~~ a 1km resolution that represented landscape heterogeneity well. Results further showed that a simple lapse-rate correction of temperature fields can already account for an important topographic effect on precipitation partitioning and has large positive

impacts on model performance. Aggregating high-resolution forcing data for coarser resolution simulations drastically reduced simulation accuracy, further underlining the need for resolutions higher than 0.25°for snow simulations in topographically complex terrain. Snow simulations were less sensitive to land-use data compared to meteorological data, but eco-physiological variables (GPP) are strongly affected by the choice of land-use forcing. The results clearly demonstrate the ~~use~~ utility of high spatial resolution and regionally detailed forcings in land surface models to better quantify and constrain the uncertainties in the represented processes, with profound implications for climate impact studies. More generally, this study highlights the utility of multi-resolution modeling experiments which bridge the gap between point-scale and spatially distributed land surface modeling~~when aiming to evaluate and improve process-based representation of variables in land surface models. Comparing process representation accuracy across a hierarchy of spatial scales, while preserving model architecture is therefore recommended for future land surface model developments.~~ .

Code and data availability. All scripts used for simulation setup and analysis can be found at https://github.com/johanna-malle/CLM5_CH. FSM2 snow simulation results can be downloaded from https://www.envidat.ch/dataset/seasonal-snow-data-wy-2016-2022. Upon publication, all CLM5 simulation results presented in this study will be available from the WSL data repository Envidat at their website under https://www.envidat.ch/.

Appendix A: Point-scale CLM5 model simulations at snow stations

Site	Name	Latitude (CH1903)	Longitude (CH1903)	Elevation [m a.s.l.]
BSG	Brissago	108390	698200	280
FRI	Frick	262700	643353	345
ALT	Altdorf	191700	690960	449
CBS	Chaebles	186320	552495	589
ABG	Labergement	178770	527540	645
MAS	Marsens	167220	571440	718
7BR	Brusio	126780	807070	800
DEH	Degersheim	247600	732600	830
SON	Sonogno	134050	703640	925
WHA	Wildhaus	229570	746130	1000
APT	Alpthal	212930	696860	1031
AIR	Airolo	153400	688910	1139
1LC	LaComballaz	136580	572640	1360
4MS	Muenster	148900	663420	1410
7ZN	Zernez	175259	802751	1475
5DF	DavosFluelastr	187400	783800	1560
6SB	SanBernardino	147290	734110	1640
YBR2	Ybrig	210311	705399	1701
7ZU	Zuoz	164590	793350	1710
7SD	Samedan	156400	786210	1750
ARO	Arosa	183320	770730	1840
LAU2	LauenenTruettlisbergpass	141633	595482	1970
VLS2	ValsAlpCalasa	170764	735166	2064
OBM2	OberMeielGrossStand	141183	582760	2097
FRA2	FrascoEfra	132853	708906	2100
VAL2	VallasciaSchneestation	155980	690126	2268
CMA2	CrapMasegnSchneestation	189875	733050	2330
OFE2	OfenpassMurtaroel	168460	818233	2359
JUL2	JulierVairana	149949	773049	2426
DAV3	DavosHanengretji	184616	778292	2455
TRU2	TrubelbodenSchneestation	135519	611306	2459
5WJ	Weissfluhjoch	189230	780845	2540
DAV2	DavosBaerentaelli	174726	782062	2558
ZNZ2	ZernezPuelschezza	175078	797312	2677
LAG2	PizLagrevSchneestation	147050	777150	2730
GOR2	GornergratSchneestation	92900	626700	2950

Table A1. Name, location and elevation of all snow station locations used in this study.

Appendix B: Land-use information data sets

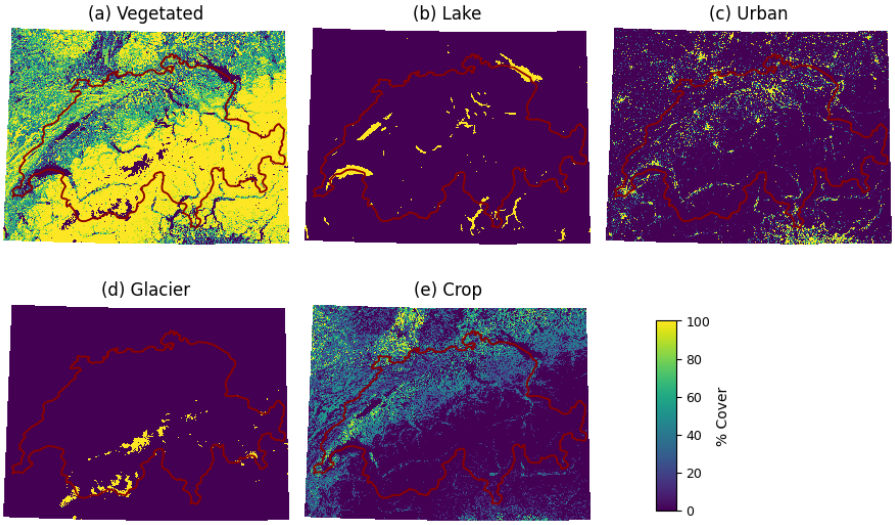

Figure B1. ~~a-c feature wiggle plots, which visualize the absolute difference in snow depth between observations and FSM2, CLM5 $Clim_{OSHD1km}$+LU_{HR1km}, CLM5 $Clim_{CRU*1km}$+LU_{HR1km} and CLM5 $Clim_{CRU1km}$+LU_{HR1km} simulations,~~ Land unit distribution per grid cell for ~~a selection of stations at elevations lower than 1000m (a), between 1000m and 2000m (b) and above 2000m (c). It is apparent across all elevation bands that FSM2 simulations match observations~~ the ~~closest, and that CLM5 forced with 1km OSHD data and based on a~~ high-resolution 1km land ~~surface~~ use dataset ~~is the next best. CLM5 with global meteorological forcing data~~ ($Clim_{CRU1km}$+LU_{HR1km}) ~~performs poorly with regards to modelling seasonal snow development, with maximal errors of over 3m, but model performance is improved when using the down-scaled global meteorological dataset to obtain meteorological input data ($Clim_{CRU*1km}$+LU_{HR1km}) with particularly dramatic improvements at low elevations. d-f each focus on one station and show the absolute difference to observations~~ as ~~well as seasonal snow depth development of the respective model runs~~used in this study. ~~In addition to the 3~~ The 5 CLM5 ~~configurations shown in a-c, in the first row of d-f, we also show CLM5 $Clim_{OSHD1km}$, $Clim_{CRU*1km}$ and $Clim_{CRU1km}$ with global~~ land ~~surface information (LU_{GI1km}). For these 3 selected examples, the HighRes case performs better for the low and high station location all 3 shown station locations, whereas the global case shows slightly better performance during the melt period for the mid-elevation station. Ultimately, it can be seen though that the effect of meteorological forcing data is substantially larger in comparison~~ units sum up to ~~differences arising from the choice of land surface information~~exactly 100%.

Appendix C: ~~Point-scale CLM5 validation at FLUXNET stations~~

~~The FLUXNET network (, Pastorello et al. (2020)) provides observations of ecosystem carbon, water, and energy fluxes at sites across the globe. A total of 6 FLUXNET site locations fall within our model domain and overlap with our modeling timespan,~~
720 ~~including a mixed forest, a coniferous forest, alpine and lowland grasslands as well as a crop site. This analysis is placed in the supplementary material since 4 out of the 6 FLUXNET station locations were lower than 1000m in elevation, and hence not~~

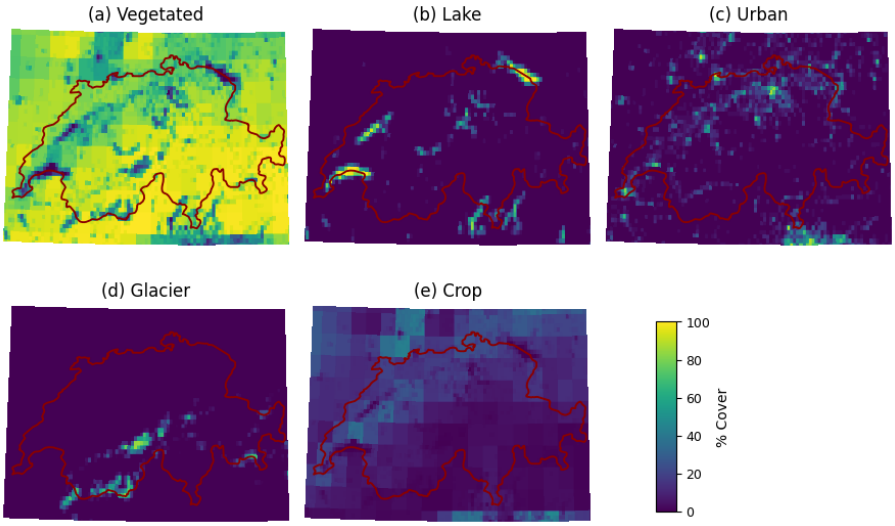

Figure B2. Land unit distribution per grid cell for the global 1km land use dataset ($LU_{Glu_{km}}$) as used in this study. The 5 CLM5 land units sum up to exactly 100%.

~~within the nival zone, preventing an extensive investigation of the link between snow cover and ecophysiological parameters at these locations. Additionally, the sensor fetch of the 35m high CH-Dav as well as the CH-Lae station towers integrates a large, heterogeneous area in complex terrain (e.g. including houses etc. for the CH-Dav site) with highly variable winds depending on the time of the day. Nevertheless we believe this analysis might still be of interest to some readers, as it validates our PTCLM simulations from a ecophysiological perspective.~~

~~Details on the sites, including information on how the prevalent vegetation types translated into CLM5 plant functional types can be found in Table **??**. Observational data for the FLUXNET tower locations were acquired from the European research infrastructure Integrated Carbon Observation System (ICOS) data product (Team and Centre, 2022), and consists of standardized observations at half-hourly temporal resolution. Gaps in the data were filled and data was quality controlled according to the FLUXNET data processing protocol (Pastorello et al., 2020). We focus on the effects of spatial resolution and~~

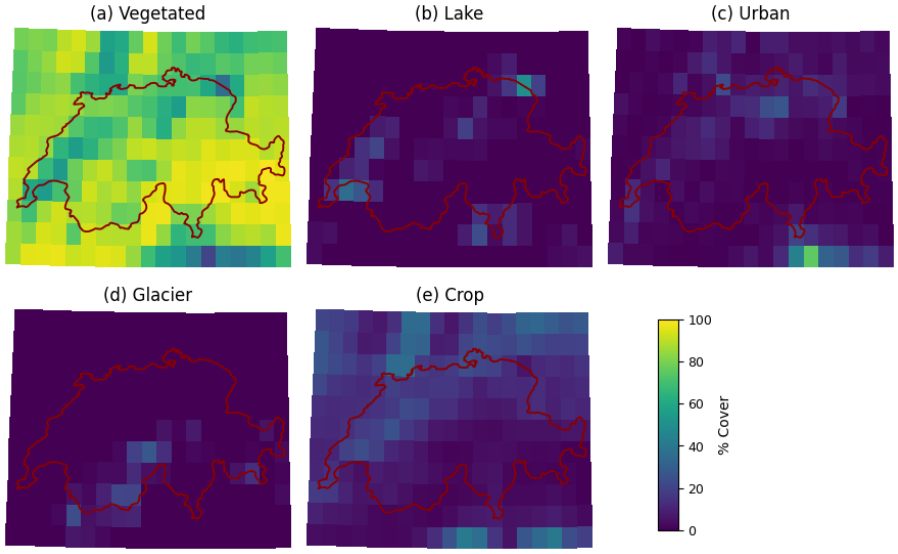

Figure B1. Land unit distribution per grid cell for the global 0.25° land use dataset ($LU_{GJ0.25°}$) as used in this study. The 5 CLM5 land units sum up to exactly 100%.

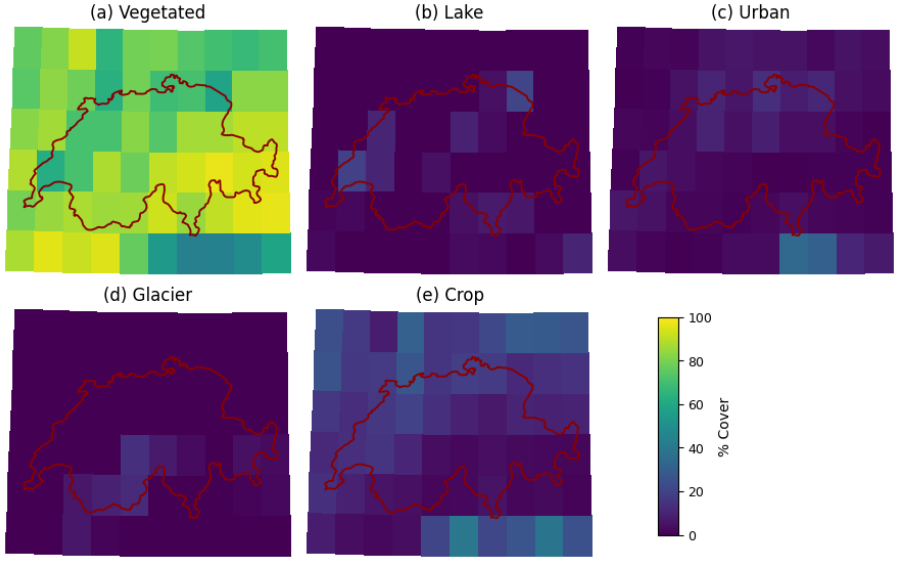

Figure B2. Land unit distribution per grid cell for the global 0.5° land use dataset ($LU_{GJ0.5°}$) as used in this study. The 5 CLM5 land units sum up to exactly 100%.

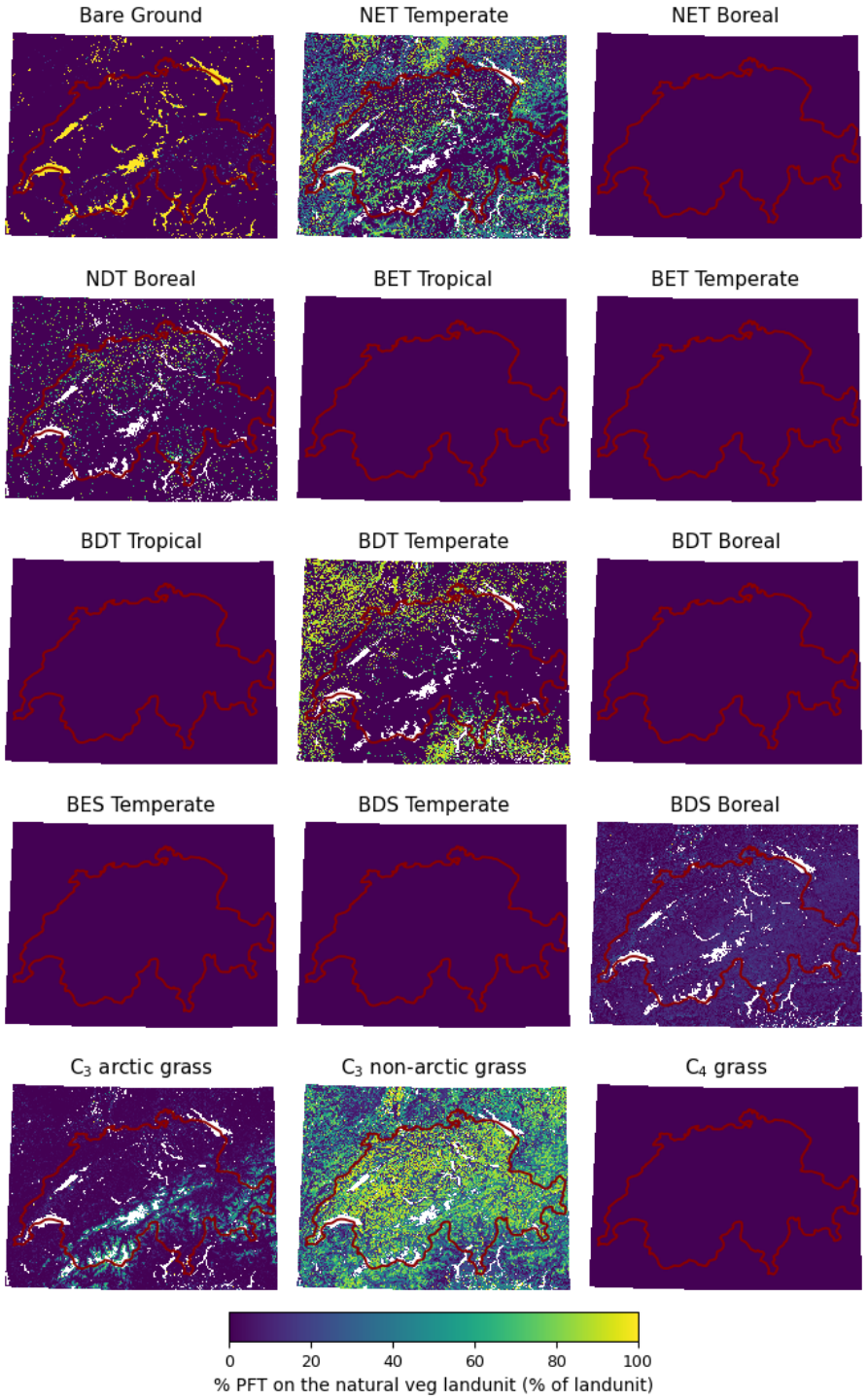

Figure B3. Patch-level Plant Functional Types (PFT) distributions for the high-resolution 1km land use dataset (LU_{HR1km}) as used in this study.

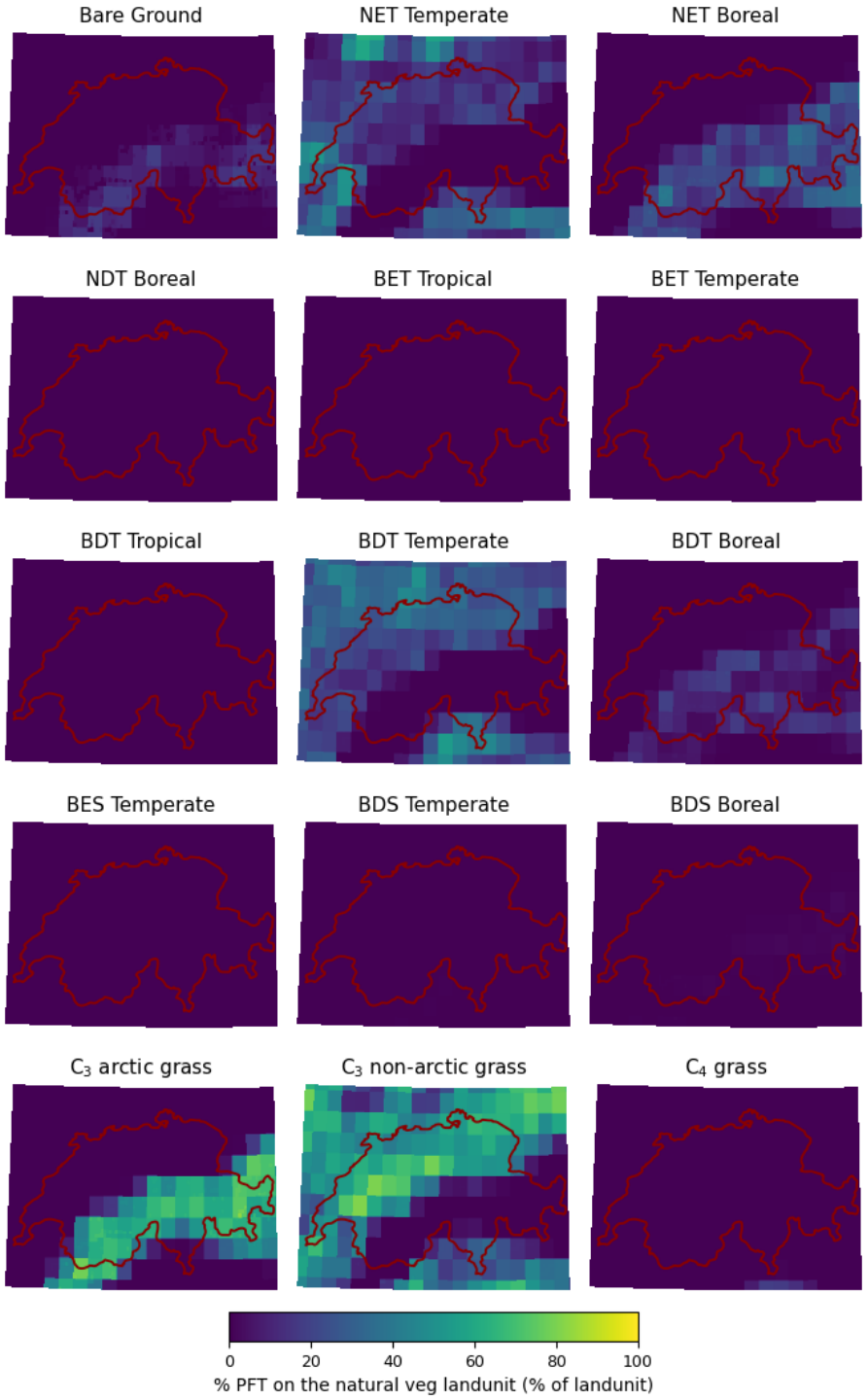

Figure B4. Patch-level Plant Functional Types (PFT) distributions for the global 1km land use dataset (LU_{Gl1km}) as used in this study.

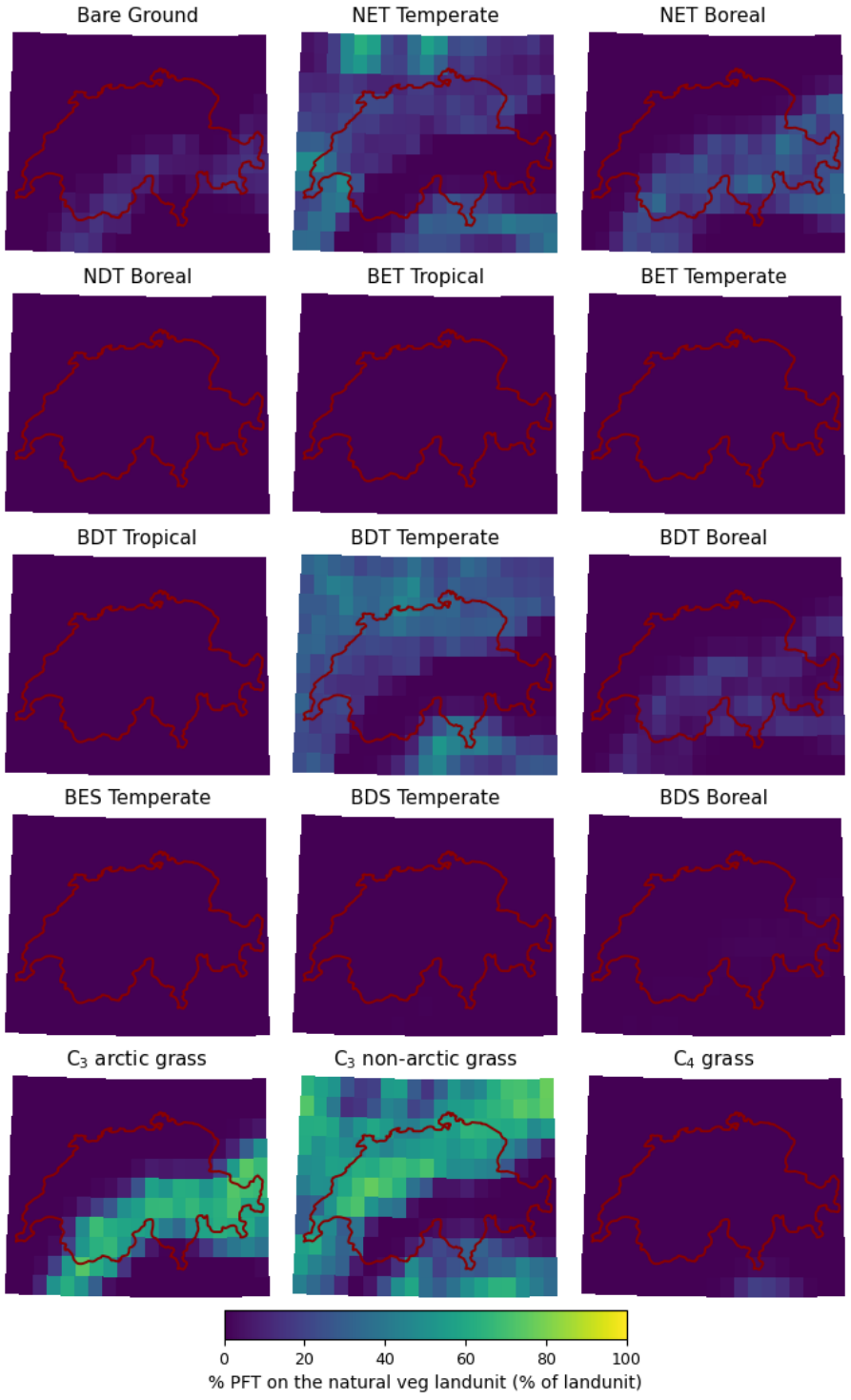

Figure B5. Patch-level Plant Functional Types (PFT) distributions for the global 0.25° land use dataset ($LU_{Gl0.25°}$) as used in this study.

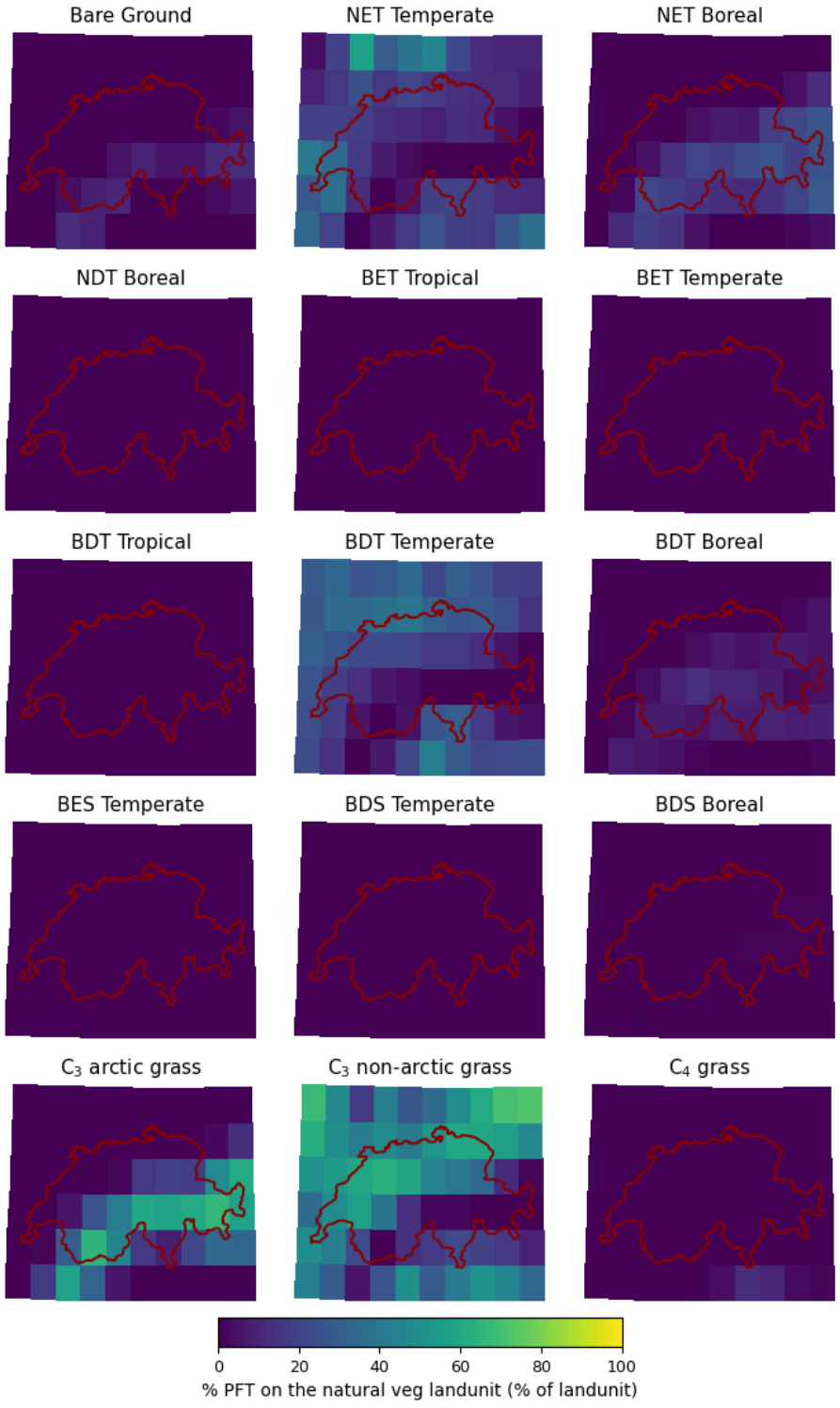

Figure B6. Patch-level Plant Functional Types (PFT) distributions for the global 0.5° land use dataset ($LU_{GI0.5°}$) as used in this study.

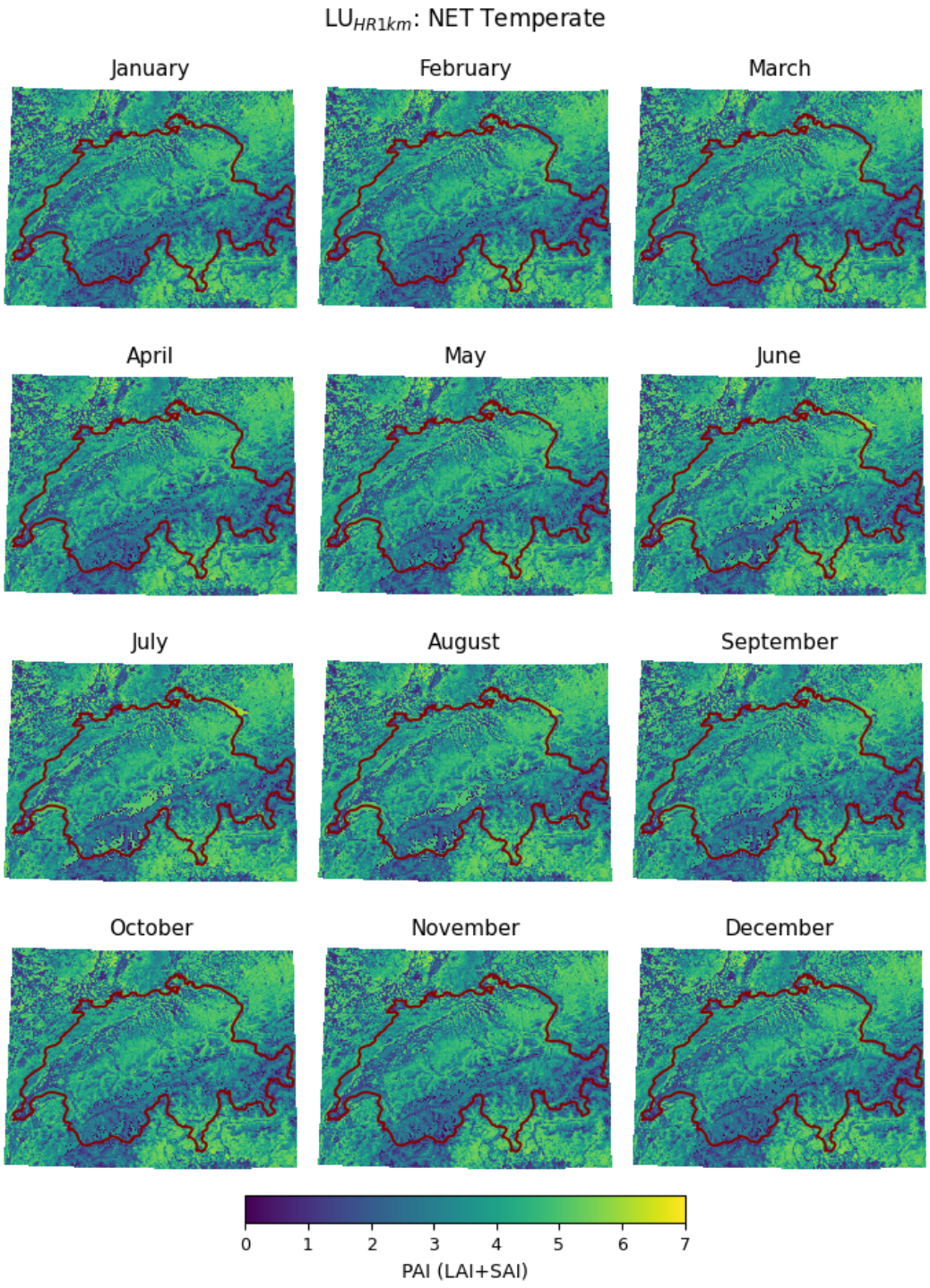

Figure B7. Monthly Plant Area Index (PAI) for temperate needle leaf evergreen trees for the high-resolution 1km land use dataset (LU_{HR1km}) as used in this study.

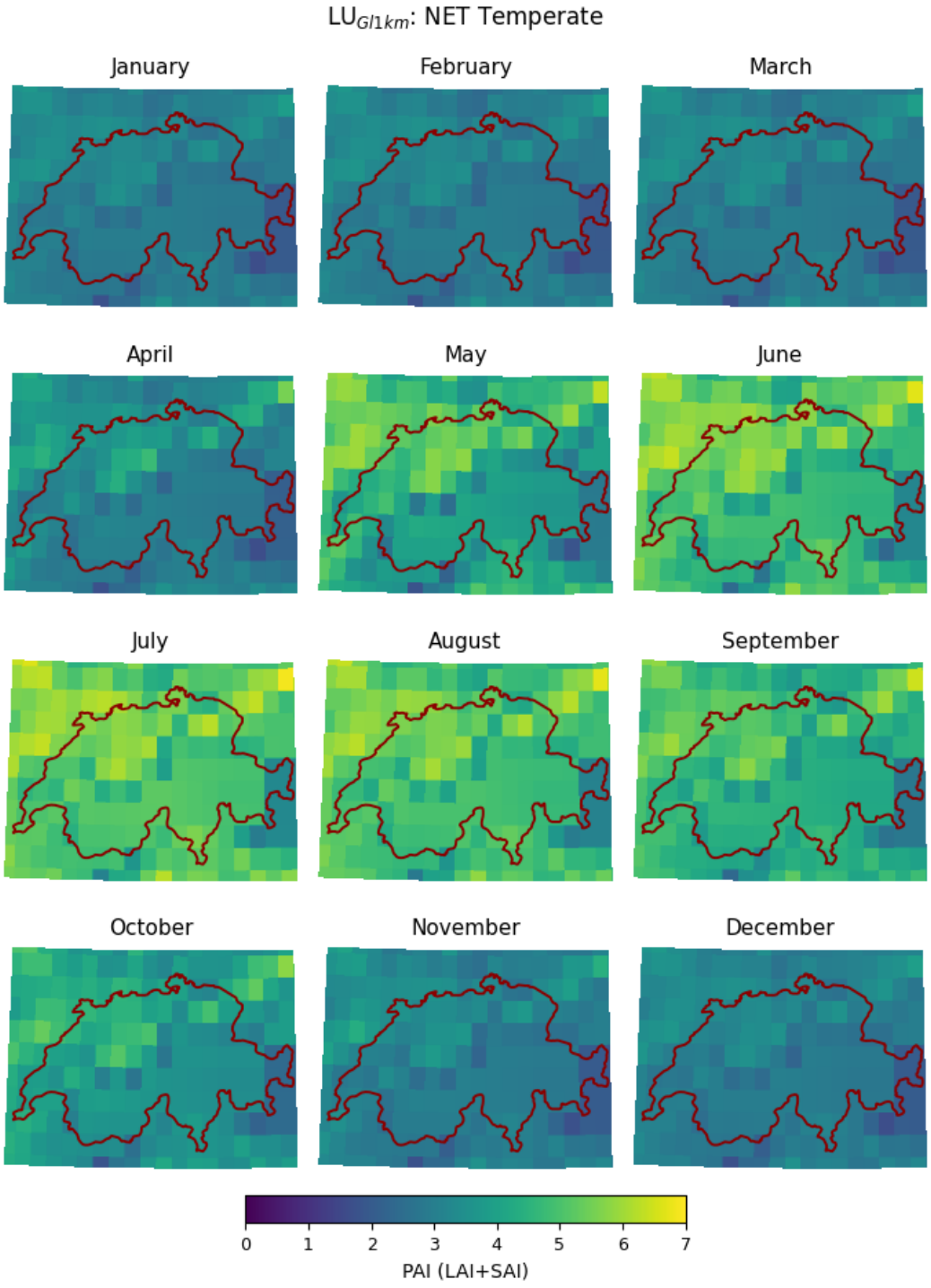

Figure B8. Monthly Plant Area Index (PAI) for temperate needle leaf evergreen trees for the global 1km land use dataset (LU$_{Gl1km}$) as used in this study.

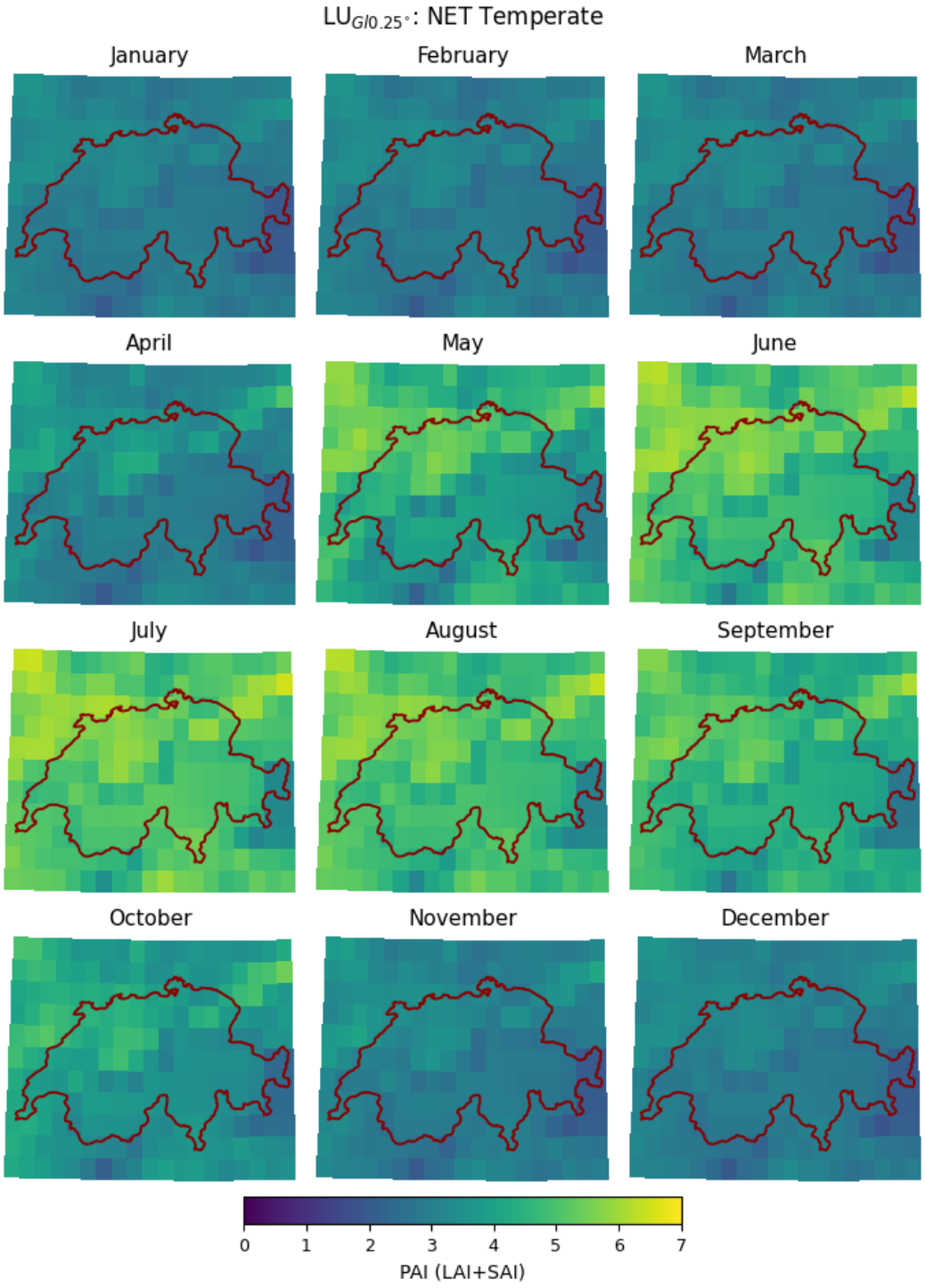

Figure B9. Monthly Plant Area Index (PAI) for temperate needle leaf evergreen trees for the global 0.25° land use dataset (LU$_{Gl0.25°}$) as used in this study.

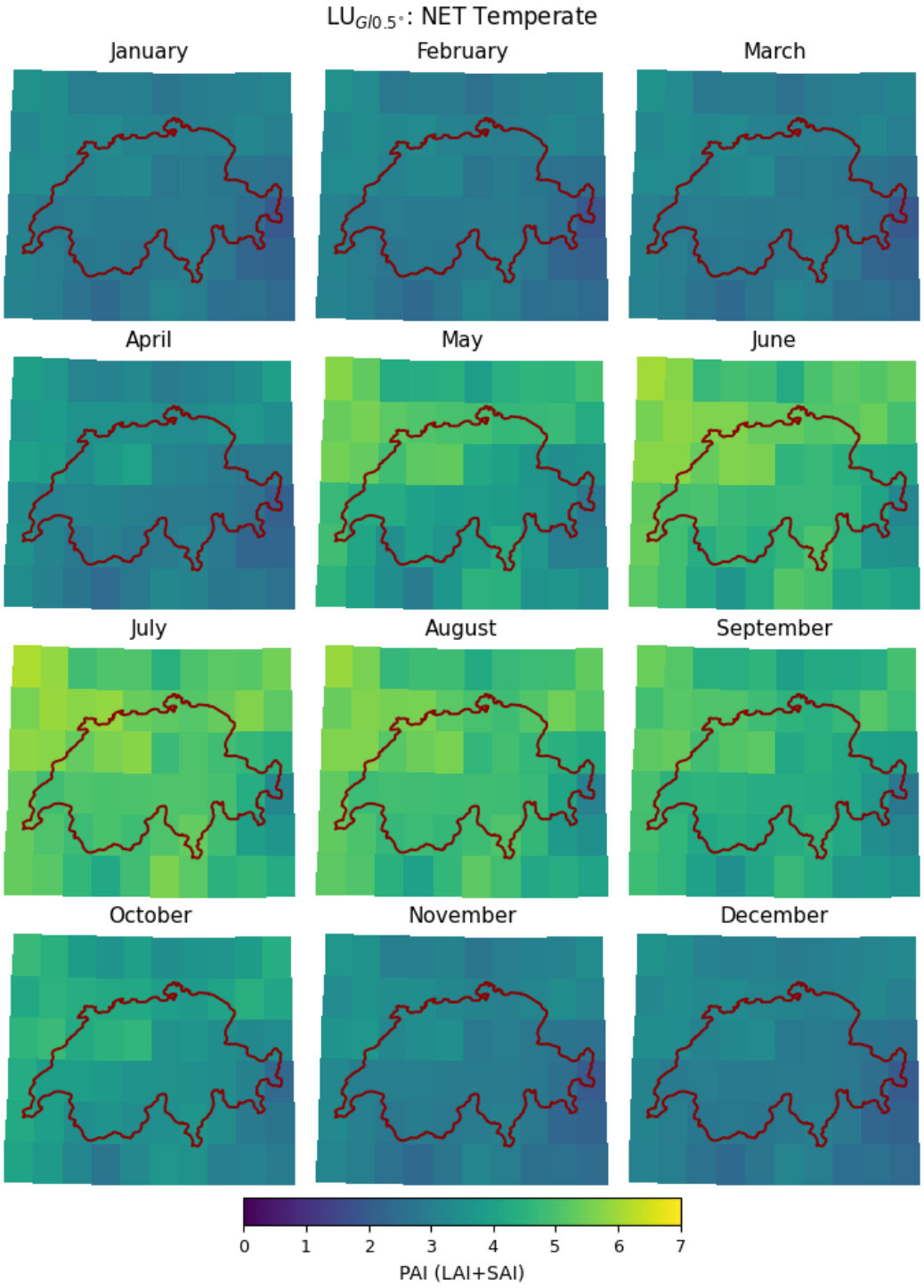

Figure B10. Monthly Plant Area Index (PAI) for temperate needle leaf evergreen trees for the global 0.5° land use dataset (LU$_{Gl0.5°}$) as used in this study.

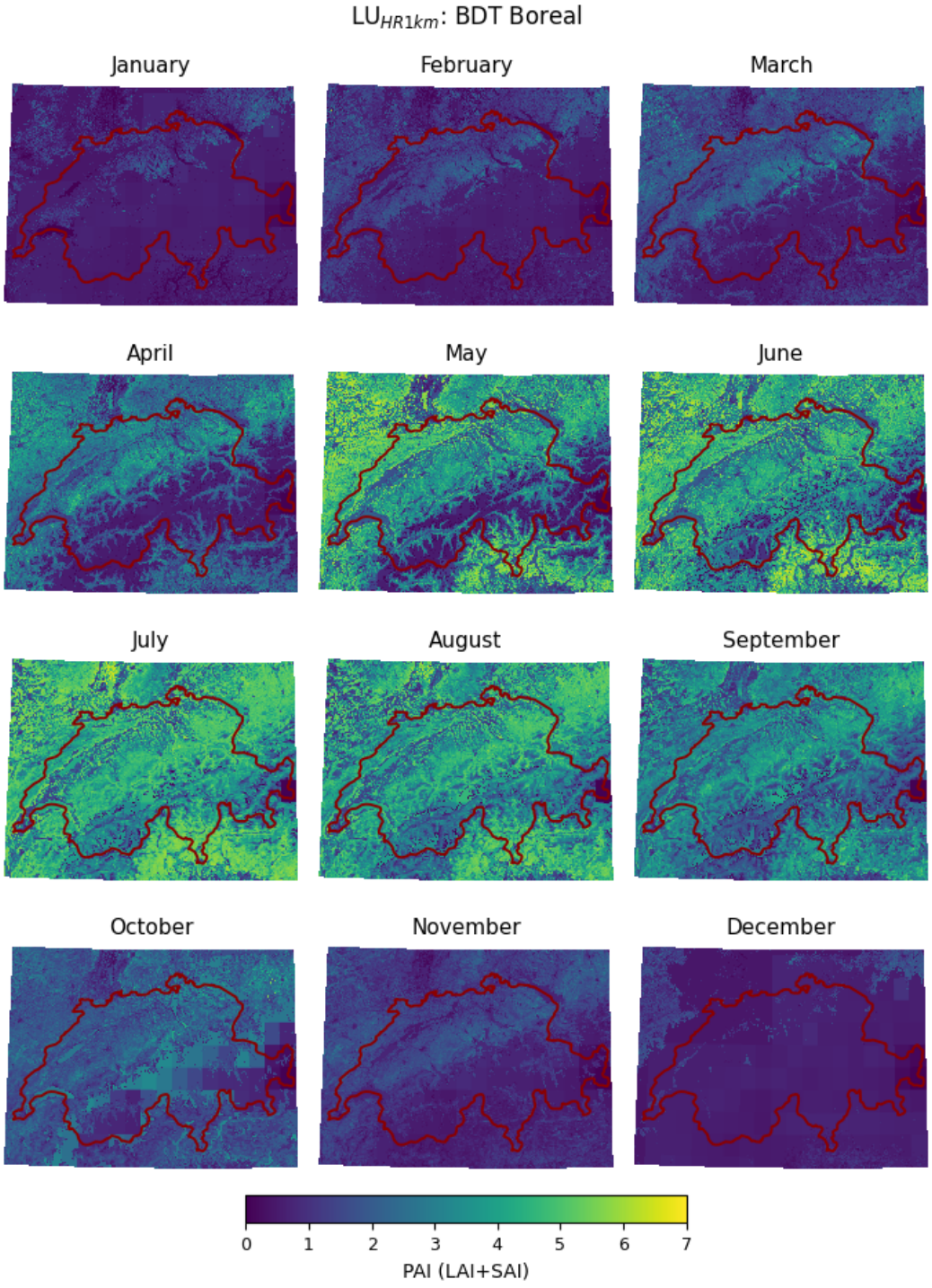

Figure B11. Monthly Plant Area Index (PAI) for boreal broad-leaf deciduous trees for the high-resolution 1km land use dataset (LU_{HR1km}) as used in this study.

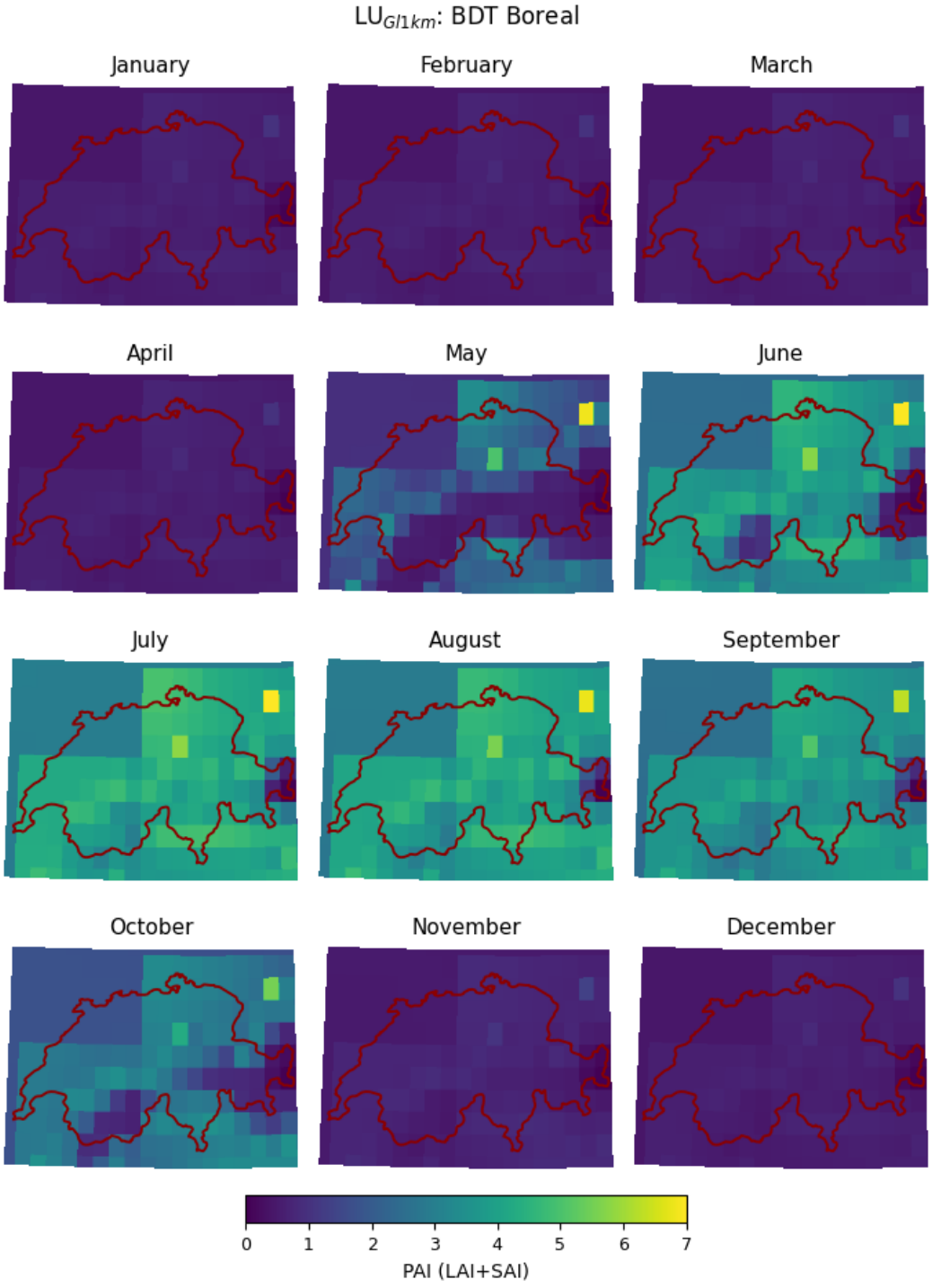

Figure B12. Monthly Plant Area Index (PAI) for boreal broad-leaf deciduous trees for the global 1km land use dataset (LU$_{Gl1km}$) as used in this study.

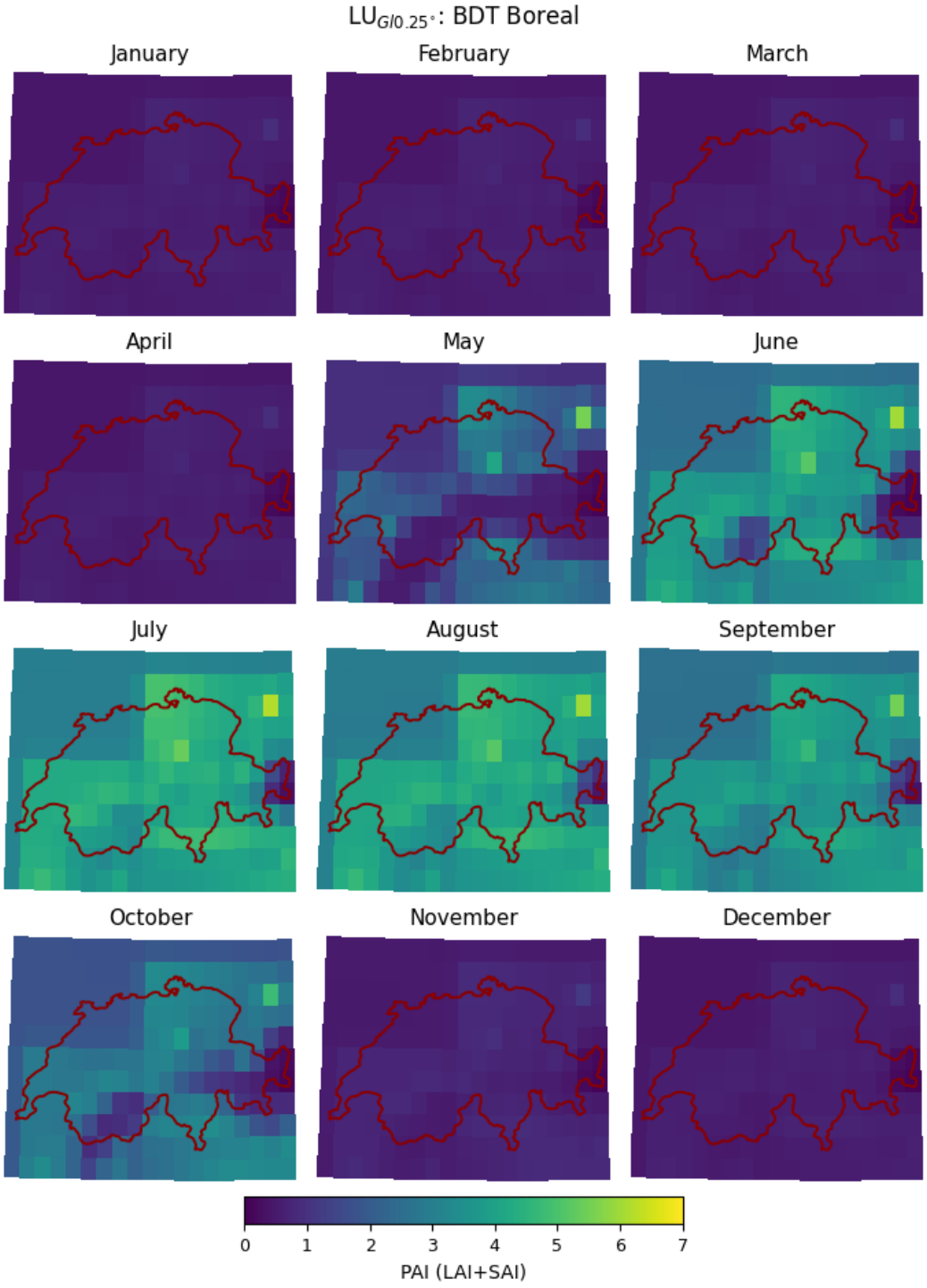

Figure B13. Monthly Plant Area Index (PAI) for boreal broad-leaf deciduous trees for the global 0.25° land use dataset (LU$_{Gl0.25°}$) as used in this study.

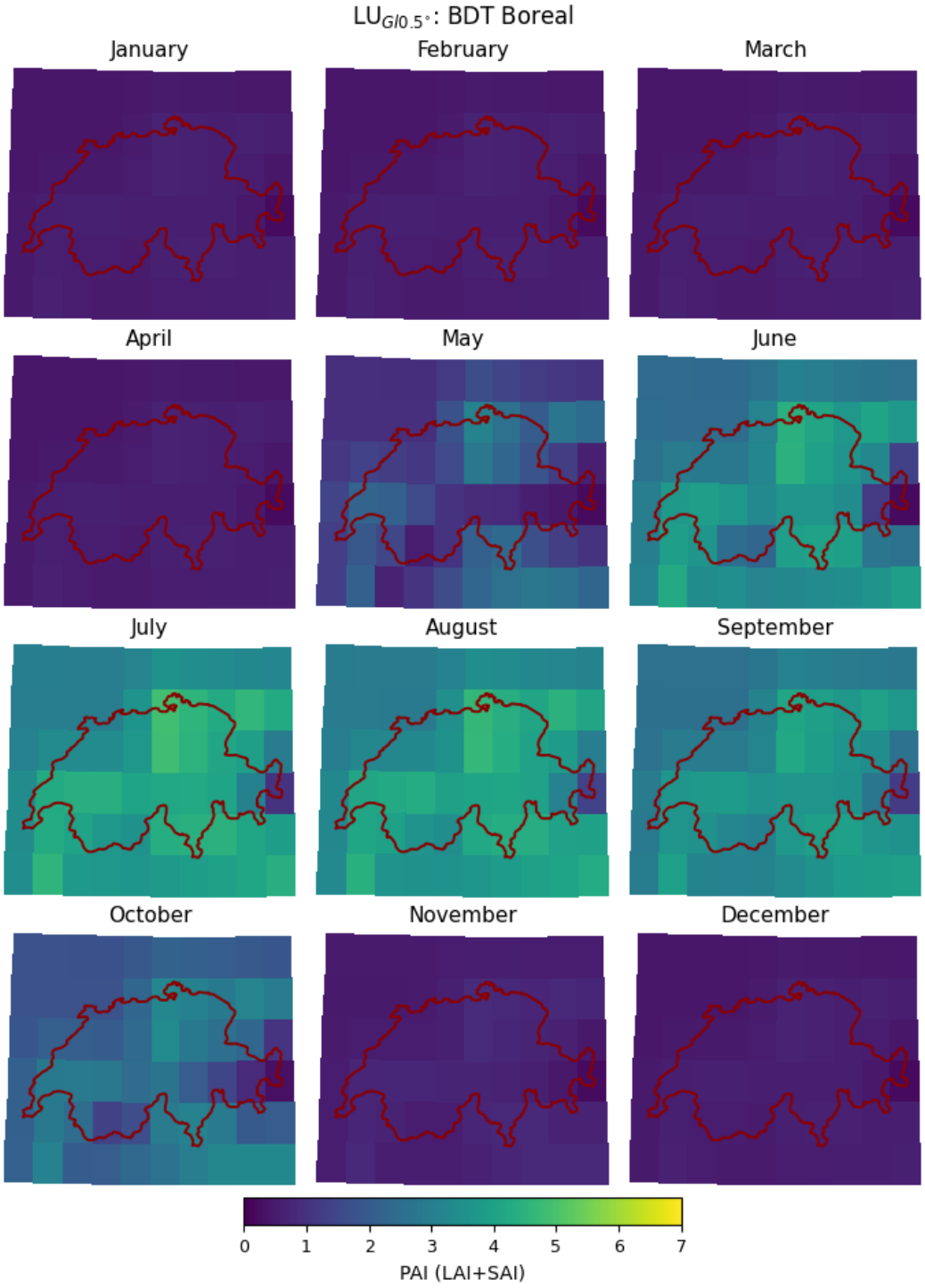

Figure B14. Monthly Plant Area Index (PAI) for boreal broad-leaf deciduous trees for the global 0.5° land use dataset (LU$_{Gl0.5°}$) as used in this study.

Appendix C: Meteorological forcing data

This section shows supporting information regarding the meteorological forcing data ~~as we compare CLM5 simulations forced with 0.5and 1km of $Clim_{CRU}$, $Clim_{CRU*}$, and $Clim_{OSHD}$~~ presented in the main part of the manuscript. First, we show the two DEMs used for lapse rate calculation in this study. We further show differences in yearly and monthly precipitation for the OSHD-based and CRU-based dataset, as well as differences in monthly temperatures between the OSHD-based, the CRU-based and the CRU* datset.

~~Name, Location, site characteristics and the selected CLM5 plant functional type for each FLUXNET site used for model performance evaluation.~~

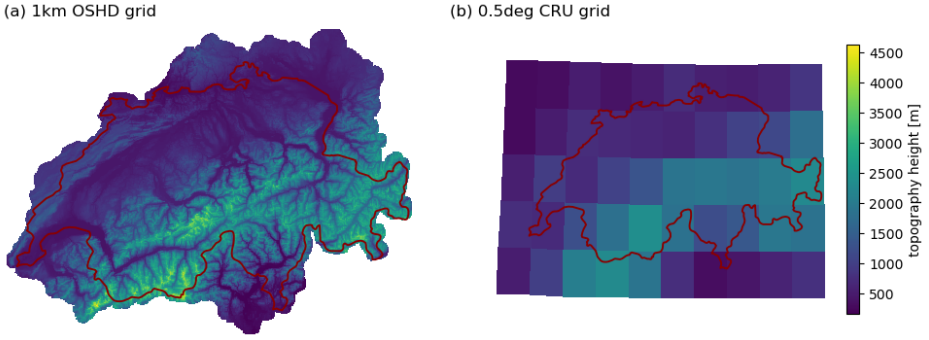

Figure C1. Comparison of digital elevation model (DEM) at (a) 1km and (b) 0.5° as used for lapse rate correction in this study.

~~The FLUXNET tower sites were used to evaluate the performance of the various CLM5 configurations regarding evapotranspiration (latent heat flux) and ecosystem carbon balance (gross primary production). For each FLUXNET site in Switzerland, we used the absolute error over all time-steps between observations and CLM5 simulations for (a) latent heat flux (LH), and (b) gross primary production (GPP). Additionally, we perform a one-way analysis of variance (ANOVA) to test for differences in absolute error between simulation results using different spatial resolution forcings. To test for the significance in differences in absolute errors we further performed a Tukey's Honestly Significant Difference (HSD) post-hoc test (Abdi and Williams, 2010) for each FLUXNET location. Additionally, in order to investigate significance across all sites we fitted a linear mixed effects model (Bates et al., 2015) with absolute error of either LH or GPP as a response and the tower site location as random effects.~~

~~Generally, performance differences between the various CLM5 simulations are small (Figure **??**), especially when compared to the pronounced effects for the snow-cover development shown in Figure 2 in the main manuscript. However, an ANOVA reported p-values <0.001 for LH and GPP at all sites, revealing significant differences in performance (absolute error) means between CLM5 configurations. A Tukey post-hoc test confirmed this (Figure **??**).~~

~~For LH, we see small improvements when using OSHD-based input data at five out of the six locations, while at CH-Cha a marginal decrease in performance when using $Clim_{OSHD}$ compared to $Clim_{CRU}$ is noticeable (Figure **??**). However, a linear mixed effects model to assess performance differences between the different CLM5 simulations revealed a significant increase~~

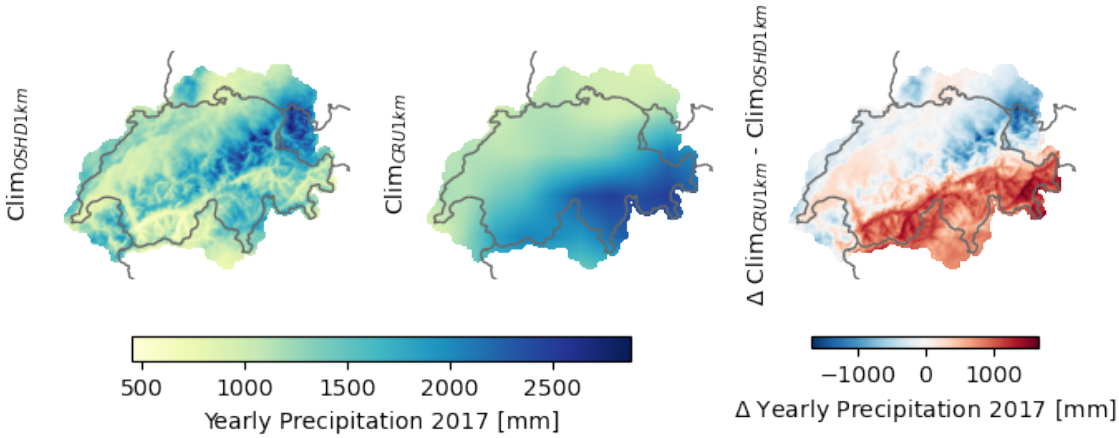

Figure C2. Total yearly precipitation input for the year 2017: OSHD-based, CRUJRA-based and a differential plot.

~~in performance with regards to latent heat flux when moving from Clim$_{CRU}$ over Clim$_{CRU*}$ to Clim$_{OSHD}$ (plot below boxplot in Figure ??a), whereby performance was further slightly enhanced when using 1km rather than 0.5forcing data (effect of resolution). Error in GPP simulations showed little variation with the different resolutions and meteorological input datasets, including overlapping extents of the confidence intervals between the different configurations.~~

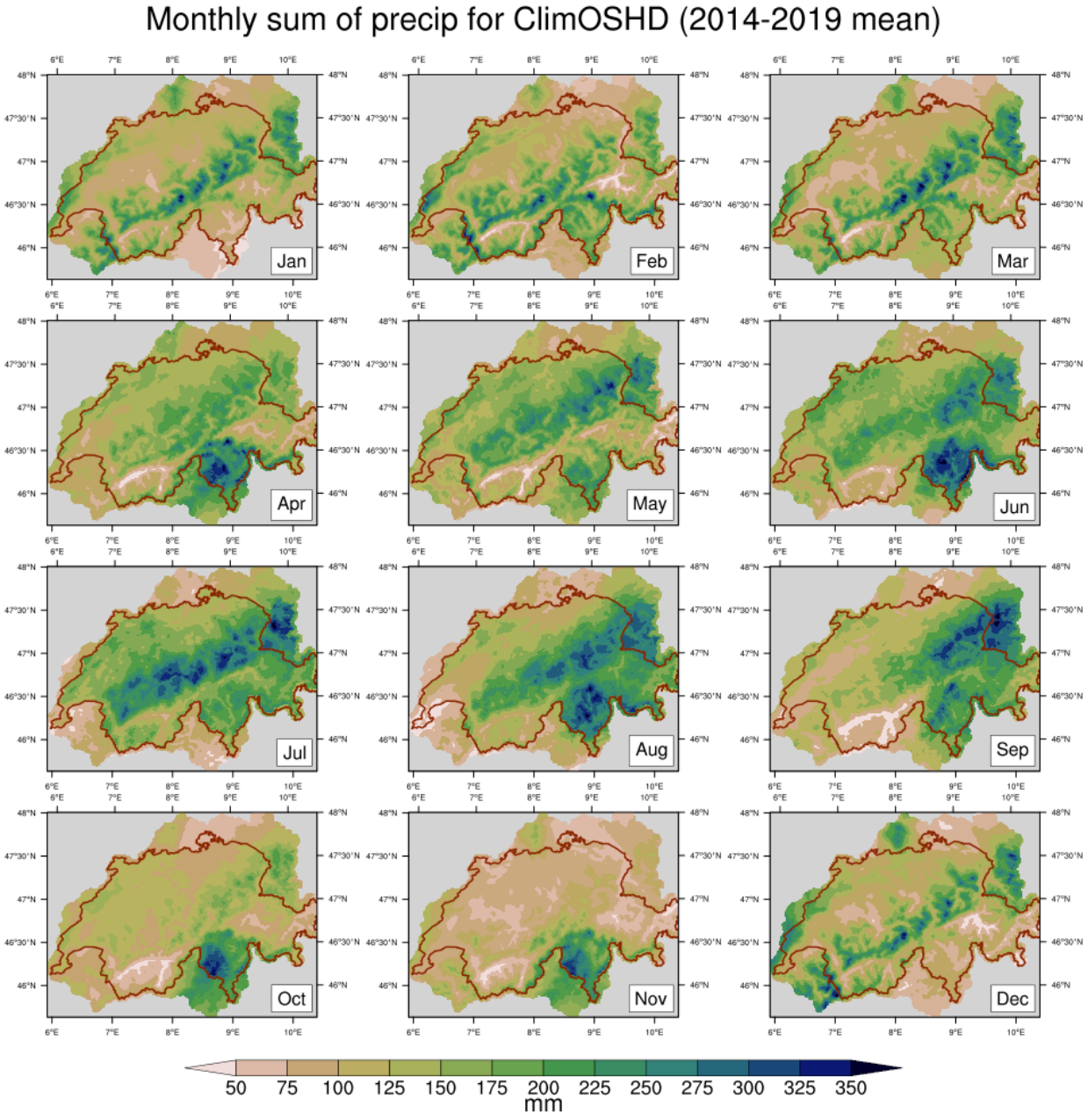

Figure C3. ~~Direct comparisons of FLUXNET observations~~ Total monthly precipitation input as averaged between 2014 and ~~CLM5 simulations of (a) latent heat flux and (b) gross primary production at six tower locations within Switzerland (see Table ??~~ 2019 for ~~details on~~ the ~~respective sites)~~ClimOSHD forcing dataset.~~Gray lines in the boxplots indicate median error, while mean error is shown with white dots. Plots below the boxplots show the coefficient estimates of a linear mixed effects model with absolute error as response, the various CLM5 configurations ($Clim_{CRU0.5°}$, $Clim_{CRU1km}$, $Clim_{CRU*0.5°}$, $Clim_{CRU*1km}$, $Clim_{OSHD0.5°}$ $Clim_{OSHD1km}$) as predictor, and the site location (CH-Aws, CH-Cha, CH-Dav, CH-Fru, CH-Lae, CH-Oe2) as random effects. Coefficients are in relation to the performance of $Clim_{CRU0.5°}$, whereby negative values indicate an increase in performance and positive values indicate a decrease in performance. Extent of lines indicates the confidence interval (with a likelihood of 95%).~~

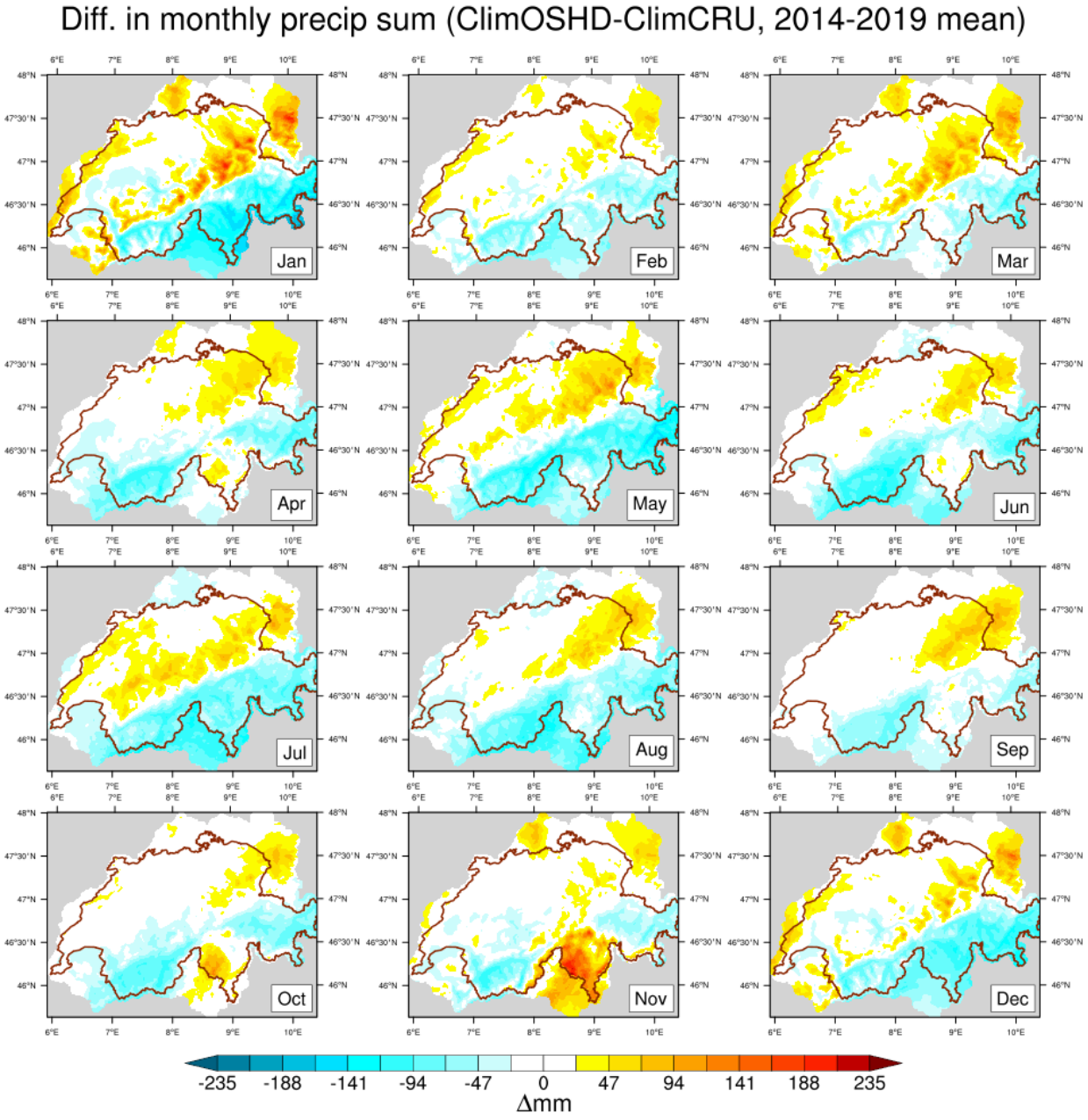

Figure C4. ~~The ANOVA reported p-values <0.001 for latent heat as well as for gross primary production, indicating differences~~ Differences in total monthly precipitation input between the ~~CLM5 simulations, hence a Tukey's post-hoc test was performed to investigate more into the differences. Tukey's post-hoc test results: Multiple comparisons at all 6 FLUXNET sites between different CLM5 configurations. Here we focus the comparison of the $Clim_{OSHD1km}$ configuration ('best-case' after the snow-evaluation) to all remaining ones ('effect of meteorological forcing'). We show absolute differences to observations (FLUXNET towers) across all time-steps for (a) latent heat~~ ClimOSHD and ~~(b) gross primary production. Dots indicate mean absolute errors and extents of each line show~~ the ~~confidence intervals (95%); any overlaps indicate a non-significant difference between CLM5 simulations (grey/black dots and lines). Green indicates a significant improvement when using OSHD-based~~ ClimCRU forcing ~~data, red indicates a worsening in performance~~dataset.~~Plots with only black indicate a non-significant difference in performance between OSHD-based and CRU-based CLM5 simulations.~~

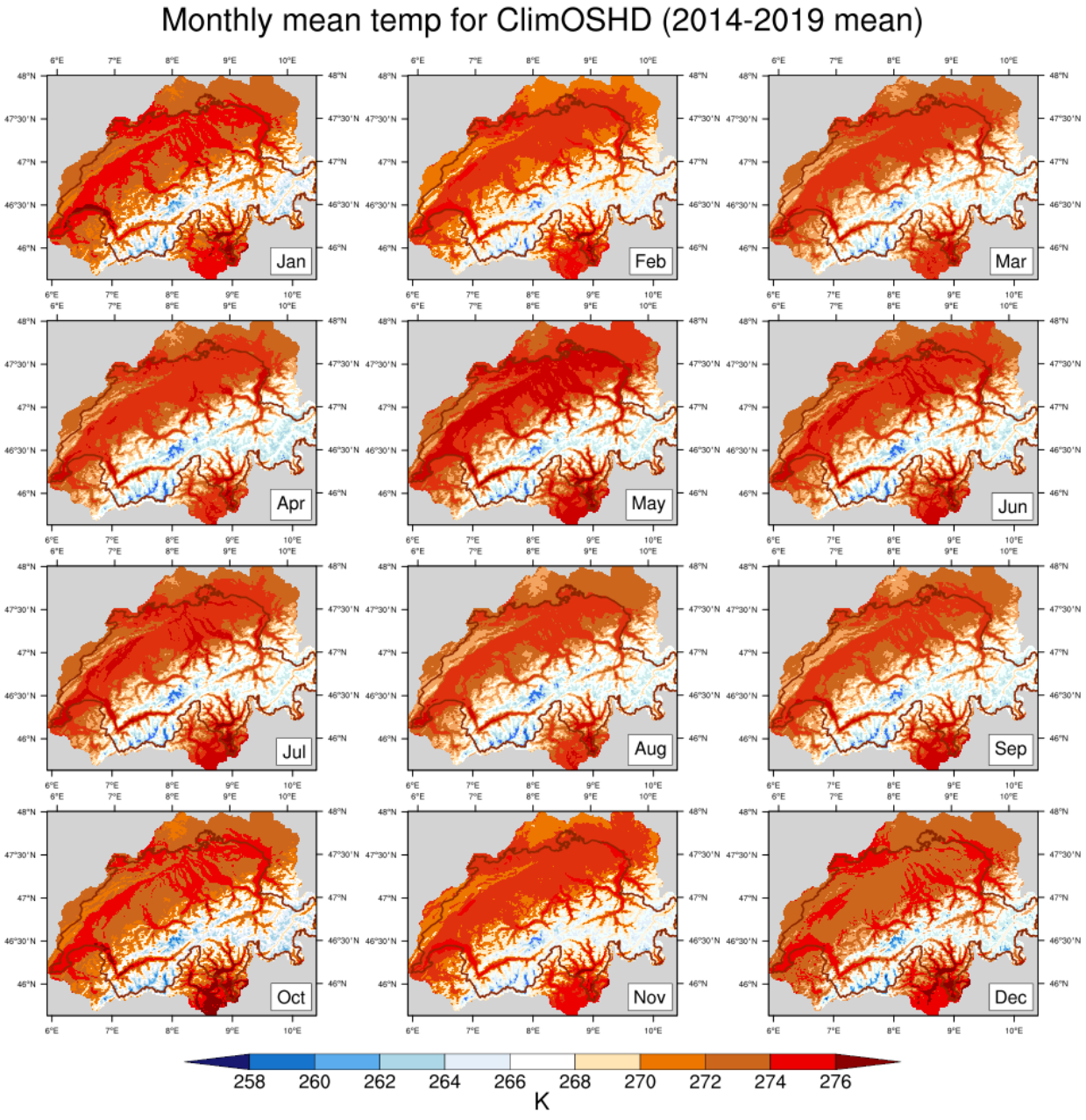

Figure C5. Mean monthly temperatures for the ClimOSHD forcing dataset.

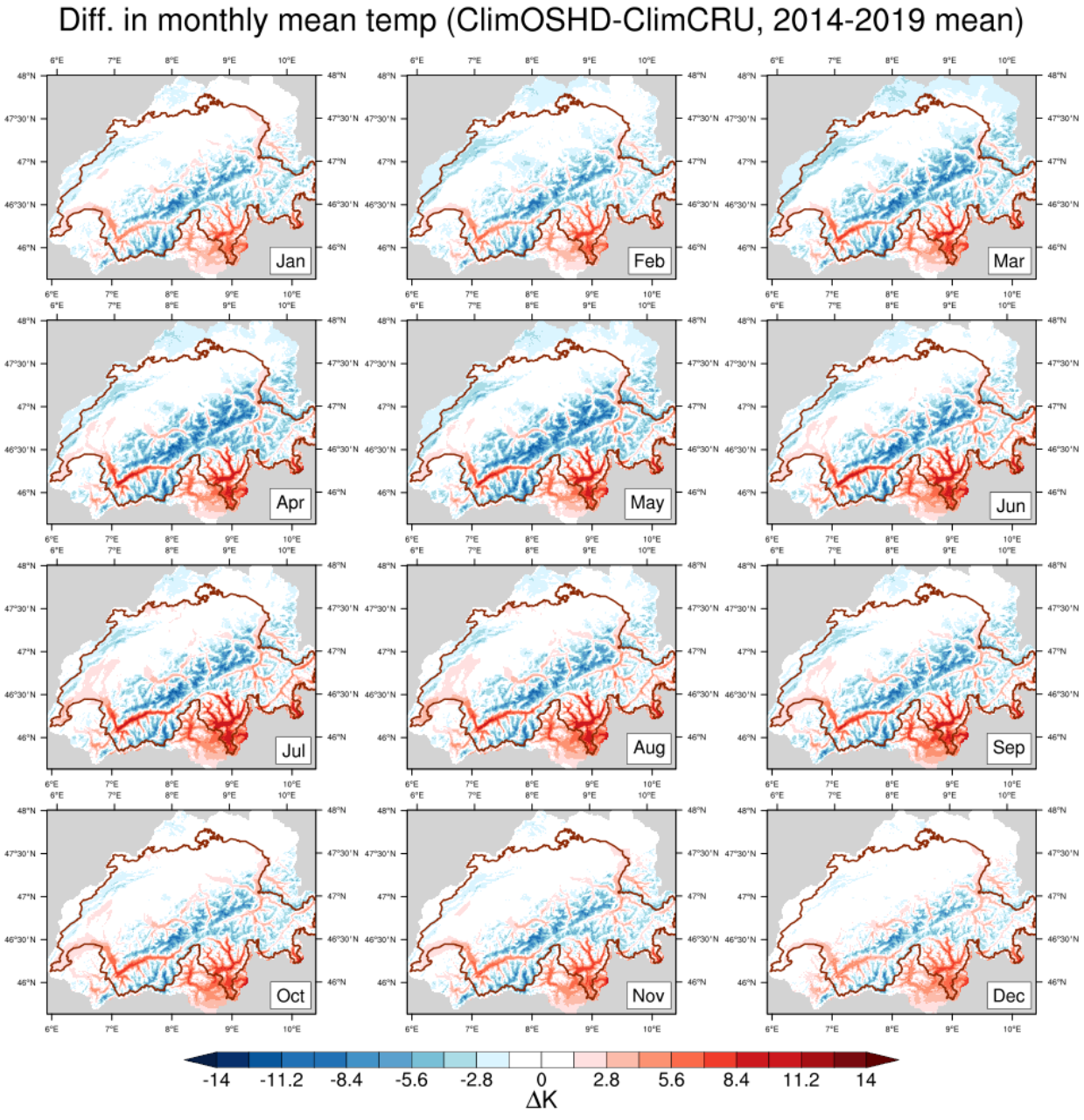

Figure C6. Differences in mean monthly temperatures between the ClimOSHD and the ClimCRU forcing dataset.

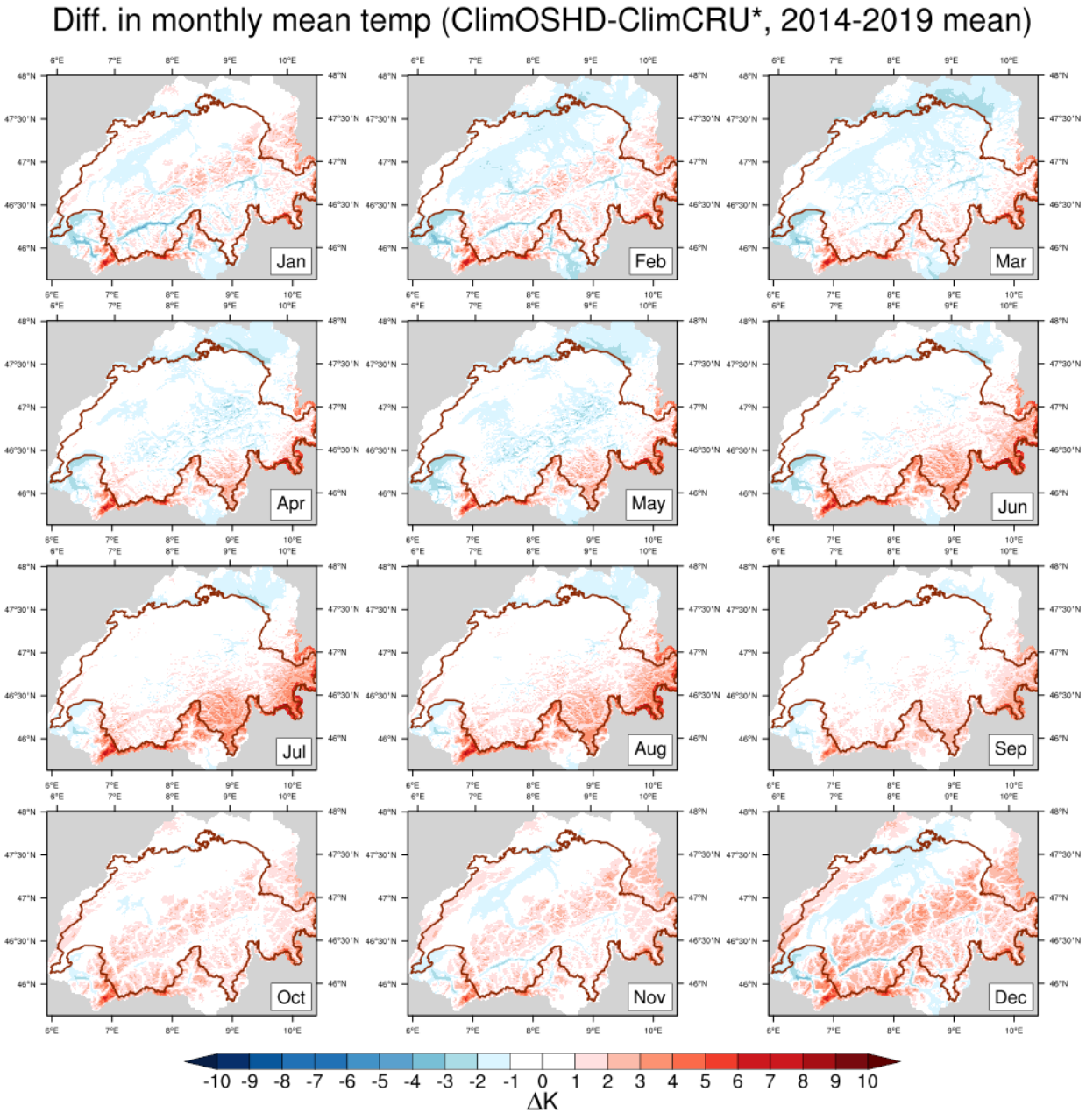

Figure C7. Differences in mean monthly temperatures between the ClimOSHD and the lapse-rate corrected ClimCRU* forcing dataset.

Appendix D: Spatially distributed CLM5 model simulations

This section shows supporting analyses for the spatially distributed CLM5 model simulations presented in the main part of the manuscript. ~~Spatial comparison of monthly-averaged gross primary production (GPP) during July and August 2017: The reference case ($Clim_{OSHD1km}$+LU_{HR1km}) is compared with simulations of all other CLM5 configurations used in this study. For the residual plots, blue indicates underestimation and red indicates overestimation with regards to the reference case.~~

~~Spatial comparison of total Evapotranspiration (ET) during the calendar year 2017: The reference case ($Clim_{OSHD1km}$+LU_{HR1km}) is compared with simulations of all other CLM5 configurations used in this study. For the residual plots, blue indicates underestimation and red indicates overestimation with regards to the reference case.~~

~~Violin plot showing distribution of all 12 CLM5 configurations across the entire model domain: monthly-averaged GPP during July and August 2017.~~

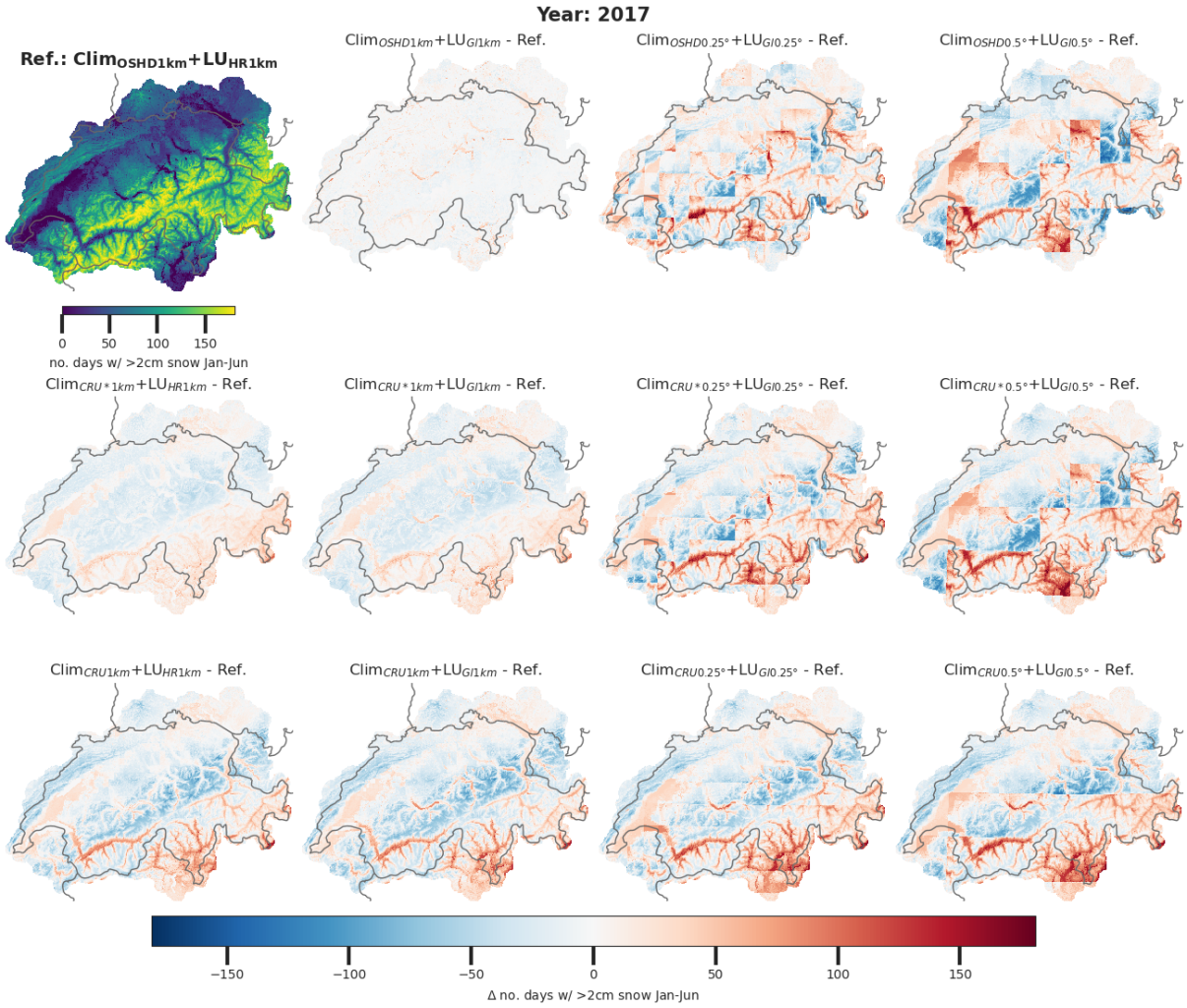

Figure D1. Spatial comparison of number of days with more than 2cm snow on the ground between January and June 2017: The reference case (Clim$_{OSHD1km}$+LU$_{HR1km}$) is compared with simulations of all other CLM5 configurations used in this study. For the residual plots, blue indicates underestimation and red indicates overestimation with regards to the reference case.

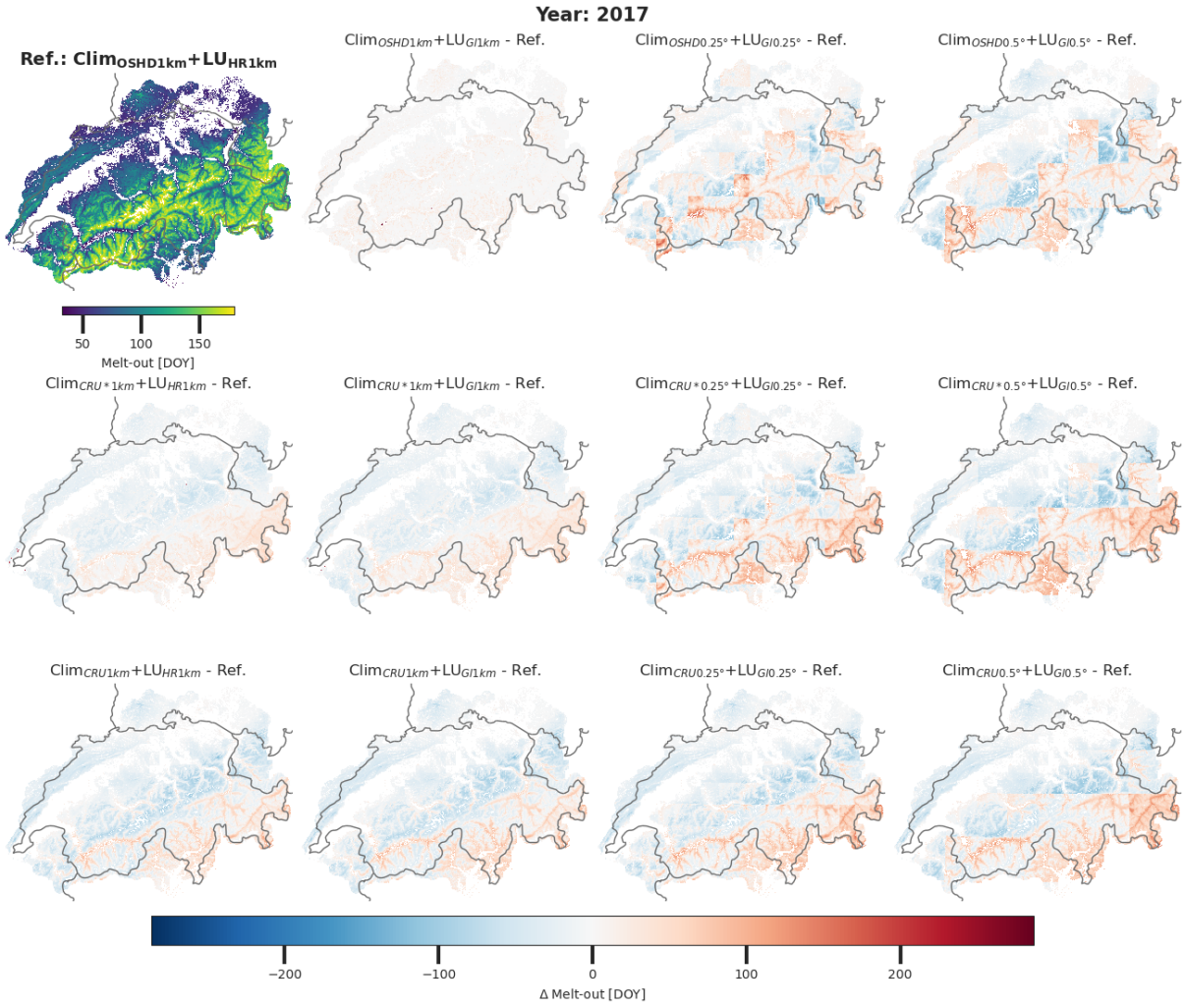

Figure D2. Spatial comparison of melt-out date (day of year) during 2017: The reference case ($Clim_{OSHD1km}$+LU_{HR1km}) is compared with simulations of all other CLM5 configurations used in this study. For the residual plots, blue indicates underestimation and red indicates overestimation with regards to the reference case.

~~Comparison of monthly gross primary production (GPP) and monthly Evapotranspiration (ET) spatially averaged across model domain for all pixels below 2000m and for all 12 CLM5 model configurations. (a) shows 3 yearly cycles between 2017 and 2020, and (b) zooms into the 2018 peak growing season period (dashed blue vertical lines in a).~~

~~Total yearly precipitation input for the year 2017: OSHD-based, CRUJRA-based and a differential plot.~~

~~Spatial plot of a) monthly-averaged GPP in July and August 2017 and b) number of days with more than 2cm of snow between January and July 2017 as simulated with our best-effort $Clim_{OSHD1km}$+LU_{HR1km} simulation. c) Correlation between number of days with more than 2cm of snow between January and July 2017 and monthly-averaged GPP in July and August 2017 as simulated with our best-effort $Clim_{OSHD1km}$+LU_{HR1km} simulation. Looking at vegetated areas across our entire modelling domain, we see that an increased number in days with more than 2cm of snow on the ground is negatively correlated with peak growing season GPP.~~

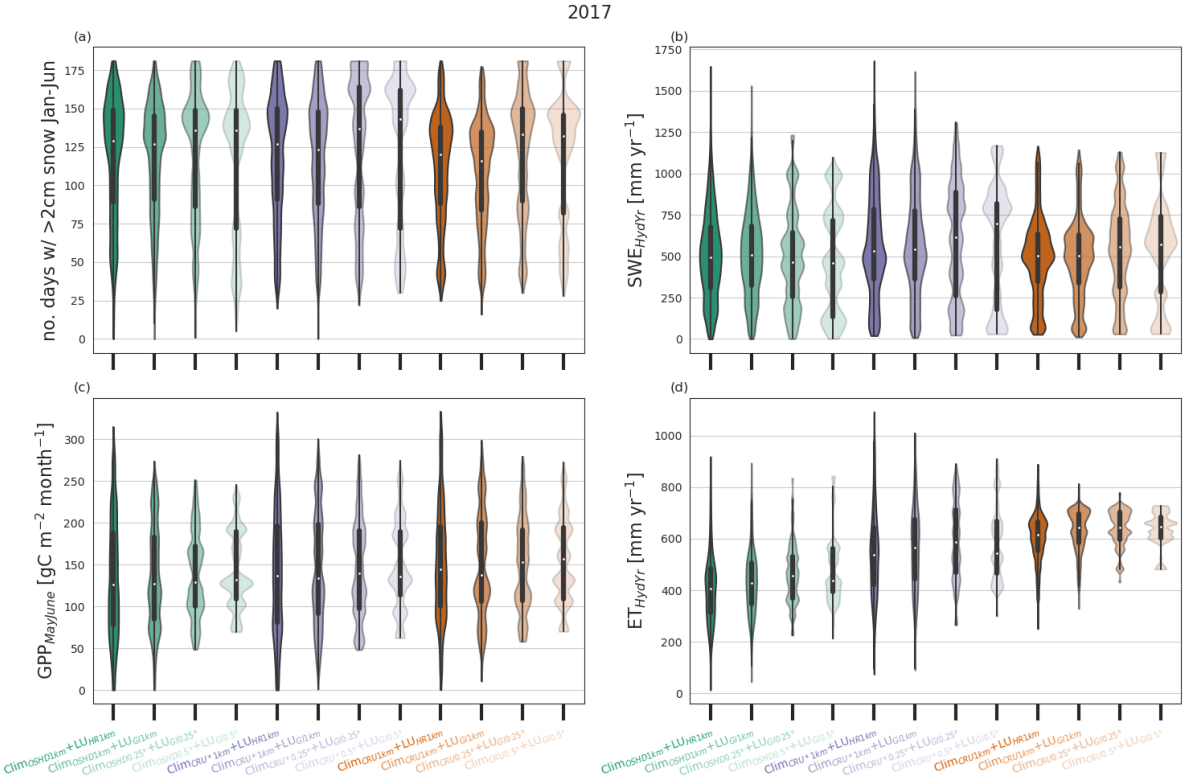

Figure D3. Violin-plots showing comparison of all 12 CLM5 model configurations for the year 2017 across the entire model domain: (a) number of days with >2cm of snow between January and June 2017, (b) cumulative SWE (total positive SWE increments; 'how much water is stored in total') during the hydrological year 2017 (1.10.2016 - 30.09.2017), (c) monthly-averaged GPP during May and June 2017and (d) total Evapotranspiration during the 2017 hydrological year. In addition to information obtained from a box plot (25^{th} + 75^{th} percentiles and median), the violin plots show a kernel density estimate of the data.

Author contributions. All authors helped design the experiments. JM set up the modelling infrastructure and performed the CLM5 simulations. JM performed the analysis, with input from all authors. JM wrote the manuscript, with contributions and feedback from all authors.

Competing interests. The authors declare that they have no conflict of interest.

Acknowledgements. The authors thank Thomas Kramer and his team for HPC support throughout this project. JM received funding from a WSL internal project call. DNK and JM were supported by the Swiss National Science Foundation SNF (project: Adohris, 205530), as was GM (project: P500PN, 202741). We further thank the team of the operational snow hydrologic service at SLF for providing input data. Developers of open source python toolboxes, particularly xarray (Hoyer and Hamman, 2017) and xesmf (Zhuang et al., 2023), have also played a crucial role in this study by enabling efficient analysis and manipulation of large datasets.

References

Abdi, H. and Williams, L. J.: Tukey's Honestly Significant Difference (HSD) Test, Encyclopedia of Research Design, 3, 1–5, http://www.utd.edu/âĹijherve, 2010.

Ali, A. A., Xu, C., Rogers, A., Fisher, R. A., Wullschleger, S. D., Massoud, E. C., Vrugt, J. A., Muss, J. D., McDowell, N. G., Fisher, J. B., Reich, P. B., and Wilson, C. J.: A global scale mechanistic model of photosynthetic capacity (LUNA V1.0), Geoscientific Model Development, 9, 587–606, https://doi.org/10.5194/gmd-9-587-2016, 2016.

Anav, A., Friedlingstein, P., Beer, C., Ciais, P., Harper, A., Jones, C., Murray-Tortarolo, G., Papale, D., Parazoo, N. C., Peylin, P., Piao, S., Sitch, S., Viovy, N., Wiltshire, A., and Zhao, M.: Spatiotemporal patterns of terrestrial gross primary production: A review, https://doi.org/10.1002/2015RG000483, 2015.

Anderson, E. A.: A Point Energy and Mass Balance Model of a Snow Cover, 1976.

Ban-Weiss, G. A., Bala, G., Cao, L., Pongratz, J., and Caldeira, K.: Climate forcing and response to idealized changes in surface latent and sensible heat, Environmental Research Letters, 6, https://doi.org/10.1088/1748-9326/6/3/034032, 2011.

Barnett, T. P., Adam, J. C., and Lettenmaier, D. P.: Potential impacts of a warming climate on water availability in snow-dominated regions., Nature, 438, 303–309, https://doi.org/10.1038/nature04141, barnett, T P
Adam, J C
Lettenmaier, D P
eng
Research Support, U.S. Gov't, Non-P.H.S.
England
2005/11/18 09:00
Nature. 2005 Nov 17;438(7066):303-9., 2005.

Bartelt, P. and Lehning, M.: A physical SNOWPACK model for the Swiss avalanche warning Part I: numerical model, Cold Regions Science and Technology, 35, 123–145, www.elsevier.com/locate/coldregions, 2002.

Bates, D., Mächler, M., Bolker, B. M., and Walker, S. C.: Fitting linear mixed-effects models using lme4, Journal of Statistical Software, 67, https://doi.org/10.18637/jss.v067.i01, 2015.

Beer, C., Reichstein, M., Tomelleri, E., Ciais, P., Jung, M., Carvalhais, N., Rödenbeck, C., Arain, M. A., and Baldocchi, D.: Covariation with Climate, Science, 329, 834–839, 2010.

Beven, K. J. and Cloke, H. L.: Comment on "Hyperresolution global land surface modeling: Meeting a grand challenge for monitoring Earth's terrestrial water" by Eric F. Wood et al., Water Resources Research, 48, 2–4, https://doi.org/10.1029/2011wr010982, 2012.

Birch, L., Schwalm, C. R., Natali, S., Lombardozzi, D., Keppel-Aleks, G., Watts, J., Lin, X., Zona, D., Oechel, W., Sachs, T., Black, T. A., and Rogers, B. M.: Addressing biases in Arctic-boreal carbon cycling in the Community Land Model Version 5, Geoscientific Model Development, 14, 3361–3382, https://doi.org/10.5194/gmd-14-3361-2021, 2021.

Blyth, E. M., Arora, V. K., Clark, D. B., Dadson, S. J., Kauwe, M. G. D., Lawrence, D. M., Melton, J. R., Pongratz, J., Turton, R. H., Yoshimura, K., and Yuan, H.: Advances in Land Surface Modelling, Current Climate Change Reports, 7, 45–71, https://doi.org/10.1007/s40641-021-00171-5, 2021.

Bonan, G. B., Lawrence, P. J., Oleson, K. W., Levis, S., Jung, M., Reichstein, M., Lawrence, D. M., and Swenson, S. C.: Improving canopy processes in the Community Land Model version 4 (CLM4) using global flux fields empirically inferred from FLUXNET data, Journal of Geophysical Research, 116, 1–22, https://doi.org/10.1029/2010jg001593, 2011.

Boone, A. A. and Etchevers, P.: An intercomparison of three snow schemes of varying complexity coupled to the same land surface model: Local-scale evaluation at an alpine site, Journal of Hydrometeorology, 2, 374–394, https://doi.org/10.1175/1525-7541(2001)002<0374:AIOTSS>2.0.CO;2, 2001.

Cheng, L., Zhang, L., Wang, Y. P., Canadell, J. G., Chiew, F. H., Beringer, J., Li, L., Miralles, D. G., Piao, S., and Zhang, Y.: Recent increases in terrestrial carbon uptake at little cost to the water cycle, Nature Communications, 8, https://doi.org/10.1038/s41467-017-00114-5, 2017.

Ciscar, J. C., Rising, J., Kopp, R. E., and Feyen, L.: Assessing future climate change impacts in the EU and the USA: Insights and lessons from two continental-scale projects, Environmental Research Letters, 14, https://doi.org/10.1088/1748-9326/ab281e, 2019.

Clark, M. P., Hendrikx, J., Slater, A. G., Kavetski, D., Anderson, B., Cullen, N. J., Kerr, T., Örn Hreinsson, E., and Woods, R. A.: Representing spatial variability of snow water equivalent in hydrologic and land-surface models: A review, https://doi.org/10.1029/2011WR010745, 2011.

Cooper, A. E., Kirchner, J. W., Wolf, S., Lombardozzi, D. L., Sullivan, B. W., Tyler, S. W., and Harpold, A. A.: Snowmelt causes different limitations on transpiration in a Sierra Nevada conifer forest, Agricultural and Forest Meteorology, 291, https://doi.org/10.1016/j.agrformet.2020.108089, 2020.

Dai, Y. and Zeng, Q.: A Land Surface Model (IAP94) for Climate Studies Part I: Formulation and Validation in Off-line Experiments, Advances in Atmospheric Sciences, 14, 1997.

Dirmeyer, P. A., Gao, X., Zhao, M., Guo, Z., Oki, T., and Hanasaki, N.: GSWP-2: Multimodel analysis and implications for our perception of the land surface, Bulletin of the American Meteorological Society, 87, 1381–1397, https://doi.org/10.1175/BAMS-87-10-1381, 2006.

Douville, H., Royer, J.-F., and Mahfouf, J.-F.: A new snow parameterization for the M6t o-France climate model Part I: validation in stand-alone experiments, Climate Dynamics, 12, 21–35, https://doi.org/10.1007/BF00208760, 1995.

Dutra, E., Viterbo, P., Miranda, P. M. A., and Balsamo, G.: American Meteorological Society Complexity of Snow Schemes in a Climate Model and Its Impact on Surface Energy and Hydrology, Source: Journal of Hydrometeorology, 13, 521–538, https://doi.org/10.2307/24912781, 2012.

Essery, R.: Aggregated and distributed modelling of snow cover for a high-latitude basin, Global and Planetary Change, 38, 115–120, https://doi.org/10.1016/S0921-8181(03)00013-4, 2003.

Essery, R.: A factorial snowpack model (FSM 1.0), Geoscientific Model Development, 8, 3867–3876, https://doi.org/10.5194/gmd-8-3867-2015, 2015.

Essery, R., Morin, S., Lejeune, Y., and Ménard, C. B.: A comparison of 1701 snow models using observations from an alpine site, Advances in Water Resources, 55, 131–148, https://doi.org/10.1016/j.advwatres.2012.07.013, 2013.

Farquhar, G. D., Caemmerer, S., and Berry, J. A.: A biochemical model of photosynthetic CO₂ assimilation in leaves of C₃ species, Planta, 149, 78–90–90, http://dx.doi.org/10.1007/BF00386231, 1980.

Fatichi, S., Ivanov, V. Y., and Caporali, E.: A mechanistic ecohydrological model to investigate complex interactions in cold and warm water-controlled environments: 1. Theoretical framework and plot-scale analysis, Journal of Advances in Modeling Earth Systems, 4, https://doi.org/10.1029/2011MS000086, 2012.

Ferguson, C. R., Wood, E. F., and Vinukollu, R. K.: A Global intercomparison of modeled and observed land-atmosphere coupling, Journal of Hydrometeorology, 13, 749–784, https://doi.org/10.1175/JHM-D-11-0119.1, 2012.

Fisher, R. A. and Koven, C. D.: Perspectives on the Future of Land Surface Models and the Challenges of Representing Complex Terrestrial Systems, Journal of Advances in Modeling Earth Systems, 12, https://doi.org/10.1029/2018MS001453, 2020.

Fisher, R. A., Wieder, W. R., Sanderson, B. M., Koven, C. D., Oleson, K. W., Xu, C., Fisher, J. B., Shi, M., Walker, A. P., and Lawrence, D. M.: Parametric Controls on Vegetation Responses to Biogeochemical Forcing in the CLM5, Journal of Advances in Modeling Earth Systems, 11, 2879–2895, https://doi.org/10.1029/2019MS001609, 2019.

Flanner, M. G. and Zender, C. S.: Snowpack radiative heating: Influence on Tibetan Plateau climate, Geophysical Research Letters, 32, 1–5, https://doi.org/10.1029/2004GL022076, 2005.

Flanner, M. G., Shell, K. M., Barlage, M., Perovich, D. K., and Tschudi, M. A.: Radiative forcing and albedo feedback from the Northern Hemisphere cryosphere between 1979 and 2008, Nature Geoscience, 4, 151–155, https://doi.org/10.1038/ngeo1062, 2011.

Friedlingstein, P., O'Sullivan, M., Jones, M. W., Andrew, R. M., Hauck, J., Olsen, A., Peters, G. P., Peters, W., Pongratz, J., Sitch, S., Quéré, C. L., Canadell, J. G., Ciais, P., Jackson, R. B., Alin, S., Aragão, L. E., Arneth, A., Arora, V., Bates, N. R., Becker, M., Benoit-Cattin, A., Bittig, H. C., Bopp, L., Bultan, S., Chandra, N., Chevallier, F., Chini, L. P., Evans, W., Florentie, L., Forster, P. M., Gasser, T., Gehlen, M., Gilfillan, D., Gkritzalis, T., Gregor, L., Gruber, N., Harris, I., Hartung, K., Haverd, V., Houghton, R. A., Ilyina, T., Jain, A. K., Joetzjer, E., Kadono, K., Kato, E., Kitidis, V., Korsbakken, J. I., Landschützer, P., Lefèvre, N., Lenton, A., Lienert, S., Liu, Z., Lombardozzi, D., Marland, G., Metzl, N., Munro, D. R., Nabel, J. E., Nakaoka, S. I., Niwa, Y., O'Brien, K., Ono, T., Palmer, P. I., Pierrot, D., Poulter, B., Resplandy, L., Robertson, E., Rödenbeck, C., Schwinger, J., Séférian, R., Skjelvan, I., Smith, A. J., Sutton, A. J., Tanhua, T., Tans, P. P., Tian, H., Tilbrook, B., Werf, G. V. D., Vuichard, N., Walker, A. P., Wanninkhof, R., Watson, A. J., Willis, D., Wiltshire, A. J., Yuan, W., Yue, X., and Zaehle, S.: Data used with permission of the Global Carbon Project under the Creative Commons Attribution 4.0 International license, Earth System Science Data, 12, 3269–3340, 2020.

Griessinger, N., Schirmer, M., Helbig, N., Winstral, A., Michel, A., and Jonas, T.: Implications of observation-enhanced energy-balance snowmelt simulations for runoff modeling of Alpine catchments, Advances in Water Resources, 133, 103 410, https://doi.org/10.1016/j.advwatres.2019.103410, 2019.

Harris, I., Jones, P. D., Osborn, T. J., and Lister, D. H.: Updated high-resolution grids of monthly climatic observations - the CRU TS3.10 Dataset, International Journal of Climatology, 34, 623–642, https://doi.org/10.1002/joc.3711, 2014.

Hoyer, S. and Hamman, J.: xarray: N-D labeled Arrays and Datasets in Python, Journal of Open Research Software, 5, 10, https://doi.org/10.5334/jors.148, 2017.

Hurk, B. V. D., Kim, H., Krinner, G., Seneviratne, S. I., Derksen, C., Oki, T., Douville, H., Colin, J., Ducharne, A., Cheruy, F., Viovy, N., Puma, M. J., Wada, Y., Li, W., Jia, B., Alessandri, A., Lawrence, D. M., Weedon, G. P., Ellis, R., Hagemann, S., Mao, J., Flanner, M. G., Zampieri, M., Materia, S., Law, R. M., and Sheffield, J.: LS3MIP (v1.0) contribution to CMIP6: The Land Surface, Snow and Soil moisture Model Intercomparison Project - Aims, setup and expected outcome, Geoscientific Model Development, 9, 2809–2832, https://doi.org/10.5194/gmd-9-2809-2016, 2016.

IPCC: Climate Change 2022: Impacts, Adaptation, and Vulnerability. Contribution of Working Group II to the Sixth Assessment Report of the Intergovernmental Panel on Climate Change, Cambridge University Press, 2022.

Jonas, T., Rixen, C., Sturm, M., and Stoeckli, V.: How alpine plant growth is linked to snow cover and climate variability, Journal of Geophysical Research: Biogeosciences, 113, https://doi.org/10.1029/2007JG000680, 2008.

Jordan, R.: A One-Dimensional Temperature Model for a Snow Cover: Technical Documentation for SNTHERM.89, 1991.

Kobayashi, S., Ota, Y., Harada, Y., Ebita, A., Moriya, M., Onoda, H., Onogi, K., Kamahori, H., Kobayashi, C., Endo, H., Miyaoka, K., and Kiyotoshi, T.: The JRA-55 reanalysis: General specifications and basic characteristics, Journal of the Meteorological Society of Japan, 93, 5–48, https://doi.org/10.2151/jmsj.2015-001, 2015.

Kraft, M. and McNamara, J. P.: Evapotranspiration across the rain–snow transition in a semi-arid watershed, Hydrological Processes, 36, https://doi.org/10.1002/hyp.14519, 2022.

Lawrence, D. M., Thornton, P. E., Oleson, K. W., and Bonan, G. B.: The partitioning of evapotranspiration into transpiration, soil evaporation, and canopy evaporation in a GCM: Impacts on land-atmosphere interaction, Journal of Hydrometeorology, 8, 862–880, https://doi.org/10.1175/JHM596.1, 2007.

Lawrence, D. M., Fisher, R. A., Koven, C., Oleson, K. W., Swenson, S. C., and Vertenstein, M.: Technical Description of version 5.0 of the Community Land Model (CLM), 2018.

Lawrence, D. M., Fisher, R. A., Koven, C. D., Oleson, K. W., Swenson, S. C., Bonan, G., Collier, N., Ghimire, B., van Kampenhout, L., Kennedy, D., Kluzek, E., Lawrence, P. J., Li, F., Li, H., Lombardozzi, D., Riley, W. J., Sacks, W. J., Shi, M., Vertenstein, M., Wieder, W. R., Xu, C., Ali, A. A., Badger, A. M., Bisht, G., van den Broeke, M., Brunke, M. A., Burns, S. P., Buzan, J., Clark, M., Craig, A., Dahlin, K., Drewniak, B., Fisher, J. B., Flanner, M., Fox, A. M., Gentine, P., Hoffman, F., Keppel-Aleks, G., Knox, R., Kumar, S., Lenaerts, J., Leung, L. R., Lipscomb, W. H., Lu, Y., Pandey, A., Pelletier, J. D., Perket, J., Randerson, J. T., Ricciuto, D. M., Sanderson, B. M., Slater, A., Subin, Z. M., Tang, J., Thomas, R. Q., Martin, M. V., and Zeng, X.: The Community Land Model Version 5: Description of New Features, Benchmarking, and Impact of Forcing Uncertainty, Journal of Advances in Modeling Earth Systems, 11, 4245–4287, https://doi.org/10.1029/2018MS001583, 2019.

Lawrence, P. J. and Chase, T. N.: Representing a new MODIS consistent land surface in the Community Land Model (CLM 3.0), Journal of Geophysical Research: Biogeosciences, 112, https://doi.org/10.1029/2006JG000168, 2007.

Lei, Y., Pan, J., Xiong, C., Jiang, L., and Shi, J.: Snow depth and snow cover over the Tibetan Plateau observed from space in against ERA5: matters of scale, Climate Dynamics, https://doi.org/10.1007/s00382-022-06376-0, 2022.

Lüthi, S., Ban, N., Kotlarski, S., Steger, C. R., Jonas, T., and Schär, C.: Projections of Alpine snow-cover in a high-resolution climate simulation, Atmosphere, 10, 1–18, https://doi.org/10.3390/atmos10080463, 2019.

Ma, X. and Wang, A.: Systematic Evaluation of a High-Resolution CLM5 Simulation over Continental China for 1979-2018, Journal of Hydrometeorology, 23, 1879 –1897, https://doi.org/10.1175/JHM-D-22, 2022.

Magnusson, J., Gustafsson, D., Huesler, F., and Jonas, T.: Assimilation of point SWE data into a distributed snow cover model comparing two contrasting methods, Water Resources Research, 50, 7816–7835, https://doi.org/10.1002/2013WR014792.Received, 2014.

Magnusson, J., Wever, N., Essery, R., Helbig, N., Winstral, A., and Jonas, T.: Evaluating snow models with varying process representations for hydrological applications, Water Resources Research, 51, 2707–2723, https://doi.org/10.1002/2014WR016498, 2015.

Magnusson, J., Eisner, S., Huang, S., Lussana, C., Mazzotti, G., Essery, R., Saloranta, T., and Beldring, S.: Influence of Spatial Resolution on Snow Cover Dynamics for a Coastal and Mountainous Region at High Latitudes (Norway), Water Resources Research, 55, 5612–5630, https://doi.org/10.1029/2019WR024925, 2019.

Male, D. H. and Granger, R. J.: Snow surface energy exchange, Water Resour. Res., 17, 609–627, https://doi.org/10.1029/WR017i003p00609, 1981.

Mankin, J. S., Viviroli, D., Singh, D., Hoekstra, A. Y., and Diffenbaugh, N. S.: The potential for snow to supply human water demand in the present and future, Environmental Research Letters, 10, 114 016, https://doi.org/10.1088/1748-9326/10/11/114016, 2015.

Mastrotheodoros, T., Pappas, C., Molnar, P., Burlando, P., Manoli, G., Parajka, J., Rigon, R., Szeles, B., Bottazzi, M., Hadjidoukas, P., and Fatichi, S.: More green and less blue water in the Alps during warmer summers, Nature Climate Change, 10, 155–161, https://doi.org/10.1038/s41558-019-0676-5, 2020.

Mazzotti, G., Essery, R., Webster, C., Malle, J., and Jonas, T.: Process-Level Evaluation of a Hyper-Resolution Forest Snow Model Using Distributed Multisensor Observations, Water Resources Research, 56, https://doi.org/10.1029/2020WR027572, 2020.

Mazzotti, G., Webster, C., Essery, R., and Jonas, T.: Increasing the Physical Representation of Forest-Snow Processes in Coarse-Resolution Models: Lessons Learned From Upscaling Hyper-Resolution Simulations, Water Resources Research, 57, https://doi.org/10.1029/2020WR029064, 2021.

Meissner, C., Schädler, G., Panitz, H. J., Feldmann, H., and Kottmeier, C.: High-resolution sensitivity studies with the regional climate model COSMO-CLM, Meteorologische Zeitschrift, 18, 543–557, https://doi.org/10.1127/0941-2948/2009/0400, 2009.

Miralles, D. G., Jiménez, C., Jung, M., Michel, D., Ershadi, A., Mccabe, M. F., Hirschi, M., Martens, B., Dolman, A. J., Fisher, J. B., Mu, Q., Seneviratne, S. I., Wood, E. F., and Fernández-Prieto, D.: The WACMOS-ET project - Part 2: Evaluation of global terrestrial evaporation data sets, Hydrology and Earth System Sciences, 20, 823–842, https://doi.org/10.5194/hess-20-823-2016, 2016.

Mott, R., Winstral, A., Cluzet, B., Helbig, N., Magnusson, J., Mazzotti, G., Quéno, L., Schirmer, M., Webster, C., and Jonas, T.: Operational snow-hydrological modeling for Switzerland, Frontiers in Earth Science, 11, https://doi.org/10.3389/feart.2023.1228158, 2023.

Mueller, B., Seneviratne, S. I., Jimenez, C., Corti, T., Hirschi, M., Balsamo, G., Ciais, P., Dirmeyer, P., Fisher, J. B., Guo, Z., Jung, M., Maignan, F., McCabe, M. F., Reichle, R., Reichstein, M., Rodell, M., Sheffield, J., Teuling, A. J., Wang, K., Wood, E. F., and Zhang, Y.: Evaluation of global observations-based evapotranspiration datasets and IPCC AR4 simulations, Geophysical Research Letters, 38, 1–7, https://doi.org/10.1029/2010GL046230, 2011.

Myers-Smith, I. H., Kerby, J. T., Phoenix, G. K., Bjerke, J. W., Epstein, H. E., Assmann, J. J., John, C., Andreu-Hayles, L., Angers-Blondin, S., Beck, P. S., Berner, L. T., Bhatt, U. S., Bjorkman, A. D., Blok, D., Bryn, A., Christiansen, C. T., Cornelissen, J. H. C., Cunliffe, A. M., Elmendorf, S. C., Forbes, B. C., Goetz, S. J., Hollister, R. D., de Jong, R., Loranty, M. M., Macias-Fauria, M., Maseyk, K., Normand, S., Olofsson, J., Parker, T. C., Parmentier, F. J. W., Post, E., Schaepman-Strub, G., Stordal, F., Sullivan, P. F., Thomas, H. J., Tømmervik, H., Treharne, R., Tweedie, C. E., Walker, D. A., Wilmking, M., and Wipf, S.: Complexity revealed in the greening of the Arctic, Nature Climate Change, 10, 106–117, https://doi.org/10.1038/s41558-019-0688-1, 2020.

Niu, G. Y., Yang, Z. L., Mitchell, K. E., Chen, F., Ek, M. B., Barlage, M., Kumar, A., Manning, K., Niyogi, D., Rosero, E., Tewari, M., and Xia, Y.: The community Noah land surface model with multiparameterization options (Noah-MP): 1. Model description and evaluation with local-scale measurements, Journal of Geophysical Research Atmospheres, 116, https://doi.org/10.1029/2010JD015139, 2011.

of East Anglia Climatic Research Unit; Harris, I. U.: CRU JRA v2.0: A forcings dataset of gridded land surface blend of Climatic Research Unit (CRU) and Japanese reanalysis (JRA) data; Jan.1901 - Dec.2018.. Centre for Environmental Data Analysis, 08.06.2022. https://catalogue.ceda.ac.uk/, Norwich: University of East Anglia, 2019.

Office., S. F. S.: The Changing Face of Land Use: Land Use Statistics of Switzerland., SFO: Neuchâtel, Switzerland, p. 32, 2001.

Oleson, K. W., Lawrence, D. M., Gordon, B., Flanner, M. G., Kluzek, E., Peter, J., Levis, S., Swenson, S. C., Thornton, E., Dai, A., Decker, M., Dickinson, R., Feddema, J., Heald, C. L., Lamarque, J.-F., yue Niu, G., Qian, T., Running, S., Sakaguchi, K., Slater, A., Stöckli, R., Wang, A., Yang, L., Zeng, X. X., Zeng, X. X., Bonan, G. B., Flanner, M. G., Kluzek, E., Lawrence, P. J., Levis, S., Swenson, S. C., Thornton, P. E., Dai, A., Decker, M., Dickinson, R., Feddema, J., Heald, C. L., Hoffman, F., Lamarque, J.-F., Mahowald, N., yue Niu, G., Qian, T., Randerson, J., Running, S., Sakaguchi, K., Slater, A., Stöckli, R., Wang, A., Yang, Z.-L., Zeng, X. X., and Zeng, X. X.: Technical Description of version 4 . 0 of the Community Land Model (CLM), http://www.ucar.edu/library/collections/technotes/technotes.jsp, 2010.

Pachauri, R. K., Allen, M. R., Barros, V. R., Broome, J., Cramer, W., Christ, R., Church, J. A., Clarke, L., Dahe, Q., Dasgupta, P., Dubash, N. K., Edenhofer, O., Elgizouli, I., Field, C. B., Forster, P., Friedlingstein, P., Fuglestvedt, J., Gomez-Echeverri, L., Hallegatte, S., Hegerl, G., Howden, M., Jiang, K., Cisneroz, B. J., Kattsov, V., Lee, H., Mach, K. J., Marotzke, J., Mastrandrea, M. D., Meyer, L., Minx, J., Mulugetta, Y., O'Brien, K., Oppenheimer, M., Pereira, J. J., Pichs-Madruga, R., Plattner, G.-K., Pörtner, H.-O., Power, S. B., Preston, B., Ravindranath, N. H., Reisinger, A., Riahi, K., Rusticucci, M., Scholes, R., Seyboth, K., Sokona, Y., Stavins, R., Stocker, T. F., Tschakert, P., van Vuuren, D., and van Ypserle, J.-P.: Climate Change 2014: Synthesis Report. Contribution of Working Groups I, II and III to the Fifth Assessment Report of the Intergovernmental Panel on Climate Change, IPCC, 2014.

Pastorello, G., Trotta, C., Canfora, E., Chu, H., Christianson, D., Cheah, Y. W., Poindexter, C., Chen, J., Elbashandy, A., Humphrey, M., Isaac, P., Polidori, D., Ribeca, A., van Ingen, C., Zhang, L., Amiro, B., Ammann, C., Arain, M. A., Ardö, J., Arkebauer, T., Arndt, S. K., Arriga, N., Aubinet, M., Aurela, M., Baldocchi, D., Barr, A., Beamesderfer, E., Marchesini, L. B., Bergeron, O., Beringer, J., Bernhofer, C., Berveiller, D., Billesbach, D., Black, T. A., Blanken, P. D., Bohrer, G., Boike, J., Bolstad, P. V., Bonal, D., Bonnefond, J. M., Bowling, D. R., Bracho, R., Brodeur, J., Brümmer, C., Buchmann, N., Burban, B., Burns, S. P., Buysse, P., Cale, P., Cavagna, M., Cellier, P., Chen, S., Chini, I., Christensen, T. R., Cleverly, J., Collalti, A., Consalvo, C., Cook, B. D., Cook, D., Coursolle, C., Cremonese, E., Curtis, P. S., D'Andrea, E., da Rocha, H., Dai, X., Davis, K. J., Cinti, B. D., de Grandcourt, A., Ligne, A. D., Oliveira, R. C. D., Delpierre, N., Desai, A. R., Bella, C. M. D., di Tommasi, P., Dolman, H., Domingo, F., Dong, G., Dore, S., Duce, P., Dufrêne, E., Dunn, A., Dušek, J., Eamus, D., Eichelmann, U., ElKhidir, H. A. M., Eugster, W., Ewenz, C. M., Ewers, B., Famulari, D., Fares, S., Feigenwinter, I., Feitz, A., Fensholt, R., Filippa, G., Fischer, M., Frank, J., Galvagno, M., Gharun, M., Gianelle, D., Gielen, B., Gioli, B., Gitelson, A., Goded, I., Goeckede, M., Goldstein, A. H., Gough, C. M., Goulden, M. L., Graf, A., Griebel, A., Gruening, C., Grünwald, T., Hammerle, A., Han, S., Han, X., Hansen, B. U., Hanson, C., Hatakka, J., He, Y., Hehn, M., Heinesch, B., Hinko-Najera, N., Hörtnagl, L., Hutley, L., Ibrom, A., Ikawa, H., Jackowicz-Korczynski, M., Janouš, D., Jans, W., Jassal, R., Jiang, S., Kato, T., Khomik, M., Klatt, J., Knohl, A., Knox, S., Kobayashi, H., Koerber, G., Kolle, O., Kosugi, Y., Kotani, A., Kowalski, A., Kruijt, B., Kurbatova, J., Kutsch, W. L., Kwon, H., Launiainen, S., Laurila, T., Law, B., Leuning, R., Li, Y., Liddell, M., Limousin, J. M., Lion, M., Liska, A. J., Lohila, A., López-Ballesteros, A., López-Blanco, E., Loubet, B., Loustau, D., Lucas-Moffat, A., Lüers, J., Ma, S., Macfarlane, C., Magliulo, V., Maier, R., Mammarella, I., Manca, G., Marcolla, B., Margolis, H. A., Marras, S., Massman, W., Mastepanov, M., Matamala, R., Matthes, J. H., Mazzenga, F., McCaughey, H., McHugh, I., McMillan, A. M., Merbold, L., Meyer, W., Meyers, T., Miller, S. D., Minerbi, S., Moderow, U., Monson, R. K., Montagnani, L., Moore, C. E., Moors, E., Moreaux, V., Moureaux, C., Munger, J. W., Nakai, T., Neirynck, J., Nesic, Z., Nicolini, G., Noormets, A., Northwood, M., Nosetto, M., Nouvellon, Y., Novick, K., Oechel, W., Olesen, J. E., Ourcival, J. M., Papuga, S. A., Parmentier, F. J., Paul-Limoges, E., Pavelka, M., Peichl, M., Pendall, E., Phillips, R. P., Pilegaard, K., Pirk, N., Posse, G., Powell, T., Prasse, H., Prober, S. M., Rambal, S., Üllar Rannik, Raz-Yaseef, N., Reed, D., de Dios, V. R., Restrepo-Coupe, N., Reverter, B. R., Roland, M., Sabbatini, S., Sachs, T., Saleska, S. R., Sánchez-Cañete, E. P., Sanchez-Mejia, Z. M., Schmid, H. P., Schmidt, M., Schneider, K., Schrader, F., Schroder, I., Scott, R. L., Sedlák, P., Serrano-Ortíz, P., Shao, C., Shi, P., Shironya, I., Siebicke, L., Šigut, L., Silberstein, R., Sirca, C., Spano, D., Steinbrecher, R., Stevens, R. M., Sturtevant, C., Suyker, A., Tagesson, T., Takanashi, S., Tang, Y., Tapper, N., Thom, J., Tiedemann, F., Tomassucci, M., Tuovinen, J. P., Urbanski, S., Valentini, R., van der Molen, M., van Gorsel, E., van Huissteden, K., Varlagin, A., Verfaillie, J., Vesala, T., Vincke, C., Vitale, D., Vygodskaya, N., Walker, J. P., Walter-Shea, E., Wang, H., Weber, R., Westermann, S., Wille, C., Wofsy, S., Wohlfahrt, G., Wolf, S., Woodgate, W., Li, Y., Zampedri, R., Zhang, J., Zhou, G., Zona, D., Agarwal, D., Biraud, S., Torn, M., and Papale, D.: The FLUXNET2015 dataset and the ONEFlux processing pipeline for eddy covariance data, Scientific data, 7, 225, https://doi.org/10.1038/s41597-020-0534-3, 2020.

Peters-Lidard, C. D., Mocko, D. M., Garcia, M., Santanello, J. A., Tischler, M. A., Moran, M. S., and Wu, Y.: Role of precipitation uncertainty in the estimation of hydrologic soil properties using remotely sensed soil moisture in a semiarid environment, Water Resources Research, 44, 1–22, https://doi.org/10.1029/2007WR005884, 2008.

Phoenix, G. K. and Bjerke, J. W.: Arctic browning: extreme events and trends reversing arctic greening, Global Change Biology, 22, 2960–2962, https://doi.org/10.1111/gcb.13261, 2016.

Pitman, A. J.: The evolution of, and revolution in, land surface schemes designed for climate models, International Journal of Climatology, 23, 479–510, https://doi.org/10.1002/joc.893, 2003.

Pongratz, J., Schwingshackl, C., Bultan, S., Obermeier, W., Havermann, F., and Guo, S.: Land Use Effects on Climate: Current State, Recent Progress, and Emerging Topics, Current Climate Change Reports, 7, 99–120, https://doi.org/10.1007/s40641-021-00178-y, 2021.

Pritchard, H. D.: Asia's shrinking glaciers protect large populations from drought stress, Nature, 569, 649–654, https://doi.org/10.1038/s41586-019-1240-1, 2019.

Qin, Y., Abatzoglou, J. T., Siebert, S., Huning, L. S., AghaKouchak, A., Mankin, J. S., Hong, C., Tong, D., Davis, S. J., and Mueller, N. D.: Agricultural risks from changing snowmelt, Nature Climate Change, 10, 459–465, https://doi.org/10.1038/s41558-020-0746-8, 2020.

Ridder, N. N., Pitman, A. J., and Ukkola, A. M.: Do CMIP6 Climate Models Simulate Global or Regional Compound Events Skillfully?, Geophysical Research Letters, 48, 1–11, https://doi.org/10.1029/2020GL091152, 2021.

Rimal, B., Sharma, R., Kunwar, R., Keshtkar, H., Stork, N. E., Rijal, S., Rahman, S. A., and Baral, H.: Effects of land use and land cover change on ecosystem services in the Koshi River Basin, Eastern Nepal, Ecosystem Services, 38, https://doi.org/10.1016/j.ecoser.2019.100963, 2019.

Rixen, C., Høye, T. T., Macek, P., Aerts, R., Alatalo, J. M., Anderson, J. T., Arnold, P. A., Barrio, I. C., Bjerke, J. W., Björkman, M. P., Blok, D., and Blume-Werry, G.: Winters are changing: Snow effects on Arctic and alpine tundra ecosystems, Arctic Science, 8, 572–608, https://doi.org/10.1139/as-2020-0058, 2022.

Rumpf, S. B., Gravey, M., Brönnimann, O., Luoto, M., Cianfrani, C., Mariethoz, G., and Guisan, A.: From white to green: Snow cover loss and increased vegetation productivity in the European Alps, Science, 376, 1119–1122, https://www.science.org, 2022.

Schaefer, K., Schwalm, C. R., Williams, C., Arain, M. A., Barr, A., Chen, J. M., Davis, K. J., Dimitrov, D., Hilton, T. W., Hollinger, D. Y., Humphreys, E., Poulter, B., Raczka, B. M., Richardson, A. D., Sahoo, A., Thornton, P., Vargas, R., Verbeeck, H., Anderson, R., Baker, I., Black, T. A., Bolstad, P., Chen, J., Curtis, P. S., Desai, A. R., Dietze, M., Dragoni, D., Gough, C., Grant, R. F., Gu, L., Jain, A., Kucharik, C., Law, B., Liu, S., Lokipitiya, E., Margolis, H. A., Matamala, R., McCaughey, J. H., Monson, R., Munger, J. W., Oechel, W., Peng, C., Price, D. T., Ricciuto, D., Riley, W. J., Roulet, N., Tian, H., Tonitto, C., Torn, M., Weng, E., and Zhou, X.: A model-data comparison of gross primary productivity: Results from the north American carbon program site synthesis, Journal of Geophysical Research: Biogeosciences, 117, 1–15, https://doi.org/10.1029/2012JG001960, 2012.

Schär, C., Fuhrer, O., Arteaga, A., Ban, N., Charpilloz, C., Girolamo, S. D., Hentgen, L., Hoefler, T., Lapillonne, X., Leutwyler, D., Osterried, K., Panosetti, D., Rüdisühli, S., Schlemmer, L., Schulthess, T. C., Sprenger, M., Ubbiali, S., and Wernli, H.: Kilometer-scale climate models: Prospects and challenges, Bulletin of the American Meteorological Society, 101, E567–E587, https://doi.org/10.1175/BAMS-D-18-0167.1, 2020.

Seneviratne, S. I., Lüthi, D., Litschi, M., and Schär, C.: Land-atmosphere coupling and climate change in Europe, Nature, 443, 205–209, https://doi.org/10.1038/nature05095, 2006.

Shi, X., Mao, J., Thornton, P. E., and Huang, M.: Spatiotemporal patterns of evapotranspiration in response to multiple environmental factors simulated by the Community Land Model, Environmental Research Letters, 8, https://doi.org/10.1088/1748-9326/8/2/024012, 2013.

Shrestha, B., Zhang, L., Sharma, S., Shrestha, S., and Khadka, N.: Effects on ecosystem services value due to land use and land cover change (1990–2020) in the transboundary Karnali River Basin, Central Himalayas, SN Applied Sciences, 4, https://doi.org/10.1007/s42452-022-05022-y, 2022.

Singh, R. S., Reager, J. T., Miller, N. L., and Famiglietti, J. S.: Toward hyper-resolution land-surface modeling: The effects of fine-scale topography and soil texture on CLM4.0 simulations over the Southwestern U.S., Water Resources Research, 51, 2648–2667, https://doi.org/10.1002/2014WR015686, 2015.

Slatyer, R. A., Umbers, K. D., and Arnold, P. A.: Ecological responses to variation in seasonal snow cover, https://doi.org/10.1111/cobi.13727, 2022.

Son, K. and Tague, C.: Hydrologic responses to climate warming for a snow-dominated watershed and a transient snow watershed in the California Sierra, Ecohydrology, 12, https://doi.org/10.1002/eco.2053, 2019.

Sterling, S. M., Ducharne, A., and Polcher, J.: The impact of global land-cover change on the terrestrial water cycle, Nature Climate Change, 3, 385–390, https://doi.org/10.1038/nclimate1690, 2013.

Swenson, S. C. and Lawrence, D. M.: A new fractional snow-covered area parameterization for the Community Land Model and its effect on the surface energy balance, Journal of Geophysical Research Atmospheres, 117, 1–20, https://doi.org/10.1029/2012JD018178, 2012.

Swiss-Federal-Statistical-Office: Waldmischungsgrad, Auflösung 100m: Geodaten, https://dam-api.bfs.admin.ch/hub/api/dam/assets/860862/master, 2013.

Tague, C. L. and Band, L. E.: RHESSys: Regional Hydro-Ecologic Simulation System-An Object-Oriented Approach to Spatially Distributed Modeling of Carbon, Water, and Nutrient Cycling, Earth Interactions, 8, https://doi.org/https://doi.org/10.1175/1087-3562(2004)8<1:RRHSSO>2.0.CO;2, 2004.

Taylor, K. E.: Summarizing multiple aspects of model performance in a single diagram, Journal of Geophysical Research: Atmospheres, 106, 7183–7192, https://doi.org/https://doi.org/10.1029/2000JD900719, 2001.

Team, W. W. . and Centre, I. E. T.: Warm Winter 2020 ecosystem eddy covariance flux product for 73 stations in FLUXNET-Archive format-release 2022-1 (version 1.0), icos carbon portal., https://doi.org/10.18160/2g60-zhak, 2022.

Thackeray, C. W. and Fletcher, C. G.: Snow albedo feedback: Current knowledge, importance, outstanding issues and future directions, Progress in Physical Geography, 40, 392–408, https://doi.org/10.1177/0309133315620999, 2016.

Thackeray, C. W., Derksen, C., Fletcher, C. G., and Hall, A.: Snow and Climate: Feedbacks, Drivers, and Indices of Change, Current Climate Change Reports, 5, 322–333, https://doi.org/10.1007/s40641-019-00143-w, 2019.

Thornton, P. E. and Zimmermann, N. E.: An improved canopy integration scheme for a Land Surface Model with prognostic canopy structure, Journal of Climate, 20, 3902–3923, https://doi.org/10.1175/JCLI4222.1, 2007.

Tsendbazar, N., Herold, M., Li, L., Tarko, A., de Bruin, S., Masiliunas, D., Lesiv, M., Fritz, S., Buchhorn, M., Smets, B., Kerchove, R. V. D., and Duerauer, M.: Towards operational validation of annual global land cover maps, Remote Sensing of Environment, 266, https://doi.org/10.1016/j.rse.2021.112686, 2021.

van Kampenhout, L., Lenaerts, J. T., Lipscomb, W. H., Sacks, W. J., Lawrence, D. M., Slater, A. G., and van den Broeke, M. R.: Improving the Representation of Polar Snow and Firn in the Community Earth System Model, Journal of Advances in Modeling Earth Systems, 9, 2583–2600, https://doi.org/10.1002/2017MS000988, 2017.

Vionnet, V., Brun, E., Morin, S., Boone, A., Faroux, S., Moigne, P. L., Martin, E., and Willemet, J. M.: The detailed snowpack scheme Crocus and its implementation in SURFEX v7.2, Geoscientific Model Development, 5, 773–791, https://doi.org/10.5194/gmd-5-773-2012, 2012.

Vitousek, P. M., Mooney, H. A., Lubchenco, J., and Melillo, J. M.: Human domination of Earth's ecosystems, Science, 277, 494–499, https://doi.org/10.1126/science.277.5325.494, 1997.

Waser, L. T., Ginzler, C., and Rehush, N.: Wall-to-Wall tree type mapping from countrywide airborne remote sensing surveys, Remote Sensing, 9, https://doi.org/10.3390/rs9080766, 2017.

Wieder, W. R., Lawrence, D. M., Fisher, R. A., Bonan, G. B., Cheng, S. J., Goodale, C. L., Grandy, A. S., Koven, C. D., Lombardozzi, D. L., Oleson, K. W., and Thomas, R. Q.: Beyond Static Benchmarking: Using Experimental Manipulations to Evaluate Land Model Assumptions, Global Biogeochemical Cycles, 33, 1289–1309, https://doi.org/10.1029/2018GB006141, 2019.

Xie, J., Jonas, T., Rixen, C., de Jong, R., Garonna, I., Notarnicola, C., Asam, S., Schaepman, M. E., and Kneubühler, M.: Land surface phenology and greenness in Alpine grasslands driven by seasonal snow and meteorological factors, Science of the Total Environment, 725, https://doi.org/10.1016/j.scitotenv.2020.138380, 2020.

Yuan, K., Zhu, Q., Zheng, S., Zhao, L., Chen, M., Riley, W. J., Cai, X., Ma, H., Li, F., Wu, H., and Chen, L.: Deforestation reshapes land-surface energy-flux partitioning, Environmental Research Letters, 16, https://doi.org/10.1088/1748-9326/abd8f9, 2021.

Yuan, K., Zhu, Q., Riley, W. J., Li, F., and Wu, H.: Understanding and reducing the uncertainties of land surface energy flux partitioning within CMIP6 land models, Agricultural and Forest Meteorology, 319, https://doi.org/10.1016/j.agrformet.2022.108920, 2022.

Zaehle, S., Medlyn, B. E., Kauwe, M. G. D., Walker, A. P., Dietze, M. C., Hickler, T., Luo, Y., Wang, Y. P., El-Masri, B., Thornton, P., Jain, A., Wang, S., Warlind, D., Weng, E., Parton, W., Iversen, C. M., Gallet-Budynek, A., Mccarthy, H., Finzi, A., Hanson, P. J., Prentice, I. C., Oren, R., and Norby, R. J.: Evaluation of 11 terrestrial carbon-nitrogen cycle models against observations from two temperate Free-Air CO2 Enrichment studies, New Phytologist, 202, 803–822, https://doi.org/10.1111/nph.12697, 2014.

Zeeman, M. J., Mauder, M., Steinbrecher, R., Heidbach, K., Eckart, E., and Schmid, H. P.: Reduced snow cover affects productivity of upland temperate grasslands, Agricultural and Forest Meteorology, 232, 514–526, https://doi.org/10.1016/j.agrformet.2016.09.002, 2017.

Zhang, T.: Influence of the seasonal snow cover on the ground thermal regime: an overview, Rev. Geophys., 43, 1–5, https://doi.org/doi:10.1029/2004RG000157, 2005.

Zhang, X., Wang, J., Gao, F., Liu, Y., Schaaf, C., Friedl, M., Yu, Y., Jayavelu, S., Gray, J., Liu, L., Yan, D., and Henebry, G. M.: Exploration of scaling effects on coarse resolution land surface phenology, Remote Sensing of Environment, 190, 318–330, https://doi.org/10.1016/j.rse.2017.01.001, 2017.

Zhao, T. and Dai, A.: The magnitude and causes of global drought changes in the twenty-first century under a low-moderate emissions scenario, Journal of Climate, 28, 4490–4512, https://doi.org/10.1175/JCLI-D-14-00363.1, 2015.

Zhuang, J., raphael dussin, Huard, D., Bourgault, P., Banihirwe, A., Raynaud, S., Malevich, B., Schupfner, M., Filipe, Levang, S., Jüling, A., Almansi, M., RichardScottOZ, RondeauG, Rasp, S., Smith, T. J., Stachelek, J., Plough, M., Pierre, Bell, R., and Li, X.: pangeo-data/xESMF: v0.7.1, https://doi.org/10.5281/ZENODO.7800141, 2023.

Zscheischler, J., Westra, S., Hurk, B. J. V. D., Seneviratne, S. I., Ward, P. J., Pitman, A., Aghakouchak, A., Bresch, D. N., Leonard, M., Wahl, T., and Zhang, X.: Future climate risk from compound events, Nature Climate Change, 8, 469–477, https://doi.org/10.1038/s41558-018-0156-3, 2018.